This theoretical work demonstrates the existence of seven new shear-horizontal surface acoustic waves (SH-SAWs) when different electrical and magnetic boundary conditions are applied. All the discovered SH-SAWs can propagate on the surface of the cubic piezoelectromagnetics along direction [101]. Calculations of the new SH-SAW features were performed for two-phase composites with the piezomagnetic phase (Metglas, Terfenol-D, Galfenol, Alfenol) and the piezoelectric phase (Tl3TaSe4, Tl3VS4, PZT). It was also found that the surface Bleustein-Gulyaev-Melkumyan wave can propagate in the cubic piezoelectromagnetics. Also, it was found that for both the sets of the eigenvector components, only single SH-SAW solution can be revealed for both groups of the cubic piezoelectromagnetics (CMEMC < 1/3 and CMEMC > 1/3). The obtained results can be utilized in fabricating smart materials in the microwave technology. It is thought that utilizing EMATs, measurements of all the new SH-SAWs propagating in the cubic piezoelectromagnetics and transversely isotropic piezoelectromagnetics can be carried out. The results can be useful for acoustoelectronics, acoustooptics, optoelectronics.

Aleksey Anatolievich Zakharenko

A.A. Zakharenko; 2005-Creator of International Institute of Zakharenko waves (IIZWs,aazaaz@inbox.ru); 1998-Diploma Engineer-Physicist (MSc) Krasnoyarsk State University, Krasnoyarsk,Russia; 2008-Certified Interior Designer,INOPROF, Krasnoyarsk; 2011-Diploma Programmer (MSc, Russian red Diploma) Siberian State Technological University,Krasnoyarsk

978-3-8473-3485-9

Seven new SH-SAWs in cubic PEMs

Aleksey Anatolievich Zakharenko

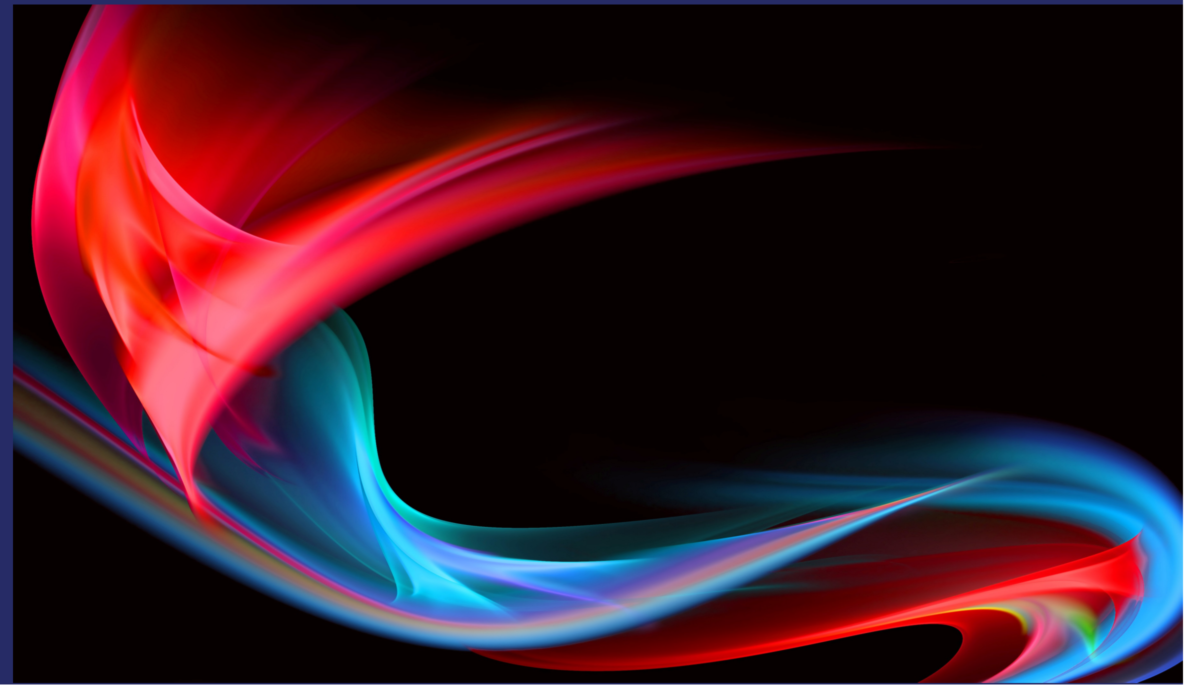

Aleksey Anatolievich Zakharenko

SEVEN NEW SH-SAWs IN CUBIC PIEZOELECTROMAGNETICS

Calculation of propagation characteristics of seven new SH-SAWs in cubic piezoelectromagnetics

LAP LAMBERT Academic Publishing

This work has been fulfilled

within the International Institute of Zakharenko Waves (IIZWs) by

ALEKSEY ANATOLIEVICH ZAKHARENKO

(E-mail: aazaaz@inbox.ru)

LAP LAMBERT Academic Publishing GmbH & Co. KG

Dudweiler Landstrasse 99 D - 66123 Saarbruecken

Phone: +49 681 3720-310 Fax: +49 681 3720 -3109

info@lap-publishing.com http://www.lap-publishing.com

Saarbruecken – Krasnoyarsk, 2011

PREFACE

This theoretical work addresses to calculations of characteristics of seven new shear-horizontal surface acoustic waves (SH-SAWs). These new SH-SAWs can propagate on the surface of the cubic piezoelectromagnetic (composite) materials concerning direction [101]. These materials can possess both piezoelectric and piezomagnetic phases. Applying different electrical and magnetic boundary conditions in the theoretical treatments, wave characteristics of the seven new SH-SAWs were obtained. Calculations of the new SH-SAW characteristics were performed for sample two-phase composite materials, consisting of the piezomagnetic phase (Metglas, Terfenol-D, Galfenol, Alfenol) and the piezoelectric phase (Tl_3TaSe_4, Tl_3VS_4, PZT) when average material properties are used. It was also found that the surface Bleustein-Gulyaev-Melkumyan (BGM) wave can propagate in the cubic piezoelectromagnetics. Also, it was found that for both the sets of the eigenvector components, only single SH-SAW solution can be revealed in the case of the cubic piezoelectromagnetics for both the CMEMC $K_{em}^2 < 1/3$ and $K_{em}^2 > 1/3$. For $K_{em}^2 < 1/3$, the seven new SH-SAWs can propagate with speeds higher than that of the surface BGM-wave and slower than that of the SH-BAW characterized by the velocity V_{tem}. For $K_{em}^2 > 1/3$, the SH-SAWs can propagate with the speeds slower than the value of the solution denoted by V_K. This is a significant difference from the case of the wave propagation in the transversely isotropic piezoelectromagnetic composites, in which two SH-SAW solutions solidly exist for each set of the boundary conditions due to two different sets of the eigenvector components and the solution V_K does not exist. Also, the dependence on the speed of light in a vacuum is revealed in the cubic piezoelectromagnetics for the suitable boundary conditions. It is obvious that the obtained results can be useful for complete understanding of wave processes in two-phase and laminated composite materials with the cubic and hexagonal symmetries in acoustoelectronics, acoustooptics, and optoelectronics. It is expected that the obtained

results can be utilized in fabricating smart materials in the microwave technology. It is thought that utilizing the electromagnetic acoustic transducers (EMATs), measurements of all the new SH-SAWs propagating in the cubic piezoelectromagnetics and transversely isotropic piezoelectromagnetic composite materials can be carried out.

PACS: 51.40.+p, 62.65.+k, 68.35.Gy, 68.35.Iv, 68.60.Bs, 74.25.Ld, 74.25.Ha, 75.20.En, 75.80.+q, 81.70.Cv

Keywords: cubic piezoelectromagnetics, magnetoelectric effect, SH-SAWs, new surface acoustic waves, EMATs.

COMMENTS BY THE AUTHOR

This book describes the theoretical work carried out for the International Institute of Zakharenko Waves (IIZWs). The author address for correspondence is as follows: A.A. Zakharenko, 660037, Krasnoyarsk-37, 17701, Krasnoyarsk, Russia (E-mail: aazaaz@inbox.ru). It is thought that this book can be interesting for researchers and students who deal with cubic and transversely-isotropic piezoelectromagnetics. Indeed, knowledge of wave properties of piezoelectromagnetics is beneficial to design of smart devices, sensors, actuators, etc. It can also represent an interest in some applications in the non-destructive testing and evaluation. Also, the obtained results in this book can allow one to choose appropriate materials to constitute piezoelectromagnetic laminate composite materials in the microwave technology. It is well-known that innovative smart composite materials are also created for the aerospace industry.

This book deals with propagation of the shear-horizontal surface acoustic waves (SH-SAWs) in cubic piezoelectromagnetics. This studying subject relates to the disciplines of Applied Physics and Electromagnetic Engineering. The descriptive term "acoustic" (rather than "elastic") follows common usage in physics, where ordinary elastic motions in crystals are called acoustic modes. This distinguishes the acoustic modes from optical ones. The optical modes involve internal degrees of freedom within a crystal unit cell. The term "acoustic" also reflects common terminology among researchers and engineers engaged in developing elastic wave devices for radar and communication systems. This arena of technological development has been strongly influenced by the philosophy, concepts, and techniques of microwave electromagnetics. This is also known as microwave acoustics. So, utilization of the term "acoustic" accurately describes the aim and scope of the book.

The International Institute of Zakharenko Waves (IIZWs) was recently created to support researches on different Zakharenko waves, as well as for monitoring the non-dispersive Zakharenko type waves in many complex systems such as the layered and quantum systems. Indeed, any complex system in which dispersive waves can propagate is of a great interest for the IIZWs. The well-known examples of dispersive waves are the dispersive Rayleigh and Bleustein-Gulyaev type waves as well as the Love and Lamb type waves. It is also stated that there are currently more than twenty papers and books relevant to the IIZWs. The International Institute of Zakharenko Waves also studies different dispersive and non-dispersive waves both theoretically and experimentally, including different applications of the waves for signal processing (filters, sensors, etc.) and the structural health monitoring.

It is worth noting that the International Institute of Zakharenko waves possessively takes all the planets and smaller natural space bodies in the space outside the Solar System to develop both the IIZWs and the planets concerning economics, ecology, and population. Also, it is thought that this is necessary in order to exclude any sale of the planets and their surfaces by any human or other. This activity of the IIZWs was also created due to a problem to find a spot for the IIZWs on Earth. Note that the single person, namely Mr. Dennis Hope from the United States of America (USA) possesses the planets in the Solar System (but Earth) who sells surfaces of the planets to individuals. It is also noted that only several thousands of planets orbiting their own stars can be currently observed in the Star Systems which are situated relatively near the Solar System. This does not mean that only several thousands of planets can exist outside the Solar System we can observe. It is expected that in average ten planets can orbit each star of enormous number of Star Systems in our Universe. It is thought that our Universe can accumulate more than 10^{999} stars.

Aleksey Anatolievich Zakharenko

Krasnoyarsk, Russia, 2011

TABLE OF CONTENTS: **PAGE**

List of Tables:

List of Figures: **PAGE**

INTRODUCTION

The beginning of this millennium demonstrates a good dynamics of development of theoretical and experimental directions of investigations of piezoelectromagnetic (PEM) composite materials. These composite materials are of interest for the engineering of different materials with either new or desired properties that are not present in single-phase materials. In composites consisting of piezoelectric and magnetostrictive phases, magnetoelectric (ME) effect represents the resulting product property, namely mechanical deformation due to magnetostriction results in a dielectric polarization owing to the piezoelectric effect. The latterly review [1] published in 2010 by Srinivasan acquaints the reader with the most recent advances in the physics of ME interactions in layered composites and nanostructures and discusses potential device applications. For instance, the magnetic-field sensors, dual electric-field- and magnetic-field-tunable microwave and millimetre-wave devices can be the potential device applications for the composites. However, this review does not cover all very significant works on bulk composites and other ME materials and phenomena since 2000.

The review paper [2] published one year earlier also focuses on demonstration of a plethora of applications of ferrites (a special class of magnetic materials using Fe as a constituent) in passive microwave components such as isolators, circulators, phase shifters, filters, and miniature antennas operating in a wide interval of work frequencies from 1 GHz to 100 GHz. It is noted that ferrites can also be utilised as magnetic recording media. There is a problem of miniaturization of the passive components. This problem can be resolved using high magnetic susceptibility of ferromagnets coupled with high dielectric permittivity of some ferroelectrics. It is mentioned that piezoelectric materials respond to applied electric field by change in dimensions or vice versa. Piezoelectrics and ferromagnets are a subclass of materials lacking centrosymmetry. Such materials can also exhibit nonlinear optical properties and can be used in optical communication and signal processing.

The 2008 review [3] overviews the brief history of ME laminated composites. Ref. [3] also discusses some of the important advancements in material couples, configurations of laminated composites consisting of piezoelectric and magnetostrictive layers, and operational modes that can dramatically enhance the ME voltage (α_{ME}) and charge coefficients. Laminated composite materials have much higher ME coefficients (giant ME effect) compared with ME single phase and two-phase particulate composite materials. The ME effect of single phase materials is scientifically very interesting and has constantly shown only small values of α_{ME} and only at low temperatures.

The ME voltage coefficient α_{ME} is defined by the following formula [3]: $\alpha_{\mathrm{ME}} = E/H$ where E and H are the bias electrical and magnetic fields, respectively. Using the tensor form following Ref. [2], the components of ME voltage coefficient $(\alpha_{\mathrm{ME}})_{ij}$ are given by

$$(\alpha_{\mathrm{ME}})_{ij} = \frac{\delta E_i}{\delta H_j} = -\frac{\alpha_{ij}}{\varepsilon_0 \varepsilon_r} \tag{1}$$

where δE_i and δH_j are the components of the AC electrical and magnetic fields, respectively. In equation (1), α_{ij} stands for the second-rank ME-susceptibility tensor, ε_0 and ε_r are the dielectric permittivity of a vacuum and the relative permittivity of a material, respectively. Note that the quantity $(\alpha_{\mathrm{ME}})_{ij}$ in equation (1) is generally measured during experiments.

Using the Landau theory and SI units, the ME effect in monocrystals can be described by writing the expansion of the free energy $F(\mathbf{E}, \mathbf{H})$ of the ME system [2, 4, 5]. Ignoring the higher order terms in the expansion, the following condition of limitation of the ME response can be obtained [2, 4]:

$$\alpha_{ij}^2 < \varepsilon_{ii} \mu_{jj} \tag{2}$$

where ε_{ij} and μ_{ij} are the dielectric permittivity and magnetic permeability tensors of the second rank, respectively. Note that the linear ME term can be less than zero, according to Ref. [2]. In PEM composite systems, a linear behavior is usually observed by means of AC magnetic field application, albeit the non-linear ME effect can be also observed in the case of bias magnetic field application. Using SI units, the components α_{ij} are expressed in s/m. However, they are dimensionless values in Gaussian units. The value of α is very small and reaches several ps/m. For instant, the following value of α is given in Ref. [4]: α = 4.13 ps/m for Cr_2O_3. The largest ME coefficients for monocrystals can have one order larger values: α = 30.6 ps/m for $LiCoPO_4$ [6], and α = 36.7 ps/m for $TbPO_4$ [7].

In contrast to the ME monocrystals, the ME laminated composites of two-phase composites can reveal several orders larger ME coefficients [1-4, 8]. The ME effect in two-phase composite materials is realized by exploiting the idea of average product properties via various connectivities *p-q* (*p*, *q* = 0, 1, 2, 3 represent the phase dimensions) [1, 2, 4, 9-12]. Therefore, the laminated composites can pertain to (2-2) connectivity in the case of thin films or to (3-2), (2-3), or (3-3) connectivities when it is necessary to treat bulk properties for some thicker films. When point (zero dimensional) inclusions of one phase are dotted across the volume of the second phase bulk material it is possible to say that one copes with (0-3) piezoelectromagnetic composites. Indeed, such zero-dimensional inclusions of the first phase must occupy a significant volume fraction in percentage to solidly change the bulk properties of the second phase to demonstrate already average product properties. Therefore, the important feature of such composite is the volume fracture of one phase into the second one.

The promising piezomagnetic (magnetostrictive) phase materials to form the composites are such Fe-containing alloys (ferrites) as Terfenol-D ($Tb_{27}Dy_{73}Fe_{195}$), Galfenol ($Fe_{81}Ga_{19}$), Alfenol ($Fe_{87}Al_{13}$), and Metglas (FeBSiC) [3, 8] which can possess the cubic symmetry of class m3m. Terfenol-D can also pertain to the transversely-isotropic symmetry of class 6 mm. However, the cubic symmetry is also possible for the rare earth alloy Terfenol-D [13, 14]. Comparing with the other magnetic materials, ferrites have large resistances and small magnetostriction. Terfenol-D [15] of ferrites has the largest magnetostriction of any known material. Notwithstanding, this alloy cannot be coprocessed with oxide ferroelectrics because sintering can oxidize the iron and significantly reduce the superior magnetostriction of such alloys [3]. Probably, Terfenol-D is not suitable for high frequency applications due to its low electrical resistance that can result in Eddy current losses [3]. However, it was found that Terfenol-D is suitable for ME laminated composited in the frequency range from 0 to 0.1 MHz.

Also, the alloy Terfenol-D can be readily substituted for the other well-known alloys Galfenol [16, 17] and Alfenol [12, 18-21]. The alloys Galfenol and Alfenol possess smaller magnetostrictions than that of Terfenol-D and are mechanically ductile whereas Terfenol-D is brittle. They are tough and not toxic, and can be machined and used without any special handling in technical devices. Indeed, the alloys can be used in magnetic transducers which are increasingly considered as actuators and sensors for copious aerospace, aeronautic, automotive, industrial, and biomedical applications [22-29]. The topical review article [30] published in 2008 describes recent development on the deformation and fracture of soft ferromagnetic materials and the mechanics of ferromagnetic composites. Also, some studies of the Fe-containing alloys are cited in Refs. [31-69] and some of the United States and international applications can be found in Refs. [70-81]. Also, one of the most promising magnetostrictive alloys is Metglas [82] which has a vast relative magnetic permeability. The Metglas magnetization is smaller than that of Terfenol-D and saturates at very low DC magnetic biases.

It is thought that Chalcogenide family materials are the suitable piezoelectric phase cubic ones which can contain no oxygen, in order to avoid oxidization of iron in the Fe-containing alloys. They belong to the cubic class $\bar{4}3m$ and can possess both zero temperature coefficients and strong piezoelectric coupling. Indeed, the Chalcogenide piezoelectric crystals such as Tl_3VS_4 and Tl_3TaSe_4 [83] can serve as the possible pair materials for the piezomagnetic alloys. The Chalcogenides represent a particularly large potential interest, especially for moderate frequency and large bandwidth. However, they are not commercially available, probably because of their mechanical softness and fabrication difficulties. On the other hand, the oxygen-containing cubic symmetry piezoelectric ceramics of the point group 23 ($Bi_{12}SiO_{20}$ and $Bi_{12}GeO_{20}$ [84] and $Bi_{12}TiO_{20}$ [85] can also have the strong piezoelectric effect) cannot be used for the purpose. Also, it is assumed that the well-known transversely-isotropic materials $Pb(Zr,Ti)O_3$ called PZT, which have the strongest piezoelectric effect, can be solidly used as the piezoelectric phase materials, for instance, a powder as the zero-dimensional inclusions in a volume of the bulk cubic piezomagnetics. So, it is possible to assume that the resulting piezoelectromagnetic composite materials will have the corresponding cubic symmetry and possess corresponding average product properties. In addition, the transversely-isotropic PZT and PVDF (polyvinylidene difluoride) together with the cubic Galfenol and Metglas were successfully used for the laminated composites [3, 60, 86, 87]. These all studies relate to experimental investigations of piezoelectromagnetics.

Concerning the theoretical investigations of wave propagation in piezoelectromagnetics, the reviews [1-3, 30] published in 2008, 2009, and 2010 did not mention about the recent theoretical achievements by Arman Melkumyan in his work [88] published in 2007. He discovered twelve new shear-horizontal surface acoustic waves (SH-SAWs) propagating in the transversely-isotropic piezoelectromagnetics and has written the new wave speeds in corresponding explicit forms. Following the theoretical work [88] by A. Melkumyan, further theoretical investigations [89] of the SH-SAW propagation in the transversely-isotropic piezoelectromagnetics also revealed the existence of additional seven new SH-SAWs and their velocities were also discovered in the corresponding explicit forms [89]. It is very interesting that discovered in the transversely-isotropic piezoelectrics approximately forty years ago, the classical surface Bleustein-Gulyaev (BG) wave speed [90, 91] can be also received for some particular cases [88, 89]. It is worth noticing that the propagation direction of the surface BG-wave should be perpendicular to an even-order symmetry axis. This soundly demonstrates connections among the theories for some SH-SAWs. Also, the authors of Ref. [92] stated that SH-SAWs can easily be produced by electromagnetic acoustic transducers (EMATs) which can offer a series of advantages over traditional piezoelectric transducers [93, 94]. It is worth noting that an improved optical method for measurements of both the phase and group velocities is described in Ref. [95]. This method allows one to measure the phase velocity with accuracy by about 2 m/s. This is true for measurements of characteristics of wave propagation in both the cubic and transversely-isotropic piezoelectromagnetics. Note that no complete theoretical calculations of wave characteristics in any cubic piezoelectromagnetics are still carried out.

The theoretical treatments of cubic materials relate to analytical and numerical studies of characteristics of wave propagation in either purely piezoelectric or purely piezomagnetic monocrystals. It is historically put together that first attempt to discover SH-SAWs was done with cubic piezoelectrics [96] before the discovery of the classical surface BG-wave [90, 91] in 1968-1969 in the transversely-isotropic piezoelectrics. In 1966, Kaganov and Sklovskaya [96] reported a possible existence of new surface waves coupled with the electrical potential in cubic piezoelectric monocrystals. Ref. [96] stated that the phase velocity V_{ph} of the new (additional) surface wave is higher than $3^{1/2}V_t/2$ and lower than V_t (according to the paper text) where V_t denotes the shear-horizontal bulk acoustic wave (SH-BAW) velocity uncoupled with the electrical potential. Also, they in Ref. [96] did not state that such SH-SAWs can propagate when the direction of wave propagation is perpendicular to an even-order symmetry axis of a piezoelectric monocrystal. However, Kaliski [97] working for the Polish Academy of Science reported in 1967 that the classical surface BG-waves [90, 91] do not exist in cubic piezoelectric crystals. Indeed, at the beginning of this Millennium the SH-SAWs were also not found in 2005 in Ref. [84] studying cubic piezoelectric monocrystals of class 23 in propagation direction (001)[100] (*Z*-cut).

However, it is indispensable to state that several attempts to find the classical surface BG-waves in cubic piezoelectrics were done after 1967, namely in 1970 [98, 99], 1972 [100], and 1989 [101]. However, these attempts [98-101] to analytically and numerically find the SH-SAWs in crystals with the cubic symmetry did not reveal the significant differences of the SH-SAW propagation in cubic crystals from that in the transversely-isotropic materials. Moreover, these studies [98-101] represented their results in such ways that the SH-SAW propagation in cubic crystals is similar to that in the transversely-isotropic materials with no significant differences pithily described below. This is in fact not trustable and looks like bogus or incorrect results. As the result, RAS Academician Gulyaev (the co-discoverer of the surface BG-waves) and Hickernell (who worked with the other co-discoverer) stated in their 2005 paper [102] that the surface BG-waves cannot exist in cubic piezoelectrics. The author of Ref. [103] agreed with the statement by Gulyaev and Hickernell.

Treating the SH-SAW propagation, the significant differences between the cubic crystals and the transversely-isotropic materials can be established based on the results obtained in Ref. [103]. The work [103] soundly demonstrated that the new SH-SAWs called the ultrasonic surface Zakharenko waves (USZWs) can exist in the cubic piezoelectric monocrystals. The very important features of the cubic piezoelectrics are the very simple values of $K_e^2 = 1/3$ and V_{aK} obtained in the explicit form in Ref. [103]. Note that the transversely-isotropic materials cannot possess these features. Therefore, all cubic piezoelectrics in contrast to the transversely-isotropic materials can be divided into two groups: the first group includes cubic piezoelectrics with $K_e^2 < 1/3$ and the second is for those with $K_e^2 > 1/3$, where K_e^2 is the coefficient of the electromechanical coupling (CEMC). For $K_e^2 < 1/3$, the USZW velocity can significantly differ from the BG-wave velocity compared with the difference between the velocity of the SH-BAW coupled with the electrical potential and the BG-wave velocity, and the value of V_{aK} is always found. For materials with $K_e^2 > 1/3$, the USZW velocity is situated slightly below the value of V_{aK}, but not slightly below the speed of the SH-BAW (this is the case for the BG-wave). Therefore, for cubic crystals with $K_e^2 > 1/3$, it is possible to treat the value of V_{aK} as the first approximation for the USZW speed due to negligible difference between them in suitable cases. However, the case of the electrical potential $\varphi = 0$ of the electrical boundary conditions demonstrates a coincidence of the USZW velocity for cubic piezoelectrics with the BG-wave velocity for the transversely-isotropic materials.

Indeed, utilization of cubic piezoelectrics in addition to the transversely-isotropic materials can broaden a list of suitable materials and represents an interest in engineering and design of SAW devices (filters, dispersive delay lines, etc.). As an important class of smart materials, piezoelectric ceramics are also broadly utilized as actuators and sensors in adaptive microelectromechanical systems [104]. In recent years, many efforts have been made in the area of wave propagation in piezoelectric media that is the subject of increasing research activity. Many important findings for the SH-SAWs on piezoelectrics have been mentioned in the historical note [105].

In theoretical paper [106], Alshits, Darinskii, and Lothe conducted a qualitative research on the existence of SH-SAWs in piezomagnetic and piezoelectric elastic half-spaces. According to Ref. [106], the piezomagnetic effect and the piezoelectric effect can be described in the same way. As a result, as in the transversely-isotropic piezoelectrics, the surface BG-waves can also propagate in the transversely-isotropic piezomagnetics, using the corresponding material characteristics for the piezomagnetic materials. Piezoelectric and piezomagnetic properties of anisotropic materials were established by Al'shits and Lyubimov in Ref. [107]. In addition, Gulyaev, Dikshtein, and Shavrov mentioned in their review paper [108] that dispersion relations for magnetoelastic SH-waves in ferromagnetics and (anti-)ferromagnetics can also lead to the surface BG-wave velocity. Also, the first study of the USZW existence in cubic piezomagnetics was theoretically performed in Ref. [14], in which the studied cubic material Galfenol can relate to both groups with $K_m^2 < 1/3$ and $K_m^2 > 1/3$, where K_m^2 is the coefficient of the magnetomechanical coupling (CMMC).

Also, it is necessary to succinctly describe the history of the researches on the magnetoelectrical (ME) effect. Notice that as early as 1894 is the year of the original prediction of the ME effect done by P. Curie [109]. He stated a possiblity for an asymmetric molecular body to be directionally polarized under the influence of a magnetic field. Later, Landau and Lifshitz [110] were the new generation theoreticians who demonstrated from symmetry considerations that a linear ME effect can be revealed in magnetically ordered crystals. On the basis of theoretical analysis, Dzyaloshinskii [111] predicted the existence of the ME effect in the antiferromagnetic Cr_2O_3. The confirmation of the prediction was published in Ref. [112] by Astrov who has carried out measurements of the electric field-induced magnetization. Later, Rado and Folen [113] have detected the magnetic field-induced polarization and also confirmed the prediction. The primary requirement for the observance of the ME effect in materials is as follows: magnetic and electric dipoles must coexist.

Also, Smolensky and Ioffe [114] in 1958 synthesized the antiferromagnetic ferroelectric perovskite ceramic with the chemical formula $Pb(Fe_{1/2}Nb_{1/2})O_3$ (PFN). Later, the presence of a weak spontaneous moment in the ferroelectric phase of grown single crystals of PFN was confirmed below 9K [115]. In addition to the antiferromagnetic Cr_2O_3 [116], the ME effect has been found in many compounds [117-132]. According to the famous classical book by Smolenskii and Chupis [129], the ME effect can exist in such materials as perovskites, pseudo-ilmenites, rare earth magnates, $BaMeF_4$ (Me = Mn, Fe, Co, Ni), Cr_2BeO_4, and inverted spinels. In 1980, Ismailzade *et al.* [130] reported the presence of linear ME effect in the antiferromagnetic-ferroelectric compound $BiFeO_3$. Its combination with barium titanate and bismuth titanate forms a big family with the general chemical formula $Bi_4Bi_{m-3}Ti_3Fe_{m-3}O_{3m+3}$ (m = 4, 5, and 8) in which ferroelectricity and magnetic nature can coexist up to high temperatures [131]. Schmid [132] has comprehensively worked on boracites which pertain to the large crystal structure family with the general chemical formula $M_3B_7O_{13}X$, where M stands for one of the following bivalent cations Mg^{2+}, Cr^{2+}, Mn^{2+}, Fe^{2+}, Co^{2+}, Ni^{2+}, Cu^{2+}, Zn^{2+}, etc. and X stands for one of the following monovalent anions $(OH)^-$, F^-, Cl^-, Br^-, I^-, or $(NO_3)^-$. In the sample material such as nickel boracite $Ni_3B_7O_{13}I$, the simultaneous presence of ferromagnetism and ferroelectricity in coexistence with ferroelasticity activates coupling between the spontaneous magnetization, spontaneous polarization, and spontaneous deformation.

For composite materials, van Suchtelen [133] introduced the concept of the product properties to realize the ME effect, which was then studied by van den Boomgaard [134], van Run *et al.* [135], and van den Boomgaard *et al.* [136] in oxygen-containing composites $BaTiO_3$-$CoFe_2O_4$. Wood and Austin [137] also studied composites and the ME effect. It is thought that the most popular composites are the transversely-isotropic ones in which hexagonal piezoelectrics $BaTiO_3$ and hexagonal piezomagnetics $CoFe_2O_4$ are used [138-142]. Using the Nye notation [143], Schmid [144] provides the tensor forms of the 58 point groups permitting the linear magnetoelectric effect. Generally, a continuous interest occurs to study the magnetoelectric effect in composites for development of smart materials in the microwave technology. Some modern researches on the ME effect in composites can be also found in Refs. [145-157]. It is thought that the most interesting possible applications of magnetoelectric materials are as follows [137, 158]:

- magnetic-electric energy converting components;
- solid state non-volatile memory;
- multi-state memory which can find application in quantum computing area;
- electrical/optical polarization components which can find applications in communication;
- light computing;
- solid state memories based on spintronics.

This work has the purpose to tersely illustrate first theoretical investigations of characteristics of the shear-horizontal surface acoustic waves (SH-SAWs) which can propagate in cubic piezoelectromagnetic composites. Chapters I and II describe thermodynamics, corresponding constitutive relations, and the equations of motion for the treated case. Chapter III acquaints the reader with material properties of the corresponding piezoelectrics and piezomagnetics, as well as studied piezoelectromagnetic composite materials consisting of them. Chapter IV discusses the boundary conditions. After that, Chapters from V to XIII cope with the calculations of wave characteristics using different electrical and magnetic boundary conditions. Chapter XIV provides some discussions for the reader on the wave propagation and the other problems. The conclusive remarks are summarized in that following Chapter XIV. After the conclusive words, a wide list of the references pertaining to various aspects of theoretical and experimental investigations of materials possessing the magnetoelectric effect is finally given.

CHAPTER I. Thermodynamics, Constitutive Relations, and Equations of Motion

Complex systems such as piezoelectrics, piezomagnetics, and piezoelectromagnetics can be described by means of several thermodynamical potentials. For example, eight thermodynamical potentials are currently used for description of thermoelectroelastic interactions in piezoelectric crystals. The thermodynamical potentials derive the equations of piezoelectric medium [159-161], and general equations for adiabatic rather than isothermal conditions may be obtained using the thermodynamical potential called the electrical enthalpy H_{el}. Adiabatic processes can be treated with the constant entropy S (S = const giving dS = 0) and only linear terms are left in a Taylor series for the electrical enthalpy H_{el} relative to an equilibrium condition $H_{el}(S_0)$ [159].

For a piezoelectromagnetic solid, energetic terms of the complex system described by a thermodynamical potential can be naturally coupled with the following sub-systems:

- elastic sub-system (stress σ_{ij} or strain η_{ij});
- electric sub-system (electrical field E_i or electrical induction D_i);
- magnetic sub-system (magnetic field H_i or magnetic flux B_i);
- thermal sub-system (temperature T or disorder value called entropy S).

For piezoelectromagnetic materials similar to piezoelectrics, the mechanical strain tensor η_{ij} defined by the following strain-displacement relation:

$$\eta_{ij} = \frac{1}{2}\left(\frac{\partial U_i}{\partial x_j} + \frac{\partial U_j}{\partial x_i}\right) \tag{I.1}$$

can be naturally taken as an independent thermodynamic mechanical variable. Expression (I.1) represents the well-known dependence of the strain tensor components η_{ij} on the corresponding partial first derivatives of the mechanical displacement components U_1, U_2, and U_3 with respect to the real space components x_1, x_2, and x_3. The indices i and j run from 1 to 3 in equation (I.1). Also, the electrical field E_i and the magnetic field H_i can be taken as independent thermodynamic electrical and magnetic variables, respectively. The components of the electrical field E_i and the magnetic field H_i are also defined by the corresponding partial first derivatives of the electrical potential φ and the magnetic potential ψ with respect to the x_1, x_2, and x_3, using the quasi-static (irrotational field) approximation:

$$E_i = -\frac{\partial \varphi}{\partial x_i} \quad \text{(I.2)}$$

$$H_i = -\frac{\partial \psi}{\partial x_i} \quad \text{(I.3)}$$

Indeed, propagation directions can exist in piezoelectromagnetic materials where both the electrical and magnetic potentials are coupled with propagating elastic waves [88, 89].

Using the independent thermodynamic mechanical, electrical, and magnetic variables, the thermodynamic potential G for a three-dimensional piezoelectromagnetic solid [89, 142, 162-164] can be written as the following function G = G(η_{ij}, E_i, H_i) where E_i and H_i are the components of the electrical field vector **E** and the magnetic field vector **H**, respectively. As a result, the coupled constitutive relations for linearly-piezoelectromagnetic solids [89, 165, 166] read:

$$\sigma_{ij} = C_{ijkl}\eta_{kl} - e_{kij}E_k - h_{kij}H_k \quad \text{(I.4)}$$

$$D_i = e_{ikl}\eta_{kl} + \varepsilon_{ik}E_k + \alpha_{ik}H_k \quad \text{(I.5)}$$

$$B_i = h_{ikl}\eta_{kl} + \alpha_{ik}E_k + \mu_{ik}H_k \quad \text{(I.6)}$$

where the indices k and l also run from 1 to 3. It is clearly seen in equations from (I.4) to (I.6) that such a piezoelectromagnetic (composite) material can possess the elastic stiffness constants C_{ijkl}, piezoelectric constants e_{kij}, piezomagnetic coefficients h_{kij}, dielectric permittivity coefficients ε_{ik}, magnetic permeability coefficients μ_{ik}, and electromagnetic constants α_{ik}.

In equation (I.4), the elastic stiffness constants C_{ijkl} are thermodynamically defined as follows:

$$C_{ijkl} = \left(\frac{\partial \sigma_{ij}}{\partial \eta_{kl}} \right)_{E,H=\text{const}} \tag{I.7}$$

In equations (I.4) and (I.5), the thermodynamic determination of the piezoelectric constants e_{kij} can be written in the following way:

$$e_{ijk} = -\left(\frac{\partial \sigma_{ij}}{\partial E_k} \right)_{\eta,H=\text{const}} = e_{ikl} = \left(\frac{\partial D_i}{\partial \eta_{kl}} \right)_{E,H=\text{const}} \tag{I.8}$$

In equations (I.4) and (I.6), the thermodynamic definition of the piezomagnetic coefficients h_{kij} can be written as follows:

$$h_{ijk} = -\left(\frac{\partial \sigma_{ij}}{\partial H_k} \right)_{\eta,E=\text{const}} = h_{ikl} = \left(\frac{\partial B_i}{\partial \eta_{kl}} \right)_{E,H=\text{const}} \tag{I.9}$$

In equation (I.5), the dielectric permittivity coefficients ε_{ik} are thermodynamically defined as follows:

$$\varepsilon_{ik} = \left(\frac{\partial D_i}{\partial E_k} \right)_{\eta,H=\text{const}} \tag{I.10}$$

In equation (I.6), the magnetic permeability coefficients μ_{ik} are thermodynamically determined as follows:

$$\mu_{ik} = \left(\frac{\partial B_i}{\partial H_k} \right)_{\eta, E=\text{const}} \tag{I.11}$$

In equations (I.5) and (I.6), the electromagnetic constants α_{ik} can be written using the following thermodynamic relations:

$$\alpha_{ik} = \left(\frac{\partial D_i}{\partial H_k} \right)_{\eta, E=\text{const}} = \left(\frac{\partial B_i}{\partial E_k} \right)_{\eta, H=\text{const}} \tag{I.12}$$

It is clearly seen in equation (I.7) that the elastic stiffness constants C_{ijkl} are defined at constant electrical and magnetic fields. Symmetry arguments allow some simplifications of the quantity of the constants C_{ijkl}. The stress tensor σ_{ij} and strain tensor η_{ij} are symmetric, i.e. $\sigma_{ij} = \sigma_{ji}$ and $\eta_{ij} = \eta_{ji}$. Thus, the stiffness tensor C_{ijkl} must have a corresponding degree of symmetry which leads to the following simplifications:

$$C_{ijkl} = C_{klij} = C_{jikl} = C_{klji} = C_{ijlk} = C_{lkij} = C_{jilk} = C_{lkji} \tag{I.13}$$

Using the Voigt notation, the constants C_{ijkl} can be written in a compact form as (6×6) matrix instead of (3×3×3×3) tensor form [143, 161, 167] which can be represented by nine (3×3) matrices. To transform a tensor form into a matrix, the following well-known rules are used for the indices: 11 → 1, 22 → 2, 33 → 3, 23 → 4, 13 → 5, 12 → 6. Therefore, the indices are changed as $ijkl \rightarrow PQ$ where the new indices P and Q run from 1 to 6. Consequently, one can construct the following matrix:

$$\left(C_{ijkl}\right)\rightarrow\left(C_{PQ}\right)=\begin{pmatrix} C_{11} & C_{12} & C_{13} & C_{14} & C_{15} & C_{16} \\ C_{21} & C_{22} & C_{23} & C_{24} & C_{25} & C_{26} \\ C_{31} & C_{32} & C_{33} & C_{34} & C_{35} & C_{36} \\ C_{41} & C_{42} & C_{43} & C_{44} & C_{45} & C_{46} \\ C_{51} & C_{52} & C_{53} & C_{54} & C_{55} & C_{56} \\ C_{61} & C_{62} & C_{63} & C_{64} & C_{65} & C_{66} \end{pmatrix} \quad \text{(I.14)}$$

For the reader, the excellent and classical books concerning the crystal symmetries and wave propagation in solids are also cited in Refs. [168-174].

The symmetry arguments also allow one to simplify the quantities of the piezoelectric constants e_{kij} and piezomagnetic coefficients h_{kij} in the similar manner. Because $\sigma_{ij} = \sigma_{ji}$ and $\eta_{ij} = \eta_{ji}$ in equations (I.8) and (I.9), the tensors e_{kij} and h_{kij} must also have corresponding degrees of symmetry. This results in the following equalities:

$$e_{kij} = e_{ijk} = e_{kji} = e_{jik} \quad \text{(I.15)}$$

$$h_{kij} = h_{ijk} = h_{kji} = h_{jik} \quad \text{(I.16)}$$

Using the Voigt notation for the piezoelectric constants e_{kij}, their (3×3×3) tensor form can be represented as the following (6×3) matrix:

$$\left(e_{ijk}\right)\rightarrow\left(e_{Pk}\right)=\begin{pmatrix} e_{11} & e_{12} & e_{13} \\ e_{21} & e_{22} & e_{23} \\ e_{31} & e_{32} & e_{33} \\ e_{41} & e_{42} & e_{43} \\ e_{51} & e_{52} & e_{53} \\ e_{61} & e_{62} & e_{63} \end{pmatrix} \text{ and } \left(e_{kij}\right)\rightarrow\left(e_{kP}\right)=\begin{pmatrix} e_{11} & e_{12} & e_{13} & e_{14} & e_{15} & e_{16} \\ e_{21} & e_{22} & e_{23} & e_{24} & e_{25} & e_{26} \\ e_{31} & e_{32} & e_{33} & e_{34} & e_{35} & e_{36} \end{pmatrix} \quad \text{(I.17)}$$

With the same notation for the piezomagnetic coefficients h_{kij}, their (3×3×3) tensor form can be represented as the following (6×3) matrix:

$$\left(h_{ijk}\right)\to\left(h_{Pk}\right)=\begin{pmatrix} h_{11} & h_{12} & h_{13} \\ h_{21} & h_{22} & h_{23} \\ h_{31} & h_{32} & h_{33} \\ h_{41} & h_{42} & h_{43} \\ h_{51} & h_{52} & h_{53} \\ h_{61} & h_{62} & h_{63} \end{pmatrix} \text{ and } \left(h_{kij}\right)\to\left(h_{kP}\right)=\begin{pmatrix} h_{11} & h_{12} & h_{13} & h_{14} & h_{15} & h_{16} \\ h_{21} & h_{22} & h_{23} & h_{24} & h_{25} & h_{26} \\ h_{31} & h_{32} & h_{33} & h_{34} & h_{35} & h_{36} \end{pmatrix} \quad \text{(I.18)}$$

The dielectric permittivity coefficients ε_{ik}, magnetic permeability coefficients μ_{ik}, and electromagnetic constants α_{ik} stand for the following symmetric tensors of the second rank (matrices):

$$\varepsilon_{ik}=\varepsilon_{ki} \quad \text{(I.19)}$$

$$\mu_{ik}=\mu_{ki} \quad \text{(I.20)}$$

$$\alpha_{ik}=\alpha_{ki} \quad \text{(I.21)}$$

The components ε_{ik}, μ_{ik}, and α_{ik} of the corresponding material constants can be also written as (3×3) matrices. They read

$$\left(\varepsilon_{ik}\right)=\begin{pmatrix} \varepsilon_{11} & \varepsilon_{12} & \varepsilon_{13} \\ \varepsilon_{21} & \varepsilon_{22} & \varepsilon_{23} \\ \varepsilon_{31} & \varepsilon_{32} & \varepsilon_{33} \end{pmatrix} \quad \text{(I.22)}$$

$$\left(\mu_{ik}\right)=\begin{pmatrix} \mu_{11} & \mu_{12} & \mu_{13} \\ \mu_{21} & \mu_{22} & \mu_{23} \\ \mu_{31} & \mu_{32} & \mu_{33} \end{pmatrix} \quad \text{(I.23)}$$

$$\left(\alpha_{ik}\right)=\begin{pmatrix} \alpha_{11} & \alpha_{12} & \alpha_{13} \\ \alpha_{21} & \alpha_{22} & \alpha_{23} \\ \alpha_{31} & \alpha_{32} & \alpha_{33} \end{pmatrix} \quad \text{(I.24)}$$

Using the definitions of the thermodynamic variables and the material constants, it is possible to write equations of motion for such piezoelectromagnetic solids. First of all, it is necessary to write some well-known equilibrium equations. Exploiting the

Maxwell equations such as div**B** = 0 and div**D** = 0, the governing mechanical, magnetostatic, and electrostatic equilibriums read:

$$\frac{\partial \sigma_{ij}}{\partial x_j} = 0 \tag{I.25}$$

$$\frac{\partial B_i}{\partial x_i} = 0 \tag{I.26}$$

$$\frac{\partial D_i}{\partial x_i} = 0 \tag{I.27}$$

From equation (I.25), the equations of motion of an elastic medium can be written in the following well-known form [175-177]:

$$\frac{\partial \sigma_{ij}}{\partial x_j} = \rho \frac{\partial^2 U_i}{\partial t^2} \tag{I.28}$$

where ρ and t are the mass density of a piezoelectromagnetics and time, respectively. In expression (I.28), the second partial derivative of the mechanical displacement components U_i with respect to time t represents an acceleration value of a unit volume $V = M/\rho$ where M is the mass of the volume. Also, the magnetostatics and electrostatics in the quasi-static approximation read:

$$\frac{\partial B_i}{\partial x_j} = 0 \tag{I.29}$$

$$\frac{\partial D_i}{\partial x_j} = 0 \tag{I.30}$$

where B_i and D_i are defined by equations (I.6) and (I.5), respectively.

With equations from (I.4) to (I.6) and definitions (I.2) to (I.3) for the electrical field E_i and the magnetic field H_i, it is possible to inscribe the following form for the coupled equations of motion defined by equations from (I.28) to (I.30) written above:

$$\rho \frac{\partial^2 U_i}{\partial t^2} = C_{ijkl} \frac{\partial^2 U_l}{\partial x_j \partial x_k} + e_{kij} \frac{\partial^2 \varphi}{\partial x_j \partial x_k} + h_{kij} \frac{\partial^2 \psi}{\partial x_j \partial x_k} \tag{I.31}$$

$$0 = e_{ijk} \frac{\partial^2 U_k}{\partial x_i \partial x_j} - \varepsilon_{ij} \frac{\partial^2 \varphi}{\partial x_i \partial x_j} - \alpha_{ij} \frac{\partial^2 \psi}{\partial x_i \partial x_j} \tag{I.32}$$

$$0 = h_{ijk} \frac{\partial^2 U_k}{\partial x_i \partial x_j} - \alpha_{ij} \frac{\partial^2 \varphi}{\partial x_i \partial x_j} - \mu_{ij} \frac{\partial^2 \psi}{\partial x_i \partial x_j} \tag{I.33}$$

These coupled equations of motion are suitable for a piezoelectromagnetic medium which possesses the piezoelectric, piezomagnetic, and piezoelectromagnetic effects.

Coupled equations from (I.31) to (I.33) mathematically represent homogeneous partial differential equations of the second order. Hence, it is well-known that solutions for such equations can be written in the following plane wave forms [89, 176, 177]:

$$U_i = U_i^0 \exp[\mathrm{j}(k_1 x_1 + k_2 x_2 + k_3 x_3 - \omega t)] \tag{I.34}$$

$$\varphi = \varphi^0 \exp[\mathrm{j}(k_1 x_1 + k_2 x_2 + k_3 x_3 - \omega t)] \tag{I.35}$$

$$\psi = \psi^0 \exp[\mathrm{j}(k_1 x_1 + k_2 x_2 + k_3 x_3 - \omega t)] \tag{I.36}$$

where the index i runs from 1 to 3.

In equations from (I.34) to (I.36), U_i^0, φ^0, and ψ^0 are the initial amplitudes which should be determined further. Also, j = $(-1)^{1/2}$ denotes the imaginary unity and ω stands for the angular frequency defined by $\omega = 2\pi\nu$ where ν is the linear frequency. The components k_1, k_2, and k_3 of the wavevector **K** directed towards the wave propagation can be written as follows:

$$(k_1, k_2, k_3) = k(n_1, n_2, n_3) \tag{I.37}$$

where n_1, n_2, and n_3 are the directional cosines: $n_1 = 1$, $n_2 = 0$ and $n_3 \equiv n_3$ for convenience. Note that the wavenumber k in the direction of wave propagation is defined by $k = 2\pi/\lambda$ where λ is the wavelength.

Utilization of the solutions given by equations from (I.34) to (I.36) and the directional cosines (I.37) for corresponding substitutions into coupled equations from (I.31) to (I.33) can lead to the following five homogeneous equations:

$$\begin{pmatrix} GL_{11}-\rho V_{ph}^2 & GL_{12} & GL_{13} & GL_{14} & GL_{15} \\ GL_{21} & GL_{22}-\rho V_{ph}^2 & GL_{23} & GL_{24} & GL_{25} \\ GL_{31} & GL_{32} & GL_{33}-\rho V_{ph}^2 & GL_{34} & GL_{35} \\ GL_{41} & GL_{42} & GL_{43} & GL_{44} & GL_{45} \\ GL_{51} & GL_{52} & GL_{53} & GL_{54} & GL_{55} \end{pmatrix} \begin{pmatrix} U_1^0 \\ U_2^0 \\ U_3^0 \\ U_4^0 \\ U_5^0 \end{pmatrix} = \begin{pmatrix} 0 \\ 0 \\ 0 \\ 0 \\ 0 \end{pmatrix} \qquad \text{(I.38)}$$

where GL_{IJ} denote the components of the modified tensor (the indices I and J run from 1 to 5) in the well-known Green-Christoffel equation [159] and V_{ph} stands for the phase velocity defined by

$$V_{ph} = \omega/k \qquad \text{(I.39)}$$

Also, $U_4^0 = \varphi^0$ and $U_5^0 = \psi^0$ are used in equations (I.38). The modified Green-Christoffel tensor GL_{IJ} is symmetric, i.e. $GL_{IJ} = GL_{JI}$. Therefore, only 15 tensor components are independent. To write below explicit forms for all 15 tensor components is not the main purpose of this work. It is thought that the readers themselves can obtain all the components GL_{IJ} in the corresponding explicit forms, using equations from (I.31) to (I.37).

Five homogeneous equations (I.38) are frequently written in the following compact form which can be met in many research paper and books concerning wave propagation in crystals:

$$\left(GL_{IJ} - \delta_{IJ}\rho V_{ph}\right)U_I^0 = 0 \qquad \text{(I.40)}$$

where the indices I and J also run from 1 to 5 and δ_{IJ} is the Kronecker delta-function, namely $\delta_{IJ} = 1$ for $I = J$, $\delta_{IJ} = 0$ for $I \neq J$, and $\delta_{44} = \delta_{55} = 0$. Equation (I.40) represents the coupled equations of motion in the well-known tensor form.

This work has an interest in research of SH-SAW propagation in cubic piezoelectromagnetics. For that reason, some highly symmetric propagation directions [175-179] must be studied. When propagation direction is changed, the number of independent material constants and their values must be also changed. However, new material constants can be obtained from the old ones. In the studied case, the material constants such as the dielectric permittivity coefficients ε_{ik}, magnetic permeability coefficients μ_{ik}, electromagnetic constants α_{ik}, piezoelectric constants e_{kij}, piezomagnetic coefficients h_{kij}, and elastic stiffness constants C_{ijkl} can be transformed using the following formulae for transformations of tensors:

$$\varepsilon_{ij} = a_{im} a_{jn} \varepsilon_{mn} \tag{I.41}$$

$$\mu_{ij} = a_{im} a_{jn} \mu_{mn} \tag{I.42}$$

$$\alpha_{ij} = a_{im} a_{jn} \alpha_{mn} \tag{I.43}$$

$$e_{ijk} = a_{im} a_{jn} a_{kp} e_{mnp} \tag{I.44}$$

$$h_{ijk} = a_{im} a_{jn} a_{kp} h_{mnp} \tag{I.45}$$

$$C_{ijkl} = a_{im} a_{jn} a_{kp} a_{lq} C_{mnpq} \tag{I.46}$$

This hard work of tensor transformations can be carried out numerically. The rules of such transformations from an original coordinate system into a new coordinate system are perfectly described in the excellent and classical books cited in Refs. [143, 176].

Suitable propagation directions on suitable crystal cuts can result in significant simplifications of the problem of wave propagation in piezoelectromagnetic materials. Indeed, certain propagation directions on certain cuts can lead to such situations when some of the *GL*-tensor components become equal to zero. For some of these cases, the matrix determinant in equation (I.38) can be written in the following simplified form:

$$\begin{vmatrix} GL_{11}-\rho V_{ph}^2 & 0 & GL_{13} & 0 & 0 \\ 0 & GL_{22}-\rho V_{ph}^2 & 0 & GL_{24} & GL_{25} \\ GL_{31} & 0 & GL_{33}-\rho V_{ph}^2 & 0 & 0 \\ 0 & GL_{42} & 0 & GL_{44} & GL_{45} \\ 0 & GL_{52} & 0 & GL_{54} & GL_{55} \end{vmatrix} == 0 \qquad (I.47)$$

It is clearly seen in equation (I.47) that the following vector from equation (I.38)

$$\left(U_1^0, U_2^0, U_3^0, U_4^0, U_5^0\right) \qquad (I.48)$$

can be readily rewritten as two vectors with the following components:

$$\left(U_1^0, 0, U_3^0, 0, 0\right) \qquad (I.49)$$

$$\left(0, U_2^0, 0, \varphi^0, \psi^0\right) \qquad (I.50)$$

Also, it is possible to write equation (I.47) in a more informative form which demonstrates that the matrix determinant in equation (I.47) actually splits into two independent determinants. This can be demonstrated as follows:

$$\begin{vmatrix} GL_{11}-\rho V_{ph}^2 & GL_{13} \\ GL_{31} & GL_{33}-\rho V_{ph}^2 \end{vmatrix} \times \begin{vmatrix} GL_{22}-\rho V_{ph}^2 & GL_{24} & GL_{25} \\ GL_{42} & GL_{44} & GL_{45} \\ GL_{52} & GL_{54} & GL_{55} \end{vmatrix} = 0 \qquad (I.51)$$

Indeed, each of them in equation (I.51) can be separately treated. Note that the vectors defined by equations (I.49) and (1.50) relate to the first and second factors in equation (I.51), respectively. For cubic piezoelectrics, the cuts and propagation directions are schematically shown in excellent works [176, 178]. It is indispensable to surely state that the highly symmetrical propagation direction are also exist in cubic piezoelectromagnetics, according to equation (I.51). Expanding the first matrix determinant in equation (I.51), a secular equation for determination of characteristics of the in-plane polarised surface Rayleigh wave [180, 181] can be obtained. In this case, the surface Rayleigh wave represents a purely mechanical wave. Expanding the second matrix determinant in equation (I.51), a secular equation for determination of characteristics of anti-plane polarized waves coupled with both the electrical potential φ and the magnetic potential ψ can be obtained. To study wave characteristics of such anti-plane polarized wave is the main purpose of this work.

Also, certain propagation directions on certain cuts can exist in cubic piezoelectrics when the surface Rayleigh wave can be coupled with the electrical potential φ [182]. It is thought that cubic and transversely-isotropic piezoelectromagnetics can possess some cases when in-plane polarised waves are also coupled with both the electrical potential φ and the magnetic potential ψ. In this case, the single possible anti-plane polarized wave represents a purely mechanical wave, namely the shear-horizontal bulk acoustic wave (SH-BAW). So, the vectors which determine the wave polarizations are as follows:

$$\left(U_1^0, 0, U_3^0, \varphi^0, \psi^0\right) \tag{I.52}$$

$$\left(0, U_2^0, 0, 0, 0\right) \tag{I.53}$$

The vectors in equations (I.52) and (I.53) serve for in-plane polarised waves and the anti-plane polarized SH-BAW, respectively.

The following chapter addresses to the theory of wave propagation in cubic piezoelectromagnetics when anti-plane polarized waves are coupled with both the electrical potential φ and the magnetic potential ψ. The certain propagation direction on the certain cut is also shown for the studied case in the following chapter.

CHAPTER II. Wave Propagation in Cubic Piezoelectromagnetics

It is indispensable to introduce the theory of propagation of shear-horizontal (SH) acoustic waves in piezoelectromagnetic (composite) materials. In this work, the studied piezoelectromagnetics have the cubic symmetry. Nevertheless, theoretical description of wave propagation in a cubic piezoelectromagnetics can be given in the same way like that in a transversely-isotropic piezoelectromagnetic composite material [89]. It was mentioned in the previous chapter that this work has an interest in propagation of shear-horizontal surface acoustic waves (SH-SAWs) when the anti-plane polarized waves are coupled with both the electrical potential φ and the magnetic potential ψ. This configuration is shown in figure II.1, in which the vector **K** exhibits the propagation direction for the studied case. Note that the SH-waves are coupled with both the potentials when the propagation direction is changed by rotation around the x_2-axis shown in figure II.1. This is similar to piezoelectrics [103, 159] and piezomagnetics [14].

The original coordinates (x'_1, x'_2, x'_3) shown in figure II.1 coincide with the crystallographic coordinates (X, Y, Z) shown in figure II.2. For the cubic system of class 23, the crystallographic coordinates (X, Y, Z) are directed along the three twofold symmetry axes. The work coordinate system (x_1, x_2, x_3), also shown in figure II.1, illuminates the propagation direction, in which the SH-waves are polarized parallel to the x_2-axis and propagate along the x_1-axis with damping towards the negative values of the x_3-axis. This propagation direction is also called direction [101] in physical acoustics. Thus, the propagation direction for the SH-waves is perpendicular to an even-order symmetry axis. This is a condition of existence of surface SH-waves in crystals, which can propagate only in certain propagation directions on certain crystal cuts. The direction of the cut normal (see the vector **N** in figure II.1) is also changed with the Euler angles (0°; θ; 0°), with which the propagation direction is changed.

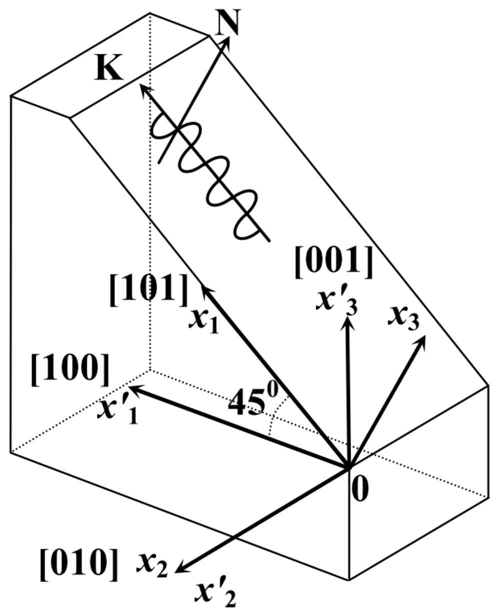

Figure II.1. The SH-SAW propagation along direction [101] for a cubic piezoelectromagnetics, using the rectangular coordinate system. The wavevector **K** is directed towards the wave propagation and **N** is the vector of surface normal.

It is necessary to introduce the cubic system based on crystallography. All the cubic crystals are characterized by presence of four threefold symmetry axes. Also, all the cubic crystals should possess even-order symmetry axes. They can be twofold and or fourfold axes. According to the work in Ref. [107], cubic symmetry materials, which can simultaneously possess both piezoelectric and piezomagnetic properties, have to relate to the crystallographic cubic classes 23 and $\bar{4}'3m'$ because the piezoelectric effect can be revealed only in non-centrosymmetric crystals. Note that a cubic class is readily distinguished by presence of threefold rotational symmetry axis denoted by number "3" on the second place in the basic cubic classes such as 23, $m3$, 432, $m3m$, and $\bar{4}3m$.

In crystallography, the point symmetry transformations include rotations, reflections, inversions, rotation-inversions, and rotation-reflections, of which the last category is equivalent to rotation-inversions. Rotation symmetries are defined in terms of the smallest rotation under which the crystal lattice is symmetric. For instance, a threefold rotation symmetry is defined as an operation with a minimum rotation angle $2\pi/3$. A threefold axis is marked with a small triangle as shown in figure II.2 and denotes a rotation through $360^0/3 = 120^0$. Also, mirror or reflection operations are denoted by the symbol "*m*" and rotation-inversion operations are denoted by the symbol "$\bar{4}$" for the cubic system. It is also noted that each crystal symmetry group is called a class. The various classes are grouped into systems (for example, the cubic system) that have to have certain physical properties in common. In general, crystallographic point groups of symmetries are defined by international symbols. It is necessary to state that no groups of crystal point symmetries have more than three generator operations such as the generator symmetry axes and mirror planes. The reader can find fundamentals of crystallography and crystallophysics in several classical books cited in Refs. [169, 183, 184].

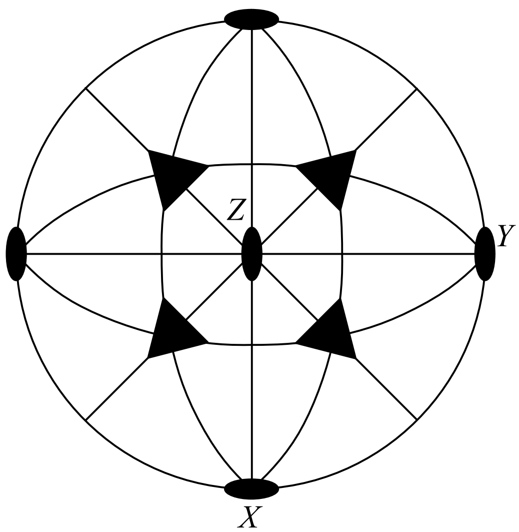

Figure II.2. The symmetry elements for the non-centrosymmetric cubic system of class 23, according to J.F. Nye [143].

In such cubic system, the material constants C_{ijkl}, e_{kij}, h_{kij}, ε_{ik}, μ_{ik}, and α_{ik} defined in the previous chapter are changed as soon as the propagation direction is changed. Also, it is assumed that the mass density ρ remains unchanged. In the crystallographic coordinate system (X, Y, Z) there are the following independent material constants: $C_{11} = C_{22} = C_{33}$, $C_{12} = C_{13} = C_{23}$, $C_{44} = C_{55} = C_{66}$, $e_{14} = e_{25} = e_{36}$, $h_{14} = h_{25} = h_{36}$, $\varepsilon_{11} = \varepsilon_{22} = \varepsilon_{33}$, $\mu_{11} = \mu_{22} = \mu_{33}$, and $\alpha_{11} = \alpha_{22} = \alpha_{33}$. The elastic stiffness constants $C_{11} = C_{22} = C_{33}$ and $C_{12} = C_{13} = C_{23}$ do not contribute in the SH-wave propagation. This is true because the matrix determinant factors in some highly symmetric propagation directions. This was demonstrated in equations (I.47) and (I.51) written in the previous chapter. For studied propagation direction [101] in a cubic piezoelectromagnetics, the transformed coordinate system (x_1, x_2, x_3) gives the following material constants:

$$C_{44} = C_{66} = C \tag{II.1}$$

$$e_{16} = -e_{34} = -e \tag{II.2}$$

$$h_{16} = -h_{34} = -h \tag{II.3}$$

$$\varepsilon_{11} = \varepsilon_{33} = \varepsilon \tag{II.4}$$

$$\mu_{11} = \mu_{33} = \mu \tag{II.5}$$

$$\alpha_{11} = \alpha_{33} = \alpha \tag{II.6}$$

The dependences of the non-zero piezoelectric constants e_{kij} and piezomagnetic coefficients h_{kij} on the propagation directions are shown in figure II.3. This figure shows the successive changes of the constants with change in the propagation direction beginning from direction [100] on the Z-cut in the crystallographic coordinate system (X, Y, Z).

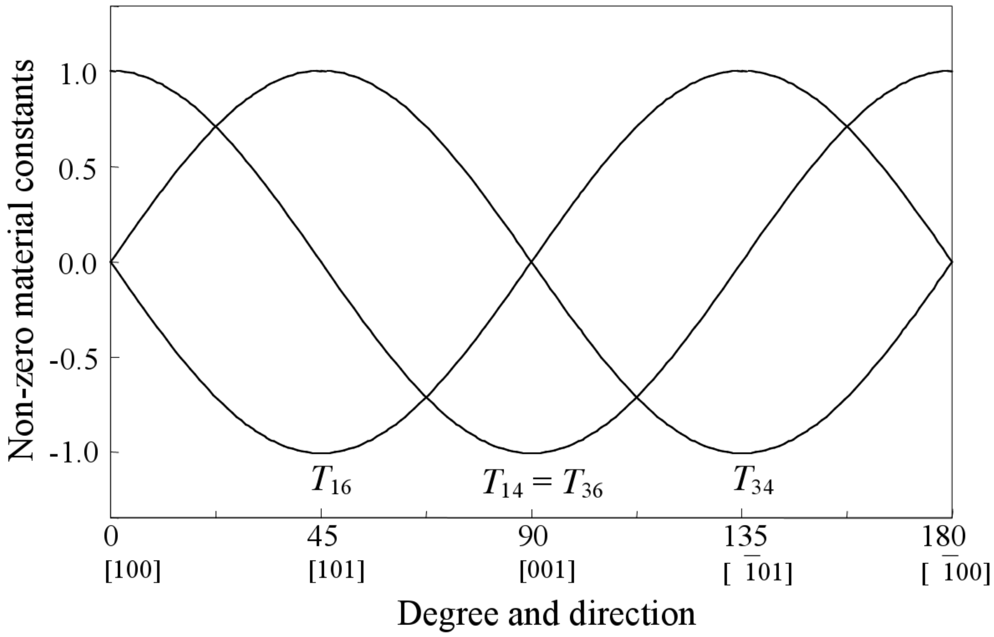

Figure II.3. The dependences of the normalized values of non-zero material constants T_{ijk} ($T_{14} = T_{36}$, T_{16}, and T_{34}) on the propagation directions with the Euler angles {0°, θ, 0°} for a cubic system. Note that here T_{ijk} represent either the piezoelectric constants e_{ijk} ($e_{14} = e_{36}$, e_{16}, and e_{34}) or the piezomagnetic coefficients h_{ijk} ($h_{14} = h_{36}$, h_{16}, and h_{34}).

Using the material constants defined by expressions from (II.1) to (II.6), it is possible to rewrite the equations of motions introduced by expressions from (I.31) to (I.33) in Chapter I. Treating only the SH-wave propagation, they can be reduced to the following simplified forms:

$$\rho \frac{\partial^2 U_2}{\partial t^2} = C_{66} \frac{\partial^2 U_2}{\partial x_1^2} + C_{44} \frac{\partial^2 U_2}{\partial x_3^2} + e_{16} \frac{\partial^2 \varphi}{\partial x_1^2} + e_{34} \frac{\partial^2 \varphi}{\partial x_3^2} + h_{16} \frac{\partial^2 \psi}{\partial x_1^2} + h_{34} \frac{\partial^2 \psi}{\partial x_3^2} \tag{II.7}$$

$$0 = e_{16} \frac{\partial^2 U_2}{\partial x_1^2} + e_{34} \frac{\partial^2 U_2}{\partial x_3^2} - \varepsilon_{11} \frac{\partial^2 \varphi}{\partial x_1^2} - \varepsilon_{33} \frac{\partial^2 \varphi}{\partial x_3^2} - \alpha_{11} \frac{\partial^2 \psi}{\partial x_1^2} - \alpha_{33} \frac{\partial^2 \psi}{\partial x_3^2} \tag{II.8}$$

$$0 = h_{16} \frac{\partial^2 U_2}{\partial x_1^2} + h_{34} \frac{\partial^2 U_2}{\partial x_3^2} - \alpha_{11} \frac{\partial^2 \varphi}{\partial x_1^2} - \alpha_{33} \frac{\partial^2 \varphi}{\partial x_3^2} - \mu_{11} \frac{\partial^2 \psi}{\partial x_1^2} - \mu_{33} \frac{\partial^2 \psi}{\partial x_3^2} \tag{II.9}$$

These equations look like those introduced in the recent book [89] concerning new surface SH-wave propagation in the transversely isotropic piezoelectromagnetics of class 6 *mm*. For a cubic piezoelectromagnetics, the main difference from the 6 *mm* material is in the forms of the piezoelectric constants e_{ijk} and the piezomagnetic coefficients h_{ijk} defined by expressions (II.2) and (II.3), respectively. This difference can drastically change the wave characteristics for some cases discussed below when the mechanical, electrical, and magnetic boundary conditions are applied.

For the simplified case of the equations of motion which corresponds to the SH-wave propagation, the solutions for the homogeneous equations from (II.7) to (II.9) then read:

$$U_{2,4,5} = U_{2,4,5}^{0} \exp\left[jk\left(n_1 x_1 + n_3 x_3 - V_{ph} t\right)\right] \tag{II.10}$$

where the directional cosines $n_1 = 1$ and $n_3 \equiv n_3$ are defined by equality (I.37) from the previous chapter. Indeed, these solutions can be used instead of those defined by equations from (I.34) to (I.36) because the common matrix determinant factors.

The coupled equations of motion written above in the simplified forms can be then written as follows:

$$\begin{pmatrix} GL_{22} - \rho V_{ph}^2 & GL_{24} & GL_{25} \\ GL_{42} & GL_{44} & GL_{45} \\ GL_{52} & GL_{54} & GL_{55} \end{pmatrix} \begin{pmatrix} U^0 \\ \varphi^0 \\ \psi^0 \end{pmatrix} = \begin{pmatrix} 0 \\ 0 \\ 0 \end{pmatrix} \tag{II.11}$$

where the initial amplitudes are $U^0 = U_2^{\,0}$, $\varphi^0 = U_4^{\,0}$, and $\psi^0 = U_5^{\,0}$, using expression (II.10). Also, the phase velocity V_{ph} is defined by expression (I.39) from Chapter I. Therefore, the eigenvector given by expression (I.50) in the previous chapter is then written as follows:

$$\left(U^0, \varphi^0, \psi^0\right) \tag{II.12}$$

The three-component eigenvector in expression (II.12) should be found unequal to zero for each eigenvalue $n_3 = k_3/k$. Suitable eigenvalues n_3 can be obtained when the following matrix determinant of the homogeneous system of equations (II.11) becomes equal to zero:

$$\begin{vmatrix} GL_{22} - \rho V_{ph}^2 & GL_{24} & GL_{25} \\ GL_{42} & GL_{44} & GL_{45} \\ GL_{52} & GL_{54} & GL_{55} \end{vmatrix} = 0 \qquad \text{(II.13)}$$

It is useful to rewrite the characteristic determinant in equation (II.13) in the following simplified form for the case:

$$\begin{vmatrix} Cm - \rho V_{ph}^2 & e(m-2) & h(m-2) \\ e(m-2) & -\varepsilon m & -\alpha m \\ h(m-2) & -\alpha m & -\mu m \end{vmatrix} = 0 \qquad \text{(II.14)}$$

where

$$m = 1 + n_3^2 \qquad \text{(II.15)}$$

A dispersion relation can be then obtained by setting the characteristic determinant in equation (II.14) equal to zero. As the result, one can get the following secular equation:

$$m \times \left[\left(1 + K_{em}^2\right)m^2 - B_t m + 4K_{em}^2\right] = 0 \qquad \text{(II.16)}$$

where

$$B_t = \left(\frac{V_{ph}}{V_{t4}}\right)^2 + 4K_{em}^2 \tag{II.17}$$

In equations (II.16) and (II.17), the velocity V_{t4} corresponds to the speed of the shear-horizontal bulk acoustic wave (SH-BAW) in the case when the SH-BAW is uncoupled with both the electrical potential φ and the magnetic potential ψ:

$$V_{t4} = \sqrt{C/\rho} \tag{II.18}$$

and the coefficient of the magnetoelectromechanical coupling (CMEMC) is defined by the following expression:

$$K_{em}^2 = \frac{\mu e^2 + \varepsilon h^2 - 2\alpha e h}{C\left(\varepsilon\mu - \alpha^2\right)} \tag{II.19}$$

It is clearly seen in definition (II.19) that the CMEMC depends on all the material constants, but the mass density ρ. It is possible to say that the electromagnetic constant α couples the other material constants forming the CMEMC and in the case of $\alpha = 0$ the CMEMC reduces to the following formula:

$$K_{em1}^2 = K_e^2 + K_m^2 \tag{II.20}$$

It is blatant that the reduced CMEMC in expression (II.20) represents a sum of two terms. The first term is the well-known coefficient of the electromechanical coupling (CEMC) for a purely piezoelectric material:

$$K_e^2 = \frac{e^2}{\varepsilon C} \tag{II.21}$$

The second term in expression (II.20) is called the coefficient of the magnetomechanical coupling (CMMC) for a purely piezomagnetic crystal:

$$K_m^2 = \frac{h^2}{\mu C} \tag{II.22}$$

Also, it is thought that it is convenient to write down expression (II.17) in the following form, in order to introduce the very important wave attribute denoted by V_{tem} below:

$$B_t = \left(1 + K_{em}^2\right)\left(\frac{V_{ph}}{V_{tem}}\right)^2 + 4K_{em}^2 \tag{II.23}$$

In expression (II.23), the velocity V_{tem} is the speed of the SH-BAW coupled with both the electrical potential φ and the magnetic potential ψ:

$$V_{tem} = V_{t4}A_K = V_{t4}\left(1 + K_{em}^2\right)^{1/2} \tag{II.24}$$

Let's return to equation (II.16) to continue the analysis in order to get all the polynomial roots in explicit forms. It is clearly seen that equation (II.16) factors. Therefore, equation (II.16) equals to zero when either the first factor or the second one zeros it. The first factor gives the following simple equation $m^{(1)} = 0$ that decisively exhibits two purely imaginary polynomial roots:

$$n_3^{(1)} = -\mathrm{j} \text{ and } n_3^{(2)} = +\mathrm{j} \tag{II.25}$$

because m is defined by expression (II.15). It is worth noting that for the transversely-isotropic piezoelectromagnetics there always occurs the second pair of the same polynomial roots given by expression (II.25), according to the recent results of book [89]. This is not true for cubic piezoelectromagnetics. However, the situation when there are two identical pairs of purely imaginary polynomial roots is possible for cubic piezoelectromagnetics. This will be further discussed.

It is also worth noticing that only such polynomial roots as those with negative sign for imaginary parts are suitable for further considerations. This choice of a negative sign for the root imaginary parts is caused by the necessary condition of damping of surface SH-wave towards the depth of the cubic crystals, namely towards the negative values of the x_3-axis shown in figure II.1. Therefore, the first eigenvector in expression (II.15) provides the following likely eigenvector:

$$\left(U^{0(1)}, \varphi^{0(1)}, \psi^{0(1)}\right) = \pm(0, -h, e) \tag{II.26}$$

because $m = 0$ results in the following:

$$\begin{pmatrix} -\rho V_{ph}^2 & -2e & -2h \\ -2e & 0 & 0 \\ -2h & 0 & 0 \end{pmatrix} \begin{pmatrix} U^0 \\ \varphi^0 \\ \psi^0 \end{pmatrix} = \begin{pmatrix} 0 \\ 0 \\ 0 \end{pmatrix} \tag{II.27}$$

The second factor in equation (II.16) leads to the following solutions of the quadratic equation:

$$m^{(2,3)} = \frac{B_t \pm \sqrt{B_t^2 - 16K_{em}^2(1 + K_{em}^2)}}{2(1 + K_{em}^2)} \tag{II.28}$$

where B is defined by expression (II.17) or (II.23). Consequently, equations (II.15) and (II.28) give the rest four polynomial roots of equation (II.16) in the following explicit forms:

$$n_3^{(3,4,5,6)} = \pm \mathrm{j}\sqrt{1 - m^{(2,3)}} \tag{II.29}$$

It is stated that the forms of the polynomial roots in equations (II.28) and (II.29) are exactly the same to those recently obtained for cubic piezoelectrics [103, 159] and cubic piezomagnetics [14]. Indeed, the found values of the eigenvalues in expression (II.29) must be either imaginary or complex for the phase velocity V_{ph} situated below the SH-BAW velocity V_{tem} defined by expression (II.24), because this work has an interest in the finding of SH-SAW. According to the recent works in Refs. [103, 159], this is not always true because the polynomial roots in equation (II.29) can be real just below the velocity V_{tem}. This unique feature also distinguishes the cubic piezoelectromagnetics from the transversely isotropic piezoelectromagnetics.

First of all, it is possible to find the situation when $m^{(2)} = m^{(3)}$ in expression (II.28). It is obvious that they are expressed as follows:

$$m^{(2)} = m^{(3)} = \frac{B_t}{2(1+K_{em}^2)} \tag{II.30}$$

giving

$$n_3^{(3)} = n_3^{(5)} = -\mathrm{j}\sqrt{1-m^{(2)}} \tag{II.31}$$

$$n_3^{(4)} = n_3^{(6)} = +\mathrm{j}\sqrt{1-m^{(2)}} \tag{II.32}$$

when the following expression under square root in formula (II.28) is equal to zero:

$$B_t^2 - 16K_{em}^2\left(1+K_{em}^2\right) = 0 \tag{II.33}$$

This equality (II.33) fulfills for some phase velocity V_{ph} that can be denoted by V_K. The value of V_K can be obtained from equation (II.33) and is defined as follows:

$$V_K = a_K V_{t4} \tag{II.34}$$

where

$$a_K = 2\sqrt{K_{em}\left(1+K_{em}^2\right)^{1/2} - K_{em}^2} \quad \text{(II.35)}$$

For comparison, the factors A_K and a_K versus the CMEMC K_{em}^2 are shown in figure II.4. It is noted that the two equal eigenvalues in expression (II.31) surely give two equal eigenvectors. All suitable eigenvalues in common forms are given in this chapter below.

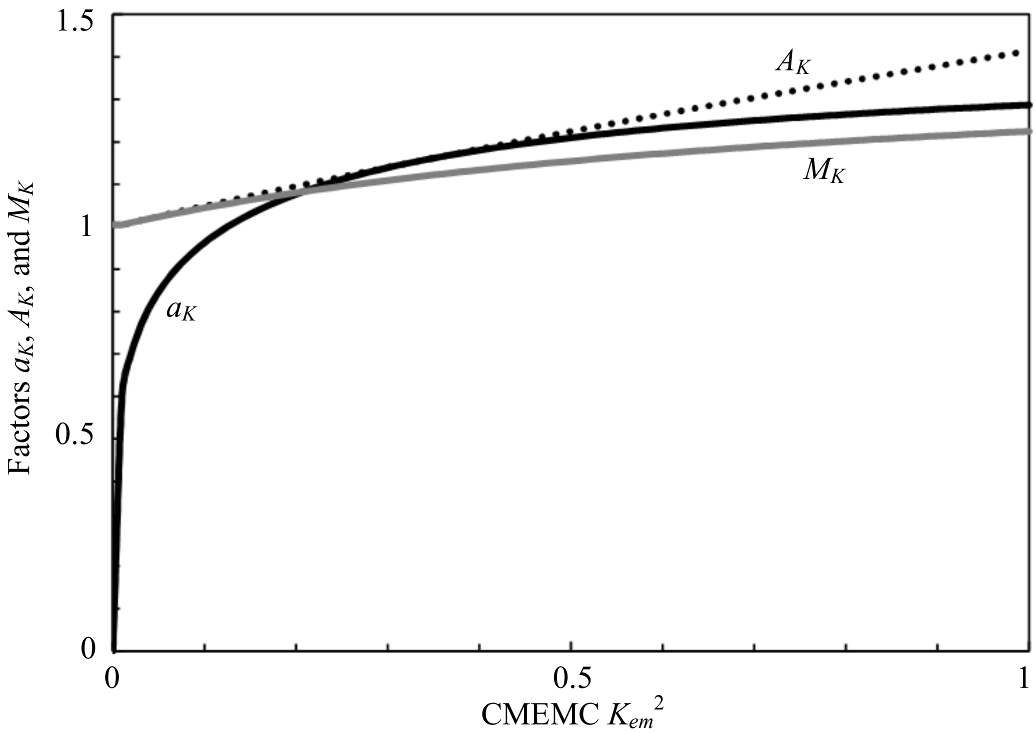

Figure II.4. The dependences of the non-dimensional factors A_K, a_K, and M_K defined by equations (II.24), (II.35), and (II.46), respectively, on the non-dimensional value of the CMEMC K_{em}^2.

Based on the results obtained in the recent works [103, 159], one can carry out some further analytical investigations of the complicated behaviors of the polynomial roots in the common forms given by formulae (II.28) and (II.29). Indeed, one can check that these four eigenvalues in expression (II.29) are complex for the phase velocity $V_{ph} > 0$ situated below the value of V_K for any value of the CMEMC $K_{em}^2 > 0$. Sample calculations of these four eigenvalues for the cubic piezoelectrics $Bi_{12}SiO_{20}$ were executed in Ref. [159]. Therefore, these complex eigenvalues can be written as follows:

$$n_3^{(3)} = \mathrm{Re}(n_3) - \mathrm{j}\,\mathrm{Im}(n_3) \tag{II.36}$$

$$n_3^{(4)} = \mathrm{Re}(n_3) + \mathrm{j}\,\mathrm{Im}(n_3) \tag{II.37}$$

$$n_3^{(5)} = -\mathrm{Re}(n_3) - \mathrm{j}\,\mathrm{Im}(n_3) \tag{II.38}$$

$$n_3^{(6)} = -\mathrm{Re}(n_3) + \mathrm{j}\,\mathrm{Im}(n_3) \tag{II.39}$$

where

$$\mathrm{Re}(n_3) = \sqrt[4]{1 - \left(\frac{V_{ph}}{V_{tem}}\right)^2} \cos\left(\frac{1}{2}\arctan\left(\frac{\sqrt{16K_{em}^2(1+K_{em}^2) - B_t^2}}{B_t - 2(1+K_{em}^2)}\right)\right) \tag{II.40}$$

$$\mathrm{Im}(n_3) = \sqrt[4]{1 - \left(\frac{V_{ph}}{V_{tem}}\right)^2} \mathrm{Abs}\left[\sin\left(\frac{1}{2}\arctan\left(\frac{\sqrt{16K_{em}^2(1+K_{em}^2) - B_t^2}}{B_t - 2(1+K_{em}^2)}\right)\right)\right] \tag{II.41}$$

In formula (II.41), the absolute value for the odd function such as sine was applied because it can change its sign. This was done in order that the eigenvalues in formulae (II.36) and (II.38) remain with a negative sign for the imaginary part. In formulas (II.40) and (II.41), the well-known formulae from the reference-book [185] on mathematics were used for the exponential and trigonometric representations of complex numbers such as

$$Z = z_1 \pm \mathrm{j}z_2 = \zeta\,\exp(\pm\mathrm{j}\vartheta) = \zeta\left(\cos(\vartheta) \pm \mathrm{j}\sin(\vartheta)\right) \tag{II.42}$$

where

$$\zeta = \sqrt{z_1^2 + z_2^2} \text{ and } \vartheta = \arctan(z_2/z_1) \tag{II.43}$$

Further, it is possible to investigate these four eigenvalues in the following range for the phase velocity V_{ph}: $V_K < V_{ph} < V_{tem}$. In this V_{ph}-range they are not complex, namely they can be imaginary or real in dependence on the CMEMC value. However, in this V_{ph}-range one peculiarity such as $V_K = V_{tem}$ occurs. It is possible to calculate the CMEMC value denoted by K_0^2 for the case of $V_K = V_{tem}$, using expressions (II.24) and (II.34) (see also figure II.4):

$$K_{em}^2\left(V_{ph} = V_K = V_{tem}\right) = K_0^2 = 1/3 \tag{II.44}$$

For $K_{em}^2 < 1/3$, one can find that all the eigenvalues given by formula (II.29) are imaginary for $V_K < V_{ph} < V_{tem}$. For $K_{em}^2 < 1/3$, two of these four eigenvalues can become real in the V_{ph}-range.

To completely understand the complicated problem, it is possible to calculate the CMEMC value denoted by K_{t4}^2 for the case of $V_K = V_{t4}$ (see also figure II.4):

$$K_{em}^2\left(V_{ph} = V_K = V_{t4}\right) = K_{t4}^2 = 1/8 \tag{II.45}$$

Also, it is very interesting to treat the case of $V_K = V_{BGM}$ where the velocity V_{BGM} stands for the surface Bleustein-Gulyaev-Melkumyan (BGM) wave [89]. The well-known SH-SAW velocity V_{BGM} can be expressed as follows:

$$V_{BGM} = V_{t4} M_K = V_{t4}\left(1 + K_{em}^2\right)^{1/2}\left[1 - \left(\frac{K_{em}^2}{1 + K_{em}^2}\right)^2\right]^{1/2} \tag{II.46}$$

Therefore, the calculated CMEMC value denoted by K_{BGM}^2 for the case of $V_K = V_{BGM}$ reads:

$$K_{em}^2\left(V_{ph}=V_K=V_{BGM}\right)=K_{BGM}^2=\frac{\sqrt{2}-1}{2}\approx 0.2071067812 \qquad \text{(II.47)}$$

The non-dimensional factor M_K defined by expression (II.46) is shown by the gray line in figure II.4 for comparison with the other non-dimensional factors A_K and a_K.

It is central to state that the existence of the SH-SAWs propagating with the velocity V_{BGM} in cubic piezoelectromagnetics will be demonstrated in Chapter V. However, it is thought that there is a problem of interpretation of the theoretical result given by formula (II.47). It is still uncertain that the surface BGM-wave can propagate in cubic piezoelectromagnetics with $V_K = V_{BGM}$. For this case, if the BGM-wave can propagate, it is possible to conclude that the value of V_K represents a true velocity and the second SH-SAW characterized by the velocity V_K can always exist in a cubic crystal for $0 < K_{em}^2 < K_0^2$, but $K_{em}^2 = K_{BGM}^2$ for $V_K = V_{BGM}$. It is noted that the existence of the solution V_K in a cubic system does not depend on applied electrical and or magnetic boundary conditions. This is a unique natural case for a cubic system. Hence, this conclusion can be also true for the corresponding velocity V_K in cubic piezoelectrics and cubic piezomagnetics.

Indeed, this is an additional problem for experimentalists to verify the SH-SAW existence for the corresponding cases of $V_K = V_{BGpe}$, $V_K = V_{BGpm}$, or $V_K = V_{BGM}$ in cubic piezoelectrics, piezomagnetics, or piezoelectromagnetics. For this problem, suitable cubic crystals must be studied. They must have the corresponding values of the CEMC, CMMC, or CMEMC obtained in this work and given by formula (II.47). One of the suitable cubic piezoelectrics is the Chalcogenide Tl_3VS_4. It belongs to the cubic class $\bar{4}3m$ and has very close value of the CEMC $K_e^2 \sim 0.2089$. This Chalcogenide was also studied in recent paper [186] concerning interfacial wave propagation along the common interface between cubic piezoelectrics. Ref. [186] also graphically shows that the velocity V_K is very close to the interfacial SH-wave solution for Tl_3VS_4. The material constants for Tl_3VS_4 are listed in the following chapter because this piezoelectrics is also used in this work as the piezoelectric phase for some piezoelectromagnetic two-phase materials.

Note that the classical surface Bleustein-Gulyaev (BG) waves in piezoelectrics and piezomagnetics can propagate with the following corresponding velocities:

$$V_{BGEC} = V_{te}\left[1-\left(\frac{K_e^2}{1+K_e^2}\right)^2\right]^{1/2} \tag{II.48}$$

$$V_{BGMO} = V_{tm}\left[1-\left(\frac{K_m^2}{1+K_m^2}\right)^2\right]^{1/2} \tag{II.49}$$

where the velocity V_{BGEC} corresponds to the electrically closed surface (φ = 0) of the piezoelectrics and the velocity V_{BGMO} corresponds to the magnetically open surface (ψ = 0) of the piezomagnetics. In expressions (II.48) and (II.49), the SH-BAW velocity V_{te} coupled with the electrical potential φ in a piezoelectrics and the SH-BAW velocity V_{tm} coupled with the magnetic potential ψ in a piezomagnetics are correspondingly defined as follows:

$$V_{te} = V_{t4}\left(1+K_e^2\right)^{1/2} \tag{II.50}$$

$$V_{tm} = V_{t4}\left(1+K_m^2\right)^{1/2} \tag{II.51}$$

In expressions (II.50) and (II.51), the SH-BAW velocity V_{t4} uncoupled with both the potentials is defined by expression (II.18) and the CEMC K_e^2 and CMMC K_m^2 are given by formulae (II.21) and (II.22), respectively.

It is worth noting that the surface BGM-wave in transversely isotropic piezoelectromagnetics exponentially decays from the crystal surface towards the depth of the crystal. This occurs due to all imaginary eigenvalues. This type of wave decay is also true for cubic piezoelectromagnetics with the CMEMC $K_{em}^2 < K_{BGM}^2$ (all imaginary eigenvalues). However, it is clear that sine-like oscillations can be added to the exponential decay for cubic piezoelectromagnetics with the CMEMC

$K_{em}^2 > K_{BGM}^2$, because there are two complex eigenvalues. This is also true for the classical surface BG-wave in cubic piezoelectrics or cubic piezomagnetics.

Also, it is expected that the SH-waves propagating with the velocity V_{BGM} can exist when they are guided by the interface between two transversely isotropic piezoelectromagnetics or two cubic piezoelectromagnetics. This assumption can be true because the interfacial SH-waves propagating with the velocity V_{BGEC} between two transversely isotropic piezoelectrics were discovered by Maerfeld and Tournois [187] in 1971. Also, they in Ref. [187] have discovered the new interfacial wave called the interfacial Maerfeld-Tournois (MT) wave. It is noted that both the classical surface BG-wave and interfacial electro-acoustic MT-wave [187] may be caused by interfacial crack propagation between two dissimilar piezoelectrics. However, the interfacial MT-waves cannot exist in cubic piezoelectrics (hence, in cubic piezomagnetics).

Ref. [186] has coped with a study of interfacial SH-wave propagation in cubic piezoelectrics and also discovered a new interfacial SH-wave guided by the interface between two dissimilar cubic piezoelectrics $Bi_{12}SiO_{20}$ and $Bi_{12}GeO_{20}$. It was also found in Ref. [186] that in such two-layer cubic systems, the interfacial SH-waves propagating with the velocity V_{BGEC} can also exist. Ref. [103] has discovered the ultrasonic surface Zakharenko wave (USZW), a new SH-SAW guided by the free surface of a cubic piezoelectrics and also found that the surface SH-waves propagating with the velocity V_{BGEC} can also exist on the metalized surface. Also, Ref. [14] has demonstrated the existence of the USZW and the surface SH-waves propagating with the velocity V_{BGMO} in cubic piezomagnetics. This means that the BG-wave velocity V_{BGEC} or V_{BGMO} can be found when different acoustic systems are treated. This fact demonstrates some similarity among different problems of SH-wave propagation.

Finally, it is necessary to write down some useful relations for $m^{(2,3)}$ defined by expression (II.28) and $n_3^{(3,5)}$ defined by expression (II.29). They are as follows:

$$m^{(2)}m^{(3)} = \frac{4K_{em}^2}{1+K_{em}^2} \tag{II.52}$$

$$m^{(2)} + m^{(3)} = \frac{B_t}{1+K_{em}^2} \tag{II.53}$$

$$m^{(2)} - m^{(3)} = \frac{\sqrt{B_t^2 - 16K_{em}^2(1+K_{em}^2)}}{1+K_{em}^2} = \sqrt{\left(m^{(2)} + m^{(3)}\right)^2 - \frac{1+K_{em}^2}{K_{em}^2}\left(m^{(2)}m^{(3)}\right)^2} \tag{II.54}$$

$$n_3^{(3)}n_3^{(5)} = -\sqrt{\left(1-m^{(2)}\right)\left(1-m^{(3)}\right)} = -\sqrt{1+m^{(2)}m^{(3)} - \left(m^{(2)}+m^{(3)}\right)} = -\sqrt{1-\left(\frac{V_{ph}}{V_{tem}}\right)^2} \tag{II.55}$$

$$\left(n_3^{(3)}\right)^2 + \left(n_3^{(5)}\right)^2 = m^{(2)} + m^{(3)} - 2 \tag{II.56}$$

$$\left(n_3^{(3)}\right)^2 - \left(n_3^{(5)}\right)^2 = m^{(2)} - m^{(3)} \tag{II.57}$$

It is possible to resolve the main problem for this chapter, namely the finding of the suitable eigenvectors in explicit forms. For this purpose, the first equation of the system of three homogeneous equations (II.11) reveals the following dependence of the eigenvector component U^0 on the other components φ^0 and ψ^0, using equation (II.14):

$$U^0 = -\varphi^0\frac{e(m-2)}{C\left(m-\gamma_K^2\right)} - \psi^0\frac{h(m-2)}{C\left(m-\gamma_K^2\right)} \tag{II.58}$$

where γ_K can be determined using the boundary conditions and can be defined as follows:

$$V_{ph}(\mathrm{SAW}) = \gamma_K V_{t4} = V_{tem}\frac{\gamma_K}{\sqrt{1+K_{em}^2}} \tag{II.59}$$

In formula (II.59), relation (II.24) between the SH-BAW velocities V_{t4} and V_{tem} is taken into account. Note that $\gamma_K = a_K$ for the case of two equal eigenvalues given by formulae (II.30) and (II.31).

Indeed, it is possible to exclude the eigenvector component U^0 from the system of three homogeneous equations (II.11), for which the matrix determinant is given by equation (II.14) in the explicit form. Thus, the resulting system of two homogeneous equations can be then written as follows:

$$\begin{pmatrix} C\varepsilon m\left(m-\gamma_K^2\right)+e^2(m-2)^2 & C\alpha m\left(m-\gamma_K^2\right)+eh(m-2)^2 \\ C\alpha m\left(m-\gamma_K^2\right)+eh(m-2)^2 & C\mu m\left(m-\gamma_K^2\right)+h^2(m-2)^2 \end{pmatrix}\begin{pmatrix} \varphi^0 \\ \psi^0 \end{pmatrix}=\begin{pmatrix} 0 \\ 0 \end{pmatrix} \tag{II.60}$$

Using expression (II.58) and the first equation of two equations (II.60), it is possible to demonstrate the first set of the eigenvectors which also contains the previously found eigenvector given by expression (II.26):

$$\begin{pmatrix} U^{0(3)} \\ \varphi^{0(3)} \\ \psi^{0(3)} \end{pmatrix}=\pm\begin{pmatrix} m^{(2)}\left(m^{(2)}-2\right)(e\alpha-h\varepsilon) \\ -C\alpha m^{(2)}\left(m^{(2)}-\gamma_K^2\right)-eh\left(m^{(2)}-2\right)^2 \\ C\varepsilon m^{(2)}\left(m^{(2)}-\gamma_K^2\right)+e^2\left(m^{(2)}-2\right)^2 \end{pmatrix} \tag{II.61}$$

$$\begin{pmatrix} U^{0(5)} \\ \varphi^{0(5)} \\ \psi^{0(5)} \end{pmatrix}=\pm\begin{pmatrix} m^{(3)}\left(m^{(3)}-2\right)(e\alpha-h\varepsilon) \\ -C\alpha m^{(3)}\left(m^{(3)}-\gamma_K^2\right)-eh\left(m^{(3)}-2\right)^2 \\ C\varepsilon m^{(3)}\left(m^{(3)}-\gamma_K^2\right)+e^2\left(m^{(3)}-2\right)^2 \end{pmatrix} \tag{II.62}$$

So, the first set of the eigenvectors is defined by expressions (II.26), (II.61), and (II.62) for the eigenvalues defined by corresponding expressions (II.25) and (II.29).

Exploiting expression (II.58) and the second equation of two equations (II.60), it is possible to express the second set of the eigenvectors which also contains the common eigenvector (II.26):

$$\begin{pmatrix} U^{0(3)} \\ \varphi^{0(3)} \\ \psi^{0(3)} \end{pmatrix}=\pm\begin{pmatrix} m^{(2)}\left(m^{(2)}-2\right)(e\mu-h\alpha) \\ -C\mu m^{(2)}\left(m^{(2)}-\gamma_K^2\right)-h^2\left(m^{(2)}-2\right)^2 \\ C\alpha m^{(2)}\left(m^{(2)}-\gamma_K^2\right)+eh\left(m^{(2)}-2\right)^2 \end{pmatrix} \tag{II.63}$$

$$\begin{pmatrix} U^{0(5)} \\ \varphi^{0(5)} \\ \psi^{0(5)} \end{pmatrix}=\pm\begin{pmatrix} m^{(3)}\left(m^{(3)}-2\right)(e\mu-h\alpha) \\ -C\mu m^{(3)}\left(m^{(3)}-\gamma_K^2\right)-h^2\left(m^{(3)}-2\right)^2 \\ C\alpha m^{(3)}\left(m^{(3)}-\gamma_K^2\right)+eh\left(m^{(3)}-2\right)^2 \end{pmatrix} \tag{II.64}$$

Accordingly, the second set of the eigenvectors is defined by expressions (II.26), (II.63), and (II.64) for the same eigenvalues (II.25) and (II.29).

It is blatant that it is more convenient to use $m^{(2,3)}$ instead of $n_3^{(3,5)}$ for further mathematical analysis to simplify the complicated problem of finding of SH-SAWs in cubic piezoelectromagnetics. This is true because the explicit forms of these two eigenvectors given by expression (II.26) and corresponding expressions from (II.61) to (II.64) are significantly more problematic than the corresponding simple forms for the transversely isotropic piezoelectromagnetics [89]. Notice that for the transversely isotropic piezoelectromagnetics [89], the first set of the eigenvector components combines ε and α, but the second set links μ and α.

It is also noted that for the case of two equal eigenvalues in expression (II.31), one can get the following two equal eigenvectors:

$$\left(U^{0(3)}, \varphi^{0(3)}, \psi^{0(3)}\right) = \left(U^{0(5)}, \varphi^{0(5)}, \psi^{0(5)}\right) \tag{II.65}$$

These equal eigenvalues and eigenvectors should give the additional solution for the phase velocity V_{ph} such as $V_{ph} = V_K$. This solution is always present and does not depend on the different electrical and magnetic boundary conditions treated in Chapters from V to XIII. The following chapter introduces the piezoelectromagnetic two-phase materials which can be engineered using cubic piezoelectrics and cubic piezomagnetics.

CHAPTER III. Piezoelectrics, Piezomagnetics, and Piezoelectromagnetic Composite Materials

This chapter acquaints the reader with some piezoelectric and piezomagnetic materials which can be used for creation of piezoelectromagnetic composite materials. It is obvious that it is necessary to treat materials with the strong piezoelectric effect as suitable candidates for coupling with piezomagnetic phase materials. Therefore, table III.1 lists the piezoelectric materials. The cubic crystals $Bi_{12}SiO_{20}$ and $Bi_{12}GeO_{20}$ of class 23 are well-known and commercially available. The other cubic structure materials such as ternary thallium Chalcogenides Tl_3VS_4 and Tl_3TaSe_4 of class $\bar{4}3m$ are also listed in the table because they are stronger piezoelectrics. However, they are commercial availability is significantly smaller than that of the other piezoelectrics listed in the table, probably due to their mechanical softness and fabrication difficulties. Also, it is well-known that many transversely-isotropic piezoelectric materials such as different Lead Zirconate Titanates (PZTs) can possess very strong piezoelectric effect compared with cubic piezoelectrics. One hexagonal piezoelectric material of Lead Zirconate Titanates called PZT-5H is also given in table III.1. It is seen in the table that this PZT-5H has doubled coefficient of the electromechanical coupling (CEMC K_e^2) compared with the strongest cubic piezoelectrics Tl_3TaSe_4.

The second group of materials is introduced in table III.2. They are piezomagnetics. It is stated that these materials represent ferrites of cubic class $m3m$. The literature about the properties of the piezoelectrics listed in table III.1 and piezomagnetics listed in table III.2 is given in the introduction of this book. According to the table, these cubic piezomagnetics possess large coefficients of the magnetomechanical coupling (CMMC K_m^2). However, this is not obligatory and the well-known ferrite called Alfenol has the CMMC K_m^2 only by about 0.08. This value is very small compared with the other ferrites from the table and even an order smaller than that for Metglas. Indeed, the Metglas CMMC $K_m^2 \sim 0.80$ is very larger and even significantly larger than those of Terfenol-D and Galfenol. Note that the structure of Terfenol-D can be both the cubic and the transversely-isotropic. It is thought that it is natural to treat the cubic structure Terfenol-D together with the other cubic piezomagnetics listed in table III.2.

Table III.1. The strongly piezoelectric cubic crystals including the Chalcogenides Tl_3VS_4 and Tl_3TaSe_4, and the transversely-isotropic material PZT.

Crystal	Class	ρ, kg/m^3	C, 10^{10} N/m^2	e, C/m^2	ε, 10^{-10} F/m	K_e^2
			Cubic system			
Tl_3VS_4	$\bar{4}3m$	6140	0.470	0.550	3.0812	0.2089
Tl_3TaSe_4	$\bar{4}3m$	7280	0.410	0.320	0.8943	0.2793
$Bi_{12}SiO_{20}$	23	9070	2.451	1.122	3.6390	0.1412
$Bi_{12}GeO_{20}$	23	9200	2.562	0.983	3.3380	0.1131
			Hexagonal system			
PZT-5H	6 *mm*	7750	2.300	17.00	150.40	0.5458

Table III.2. The piezomagnetic ferrites such as cubic Terfenol-D, Galfenol, Alfenol, and Metglas. It is noted that T stands for Tesla units and [T] = [N/(A×m)].

Name	Class	ρ, kg/m^3	C, 10^{10} N/m^2	h, T	μ, 10^{-6} N/A^2	K_m^2
Terfenol-D	*m*3*m*	7800	0.6100	97.1190	2.74889	0.562498
Galfenol	*m*3*m*	7973	12.700	3331.34	206.830	0.422494
Alfenol	*m*3*m*	7848	12.300	824.627	66.85795	0.082691
Metglas	*m*3*m*	7180	10.447	28367.248	9550.00	0.806565

As a result, it is possible to have attempts to experimentally obtain some piezoelectromagnetic composite materials consisting of the piezoelectrics and piezomagnetics listed in corresponding tables III.1 and III.2. This work has an interest in study of cubic piezoelectromagnetics. Therefore, the material constants for several cubic piezoelectromagnetics (PEMs) are listed in table III.3. This is the first attempt to theoretically predict some wave properties of the piezoelectromagnetic composites listed in the table. Indeed, the material constants of the formed piezoelectromagnetics must have the average material properties borrowed from the corresponding piezoelectric and piezomagnetic phases. However, the very important parameter such as the electromagnetic constants α can be experimentally determined for each piezoelectromagnetic composite. To theoretically predict possible values of this material constant, it is possible to treat several values of the constant α in order to find out an influence of the value of the parameter α on some wave properties of the piezoelectromagnetics. Therefore, three different values of the parameter α were introduced in the table for each piezoelectromagnetics.

Table III.3. The piezoelectromagnetic composite materials consisting of the piezoelectrics and piezomagnetics listed in tables III.1 and III.2, respectively. For the piezoelectromagnetic composite materials, the values of the corresponding electromagnetic constants α are as follows: $\alpha^2 = 0.01\varepsilon\mu$, $0.0001\varepsilon\mu$, and $0.000001\varepsilon\mu \times 10^{-16}$ [s^2/m^2] for $(K_{em}^2)_1$, $(K_{em}^2)_2$, and $(K_{em}^2)_3$, respectively.

PEM	ρ, kg/m^3	C, 10^{10} N/m^2	e, C/m^2	h, T	ε, 10^{-10} F/m
Metglas–PZT-5H	7465.0	6.3735	8.500	14183.624	75.2000
Tl_3TaSe_4–Terfenol-D	7540.0	0.5100	0.160	48.55950	0.44715
Galfenol–Tl_3VS_4	7056.5	6.5850	0.275	1665.670	1.54060
Galfenol–Tl_3TaSe_4	7626.5	6.5550	0.160	1665.670	0.44715
Alfenol–Tl_3VS_4	6994.0	6.3850	0.275	412.3135	1.54060

PEM	μ, 10^{-6} N/A^2	$\varepsilon\mu$, 10^{-16}	$(K_{em}^2)_1$	$(K_{em}^2)_2$	$(K_{em}^2)_3$
Metglas–PZT-5H	4775.00	359080.0	0.756205726	0.805544722	0.811147029
Tl_3TaSe_4–Terfenol-D	1.374445	0.614583	0.413927670	0.444811780	0.448265638
Galfenol–Tl_3VS_4	103.415	159.3211	0.407928334	0.413810203	0.414761214
Galfenol–Tl_3TaSe_4	103.415	46.24202	0.410159006	0.416861038	0.417895963
Alfenol–Tl_3VS_4	33.428975	51.50068	0.083218461	0.086849117	0.087285935

It is clearly seen in table III.3 that these different values of the α do not significantly change the very important parameter K_{em}^2 called the coefficient of the magnetoelectromechanical coupling (CMEMC). The first value of α is one order larger than the second and the second value is one order larger than the third. As a result, the first value of K_{em}^2 denoted by $(K_{em}^2)_1$ is larger than the second and the second value denoted by $(K_{em}^2)_2$ is slightly larger than the third, $(K_{em}^2)_3$. It is noted that the wave properties of the transversely isotropic piezoelectromagnetics studied in book [89] depend on both the parameters K_{em}^2 and α. Therefore, it is expected that this can be true for any cubic piezoelectromagnetics. Also, it is necessary to state that only the composite material Alfenol–Tl_3VS_4 has the CMEMC values of $K_{em}^2 < 1/3$ and the rest cubic composites have the values of $K_{em}^2 > 1/3$. The highest value of K_{em}^2 was calculated for Metglas–PZT-5H, $K_{em}^2 \sim 0.81$. This value is already very large, but significantly less than unity.

Also, it is necessary to briefly discuss the cubic piezoelectromagnetic composites listed in table III.3. The first composite consists of cubic piezomagnetics Metglas and the transversely isotropic piezoelectrics PZT-5H. However, it is expected that the resulting piezoelectromagnetic composite must relate to the cubic structure of class 23. The transversely isotropic Lead Zirconate Titanate $Pb(Zr,Ti)O_3$ such as PZT-5H was used because its properties are well-known. Lead-based ceramics have excellent dielectric and piezoelectric properties and are currently the dominant material system for sensors, actuators, and resonators. However, there is the problem of toxicity of lead-based composite materials [188]. Indeed, the recent paper [188] by Bichurin *et al.* discussed this problem and conducted experimental results with Pb-free piezoelectric compositions. They presented results on the magnetoelectric performance of Ni-NKN, Ni-NBTBT and NZFO-NKN, NZFO-NBTBT systems, where NKN = $(Na,K)NbO_3$, NBTBT = $Na_{0.5}Bi_{0.5}TiO_3$-$BaTiO_3$, and NZFO = $Ni_{1-x}Zn_xFe_2O_4$ and discussed their importance as an environmentally friendly alternative. Possible alternatives can be the following solid solutions: NKN-$LiNbO_3$ [189], NKN-$LiTaO_3$ [190], NKN-$LiSbO_3$ [191], NKN-$Li(Nb,Ta,Sb)O_3$ [192], NKN-$BaTiO_3$ [193], NKN-$SrTiO_3$ [194, 195], and NKN-$CaTiO_3$ [196]. They have received considerable attention mainly for two reasons: piezoelectric properties exist over a wide range of temperature, and several possibilities can be used for substitutions and additions. Ref. [188] also described the magnetostrictive phase by the way when it has a cubic symmetry. It was also mentioned in Ref. [188] that an interesting possibility for one can be the problem of finding of lead-free ceramics with a high piezoelectric performance in order to combine it with magnetostrictive material with high piezomagnetic coefficient. To obtain environment-friendly magnetoelectric composite materials with desired sensitivity is a problem for the last two decades.

According to Ref. [8], piezoelectromagnetic composite materials still need some important issues addressed when fabricating the sintered or in situ magnetoelectric particulate composites to obtain superior magnetoelectric response.

- no chemical reaction should occur between the magnetostrictive and piezoelectric materials during the sintering process. The chemical reaction may cause decrease in the magnetostrictive or piezoelectric properties of either phase;
- the resistivity of the magnetostrictive phase should be as large as possible. If the resistivity of the magnetostrictive phase is low, the leakage current causes significant difficulties for the electric poling process and reduces the magnetoelectric properties of the composites. The ferrite particles can form connected chains, and the electric resistivity of the composites is significantly reduced due to the lower resistivity of the ferrite. Therefore, good dispersion of the ferrite particles in the matrix is required. This can allow one to sustain sufficient electric resistivity of the composite;
- for good mechanical coupling, pores as mechanical defects at the interface between the two phases should not exist in the composite.

There are many problems of fundamental importance in a theoretical study of piezoelectric-piezomagnetic composite materials. The obtained solutions can be complex functions of the shape of inclusions, phase properties, and volume fraction of the inclusions of one phase into the second for two-phase composites. For example, the theoretical work [197] treated a number of problems which cover a range from the derivation of the analytical expressions for the magneto-electro-elastic Eshelby tensors to the analysis of the magnetoelectric coupling effect which is a new property exhibited in the piezoelectric-piezomagnetic composite. However, only the transversely isotropic cases for the matrix and inclusions with different magneto-electro-elastic moduli were used for simplicity. The possible shapes of inclusions are of elliptic cylinder, circular cylinder, disk, and ribbon. Also, closed-form solutions for the magnetoelectric coupling coefficients are compactly presented. The obtained results of the theoretical investigations in Ref. [197] can be helpful in understanding the magnetoelectroelastic behaviour of the composite material with inclusions.

The magnetoelectroelastic inclusions and inhomogeneity problems are also discussed in Ref. [198]. This work also developed a numerical algorithm to evaluate the magnetoelectroelastic Eshelby tensors for the general material symmetry and ellipsoidal inclusion shape. Li [198] has theoretically studied the average magnetoelectroelastic field in a multi-inclusion or inhomogeneity embedded in an infinite matrix. Li has shown that the average field in an annulus surrounding an inclusion embedded in an infinite magnetoelectroelastic medium only depends on the shapes and orientations of two ellipsoids, which generalizes observation in elasticity by Tanaka and Mori. The average field in a multi-inclusion can be determined exactly. Using the equivalent-inclusion concept, the average field in a multi-inhomogeneity can be also obtained. The obtained solutions of multi-inclusion and inhomogeneity problems can serve as basis for an averaging scheme to model the effective magnetoelectroelastic moduli of heterogeneous materials. This generalizes Nemat-Nasser and Hori's multi-inclusion model in elasticity. It is noted that Li [197] proposed model which recovers Mori-Tanaka and self-consistent approaches as special cases. Finally, he provided some numerical results to demonstrate the applicability of the model and discussed the potential techniques to enhance the magnetoelectric effect in practical composites are also discussed.

The purpose of this book is not to treat all possible influences of different inclusions of one phase into the matrix of the second phase. It is possible that this influence can be significant or not. It is expected that the value of the electromagnetic constant α can be sensitive to the problems. However, the significant sensitivity of the CMEMC K_{em}^2 on the dramatic change in the constant α (see table III.3) is questionable. Therefore, it is expected that any dramatic change in the constant α can slightly change the propagation velocity of the shear-horizontal bulk acoustic wave (SH-BAW) in a bulk piezoelectromagnetics. As the result, any found SH-SAW velocity will follow the SH-BAW velocity because it should be situated slightly below the SH-BAW velocity. Also, the second set of the theoretical problem is to use different boundary conditions. Therefore, the next chapter describes the electrical, magnetic, and mechanical boundary conditions which can strongly influence on the propagation characteristics of the surface acoustic waves.

The previous chapter provided material constants for piezoelectromagnetic solids. However, figure II.1 from Chapter II showed the configuration when there is a contact of the corresponding surface of a cubic piezoelectromagnetics with a vacuum. Therefore, it is also necessary to introduce the vacuum material constants and the corresponding expressions. For a vacuum (free space), the elastic constant C_0 is as follows: C_0 = 0.001 Pa [199]. This value of C_0 is thirteen orders smaller than that for a condensed matter (solid). Thus, it is too negligible to account this value in calculations. Also, the vacuum dielectric permittivity constant has the following value: $\varepsilon_0 = 10^{-7}/(4\pi C_L^2) = 8.854187817\times10^{-12}$ [F/m] where $C_L = 2.99782458\times10^{8}$ [m/s] is the speed of light in a vacuum. Also, the Laplace equation of type $\Delta\varphi_f = 0$ can be written as follows:

$$\left(k_1^2 + k_3^2\right)\varphi_{f0} = 0 \tag{IV.1}$$

The electrical potential φ_{f0} can be expressed in the following form:

$$\varphi_{f0} = F^{(E0)} \exp\left(-k_1 x_3\right)\exp\left[\mathrm{j}\left(k_1 x_1 - \omega t\right)\right] \tag{IV.2}$$

Also, the vacuum magnetic permeability constant μ_0 must be used, $\mu_0 = 4\pi\times10^{-7}$ [H/m] = $12.5663706144\times10^{-7}$ [H/m]. The Laplace equation of type $\Delta\psi_f = 0$ is written in the following form:

$$\left(k_1^2 + k_3^2\right)\psi_{f0} = 0 \tag{IV.3}$$

The magnetic potential in a vacuum reads:

$$\psi_{f0} = F^{(M0)} \exp(-k_1 x_3)\exp[\mathrm{j}(k_1 x_1 - \omega t)] \tag{IV.4}$$

According to the configuration shown in figure II.1, the electrical and magnetic potentials in expressions (IV.2) and (IV.4) must exponentially decrease for $k_1 > 0$ with increase in the coordinate $x_3 > 0$.

In equations (IV.2) and (IV.4), the weight factors $F^{(E0)}$ and $F^{(M0)}$ serve for determination of the electrical and magnetic potentials. These potentials can be also determined in a solid. For this purpose, complete mechanical, electrical, and magnetic characteristics are utilized. For a solid piezoelectromagnetics, the complete mechanical displacement U^{Σ}, complete electrical potential φ^{Σ}, and complete magnetic potential ψ^{Σ} can be written in the plane wave forms as follows:

$$U^{\Sigma} = \sum_{p=1,3,5} F^{(p)} U^{0(p)} \exp\left[\mathrm{j}k\left(n_1 x_1 + n_3^{(p)} x_3 - V_{ph} t\right)\right] \tag{IV.5}$$

$$\varphi^{\Sigma} = \sum_{p=1,3,5} F^{(p)} \varphi^{0(p)} \exp\left[\mathrm{j}k\left(n_1 x_1 + n_3^{(p)} x_3 - V_{ph} t\right)\right] \tag{IV.6}$$

$$\psi^{\Sigma} = \sum_{p=1,3,5} F^{(p)} \psi^{0(p)} \exp\left[\mathrm{j}k\left(n_1 x_1 + n_3^{(p)} x_3 - V_{ph} t\right)\right] \tag{IV.7}$$

These weight factors $F^{(1)}$, $F^{(3)}$, and $F^{(5)}$ in expressions from (IV.5) to (IV.7) can be determined from equations in which suitable boundary conditions are accounted. These forms of the complete characteristics in expressions from (IV.5) to (IV.7) can be used in the boundary conditions described below.

For a studied cubic piezoelectromagnetics, the mechanically free surface is used as one of the possible mechanical boundary conditions at the interface $x_3 = 0$ shown in figure II.1. Also, the electrical and magnetic boundary conditions at the interface $x_3 = 0$ between a vacuum and the piezoelectromagnetic half-space must be satisfied. In 1992, the realization of the mechanical, electrical, and magnetic boundary conditions is described by V.I. Al'shits, A.N. Darinskii, and J. Lothe in Ref. [106]. It is well-known that the electrical boundary conditions must satisfy the cases of the electrically closed surface (the electrical potential $\varphi = 0$) and electrically open surface (the electrical displacement component $D_3 = 0$). For example, the electrically closed surface can be realized by surface metallization. Also, the well-known magnetic boundary conditions of the magnetically closed surface (the magnetic flux component $B_3 = 0$) and magnetically open surface (the magnetic potential $\psi = 0$) can occur. According to Ref. [106], the case of $\psi = 0$ can be realized when a crystal surface contacts with a ferromagnetic covering characterized by a relative magnetic susceptibility $\mu_r >> 1$.

Concerning the mechanically free surface, the mechanical boundary condition for the normal component of the stress tensor $\sigma_{32}(x_3 = 0) = 0$ at the interface $x_3 = 0$ between the crystal surface and a vacuum can be written as follows:

$$\begin{aligned}\sigma_{32} = {} & F_1 k_3^{(1)}\left[CU^{0(1)} + e\varphi^{0(1)} + h\psi^{0(1)}\right] \\ & + F_2 k_3^{(3)}\left[CU^{0(3)} + e\varphi^{0(3)} + h\psi^{0(3)}\right] + F_3 k_3^{(5)}\left[CU^{0(5)} + e\varphi^{0(5)} + h\psi^{0(5)}\right]\end{aligned} \quad \text{(IV.8)}$$

where $F_1 = F^{(1)}$, $F_2 = F^{(3)}$, and $F_3 = F^{(5)}$.

The electrical boundary conditions at the interface $x_3 = 0$ can be described as follows:

- Continuity of the electrical displacement normal component D_3 at the interface $x_3 = 0$, namely

$$D_3 = D_3^f \quad \text{(IV.9)}$$

where

$$\begin{aligned}D_3 = {} & F_1 k_3^{(1)}\left[eU^{0(1)} - \varepsilon\varphi^{0(1)} - \alpha\psi^{0(1)}\right] \\ & + F_2 k_3^{(3)}\left[eU^{0(3)} - \varepsilon\varphi^{0(3)} - \alpha\psi^{0(3)}\right] + F_3 k_3^{(5)}\left[eU^{0(5)} - \varepsilon\varphi^{0(5)} - \alpha\psi^{0(5)}\right]\end{aligned} \quad \text{(IV.10)}$$

and the vacuum characteristics D_3^f can be defined by

$$D_3^f = -F_E \varphi_0^f \mathrm{j} k_1 \varepsilon_0 \quad \text{(IV.11)}$$

- Continuity of the electrical potential φ at the interface:

$$\varphi = \varphi^f \tag{IV.12}$$

where

$$\varphi = F_1\varphi^{0(1)} + F_2\varphi^{0(3)} + F_3\varphi^{0(5)} \tag{IV.13}$$

In condition (IV.12), the electrical potential φ^f in a vacuum is

$$\varphi^f = F_E\varphi_0^f \tag{IV.14}$$

Also, the magnetic boundary conditions can be expressed as follows:

- Continuity of the magnetic flux normal component B_3 at $x_3 = 0$, namely

$$B_3 = B_3^f \tag{IV.15}$$

where

$$\begin{aligned} B_3 = {} & F_1k_3^{(1)}\left[hU^{0(1)} - \alpha\varphi^{0(1)} - \mu\psi^{0(1)}\right] \\ & + F_2k_3^{(3)}\left[hU^{0(3)} - \alpha\varphi^{0(3)} - \mu\psi^{0(3)}\right] + F_3k_3^{(5)}\left[hU^{0(5)} - \alpha\varphi^{0(5)} - \mu\psi^{0(5)}\right] \end{aligned} \tag{IV.16}$$

In expression (IV.15), the value of B_3^f for a vacuum is expressed as follows:

$$B_3^f = -F_M\psi_0^f \,\mathrm{j}k_1\mu_0 \tag{IV.17}$$

- Continuity of the magnetic potential ψ at $x_3 = 0$:

$$\psi = \psi^f \tag{IV.18}$$

where

$$\psi = F_1\psi^{0(1)} + F_2\psi^{0(3)} + F_3\psi^{0(5)} \tag{IV.19}$$

The magnetic potential ψ^f in a vacuum used in equation (IV.18) is defined by

$$\psi^{f} = F_M \psi_0^{f} \tag{IV.20}$$

This brief review of the different boundary conditions introduced in this chapter can allow the reader to grasp the following chapters. The following chapters study the influence of different electrical and magnetic boundary conditions applied at the interface between the cubic piezoelectromagnetics and a vacuum. It is thought that the case of the electrically closed surface (the electrical potential $\varphi = 0$) and the magnetically open surface (the magnetic potential $\psi = 0$) is a common realization of the boundary conditions to commence the analysis. This is the case of study for Chapter V.

CHAPTER V. The Case of $\sigma_{32} = 0$, $\varphi = 0$, and $\psi = 0$ at $x_3 = 0$

The main purpose of this chapter is a demonstration of some similarity between problems of SH-SAW propagation in the transversely isotropic piezoelectromagnetics studied in the book cited in Ref. [89] and cubic ones studied in this work. Certainly, it is thought that the surface Bleustein-Gulyaev-Melkumyan (BGM) wave [88, 89] can propagate in piezoelectromagnetics revealing the cubic symmetry. Note that the theoretical publication [88] in which the surface BGM-wave propagation was first demonstrated relates to the beginning of this millennium. However, the classical surface Bleustein-Gulyaev (BG) wave propagation [90, 91] in transversely isotropic piezoelectrics was theoretically demonstrated significantly earlier, namely about forty years ago. This quite large difference in time between these two very important events is caused by serious difficulties in theoretical analysis when a piezoelectromagnetic system is treated. Indeed, more parameters must be accounted for transversely isotropic piezoelectromagnetics compared with piezoelectrics or piezomagnetics of the same symmetry system.

To analytically treat a cubic piezoelectromagnetics concerning the existence of SH-SAW propagation is very complicated theoretical problem. This is true because the theoretical description of SH-SAW propagation is problematic even in the case of significantly more simple system such as a cubic piezoelectrics (hence, cubic piezomagnetics). Therefore, one can find that transversely isotropic materials are researched more widely compared with cubic ones. Consequently, experimentalists prefer to deal with transversely isotropic materials (piezoelectrics, piezomagnetics, and piezoelectromagnetics). Moreover, it is thought that this work dealing with cubic piezoelectromagnetics is the first one. Therefore, it also has the purpose to pave the way for theoreticians and experimentalists in the direction of investigations of SH-SAW propagation in cubic piezoelectromagnetics.

In 2007, Arman Melkumyan [88] has theoretically treated a problem of SH-wave propagation guided by the interface between the transversely isotropic piezoelectromagnetic solid of class 6 *mm* and a vacuum. Ref. [89] has graphically shown the propagation direction perpendicular to the sixfold symmetry axis. In Refs. [88, 89], it was used the mechanical boundary condition such as the normal component of the stress tensor at the interface must vanish, namely $\sigma_{32}(x_3 = 0) = 0$. Besides the mechanical boundary condition, different electrical and magnetic boundary conditions were applied at the interface $x_3 = 0$. He has found that the SH-SAW called the surface BGM-wave can propagate along the electrically closed surface (electrical boundary condition of $\varphi = 0$) when the surface is also magnetically open (magnetic boundary condition of $\psi = 0$).

The interface $x_3 = 0$ for the case of cubic piezoelectromagnetics is shown in figure II.1 of Chapter II. It is a key point to mention here that in this work, the SH-waves propagate in direction [101]. In this work, utilization of the same mechanical, electrical, and magnetic boundary conditions (namely, $\sigma_{32} = 0$, $\varphi = 0$, and $\psi = 0$) at the surface $x_3 = 0$ of a cubic piezoelectromagnetics leads to the following system of three homogeneous equations also used in Ref. [89]:

$$\begin{pmatrix} k_3^{(1)}\left[CU^{0(1)} + e\varphi^{0(1)} + h\psi^{0(1)}\right] & k_3^{(3)}\left[CU^{0(3)} + e\varphi^{0(3)} + h\psi^{0(3)}\right] & k_3^{(5)}\left[CU^{0(5)} + e\varphi^{0(5)} + h\psi^{0(5)}\right] \\ \varphi^{0(1)} & \varphi^{0(3)} & \varphi^{0(5)} \\ \psi^{0(1)} & \psi^{0(3)} & \psi^{0(5)} \end{pmatrix} \begin{pmatrix} F_1 \\ F_2 \\ F_3 \end{pmatrix} = \begin{pmatrix} 0 \\ 0 \\ 0 \end{pmatrix} \quad \text{(V.1)}$$

For this set of the boundary conditions, relatively simple system of three homogeneous equations (V.1) can provide explicit forms for the suitable SH-SAW velocity and the weight factors F_1, F_2, and F_3. However, all of them must be obtained in this chapter below.

In three-equation system (V.1), the third-order boundary-condition determinant (BCD3) of the coefficient matrix can be then written in more explicit form. For this purpose, it is possible to use the first set of three eigenvectors with the components defined by expressions (II.26), (II.61), and (II.62) for the eigenvalues defined by corresponding expressions (II.25) and (II.29) in Chapter II. In order to find the weight factors F_1, F_2, and F_3 for suitable SH-SAW phase velocity V_{ph}, the BCD3 must vanish. After some transformations, the matrix BCD3 can be then led to the following simplified form:

$$\begin{vmatrix} 0 & n_3^{(3)}m^{(2)} & n_3^{(5)}m^{(3)} \\ h & C\alpha m^{(2)}\left(m^{(2)}-\gamma_K^2\right)+eh\left(m^{(2)}-2\right)^2 & C\alpha m^{(3)}\left(m^{(3)}-\gamma_K^2\right)+eh\left(m^{(3)}-2\right)^2 \\ e & C\varepsilon m^{(2)}\left(m^{(2)}-\gamma_K^2\right)+e^2\left(m^{(2)}-2\right)^2 & C\varepsilon m^{(3)}\left(m^{(3)}-\gamma_K^2\right)+e^2\left(m^{(3)}-2\right)^2 \end{vmatrix}=0 \quad \text{(V.2)}$$

Expanding the BCD3 in expression (V.2), a quite complicated secular equation can be then obtained. However, this secular equation can be significantly simplified and the final form of it can be given as follows:

$$n_3^{(3)}\left(m^{(3)}-\gamma_K^2\right)-n_3^{(5)}\left(m^{(2)}-\gamma_K^2\right)=0 \quad \text{(V.3)}$$

Using definition (II.15) for m from Chapter II, it is possible to write equation (V.3) without m. The secular equation can be then written only with the eigenvalues n_3 defined by (II.29) from Chapter II. It now reads:

$$n_3^{(3)}\left[\left(n_3^{(5)}\right)^2+1-\gamma_K^2\right]-n_3^{(5)}\left[\left(n_3^{(3)}\right)^2+1-\gamma_K^2\right]=0 \quad \text{(V.4)}$$

It is clearly seen in equation (V.4) that some rearrangement of the terms can further simplify it. Therefore, the final form of the secular equation is as follows:

$$n_3^{(3)}n_3^{(5)}=1-\gamma_K^2 \quad \text{(V.5)}$$

Utilizing the useful relation in expression (II.55) for the eigenvalues and definition (II.59) for the value of γ_K, one can obtain the following equation which already openly contains the phase velocity V_{ph}:

$$1-\left(\frac{V_{ph}}{V_{tem}}\right)^2=1-2\left(\frac{V_{ph}}{V_{t4}}\right)^2+\left(\frac{V_{ph}}{V_{t4}}\right)^4 \tag{V.6}$$

At the following step for simplification of equation (V.6), it is possible to use the velocity V_{tem} expressed by relation (II.24) instead of the velocity V_{t4} defined by expression (II.18) in Chapter II.

$$1+2K_{em}^2=\left(1+K_{em}^2\right)^2\left(\frac{V_{ph}}{V_{tem}}\right)^2 \tag{V.7}$$

Therefore, it is possible to write the following well-known form for the velocity of the surface Bleustein-Gulyaev-Melkumyan (BGM) wave [88, 89, 200]:

$$V_{BGM}=V_{tem}\left[\frac{1+2K_{em}^2}{\left(1+K_{em}^2\right)^2}\right]^{1/2} \tag{V.8}$$

In equations (V.7) and (V.8), the coefficient of the magnetoelectromechanical coupling (CMEMC) K_{em}^2 is given in the well-known compact form written in expression (II.19) in Chapter II.

For some further analytical investigations done in Ref. [200], it is thought that the form of equation (V.8) can be conveniently written in the following form:

$$V_{BGM}=V_{tem}\left[1-b^2\right]^{1/2} \tag{V.9}$$

where

$$b = \frac{K_{em}^2}{1 + K_{em}^2} \tag{V.10}$$

Also, it is necessary to mention that formula (V.8) for the velocity V_{BGM} can be readily reduced to the well-known velocity of the classical surface Bleustein-Gulyaev (BG) waves [90, 91] defined by corresponding equations (II.48) and (II.49) from Chapter II. This is true when $K_{em}^2 \to K_e^2$ ($h = 0$ and $\alpha = 0$ for a piezoelectrics) or $K_{em}^2 \to K_m^2$ ($e = 0$ and $\alpha = 0$ for a piezomagntics).

Using equations (V.1) and (V.2), tree equations for determination of the weight factors F_1, F_2, and F_3 can be then written as follows:

$$\begin{pmatrix} 0 & n_3^{(3)} m^{(2)} & n_3^{(5)} m^{(3)} \\ h & C\mu m^{(2)}\left(m^{(2)} - \gamma_K^2\right) + h^2\left(m^{(2)} - 2\right)^2 & C\mu m^{(3)}\left(m^{(3)} - \gamma_K^2\right) + h^2\left(m^{(3)} - 2\right)^2 \\ e & C\alpha m^{(2)}\left(m^{(2)} - \gamma_K^2\right) + eh\left(m^{(2)} - 2\right)^2 & C\alpha m^{(3)}\left(m^{(3)} - \gamma_K^2\right) + eh\left(m^{(3)} - 2\right)^2 \end{pmatrix} \begin{pmatrix} F_1 \\ F_2 \\ F_3 \end{pmatrix} = \begin{pmatrix} 0 \\ 0 \\ 0 \end{pmatrix} \tag{V.11}$$

It is noted that the explicit forms of the weight factors F_1, F_2, and F_3 in equation (V.1) can be very complicated. Using expression (V.11), it is possible to get the factors F_2 and F_3 from the first equation in three-equation system (V.11). Using them for the second or third equation in (V.1), it is possible to obtain the weight factor F_1. Therefore, all the weight factors for this case can be written in compact forms as follows:

$$F_1 = \left(\psi^{0(3)} n_3^{(5)} m^{(3)} - \psi^{0(5)} n_3^{(3)} m^{(2)}\right)/e \tag{V.12}$$

$$F_2 = -n_3^{(5)} m^{(3)} \tag{V.13}$$

$$F_3 = n_3^{(3)} m^{(2)} \tag{V.14}$$

It is thought that these compact forms of the weight factors F_1, F_2, and F_3 in equations (V.12), (V.13), and (V.14) are convenient for calculations. It is noted that these factors depend on the values explicitly defined in Chapter II. Also, they look like significantly complicated characteristics compared with those for the surface BGM wave propagation in the transversely isotropic piezoelectromagnetics [89].

Also, it is necessary here to state that when the reader will use the second set of three eigenvectors with the components defined by expressions (II.26), (II.63), and (II.64) for the same eigenvalues defined by corresponding expressions (II.25) and (II.29) in Chapter II, the obtained explicit form for the propagation wave velocity will be exactly the same SH-SAW velocity defined by relation (V.8). Indeed, in this case of the boundary conditions, the use of the both sets of the eigenvectors leads to the same result. This is like the case of SH-SAW propagation in the transversely isotropic piezoelectromagnetics.

For a solid piezoelectromagnetics, the complete mechanical displacement U^{Σ}, complete electrical potential φ^{Σ}, and complete magnetic potential ψ^{Σ} are given in the plane wave forms written in expressions from (IV.5) to (IV.7) in the previous chapter. Using findings obtained in this chapter, the complete displacement and potentials can be then introduced as follows:

$$U^{\Sigma} = \left\{F_2 U^{0(3)} \exp\left[\mathrm{j}kn_3^{(3)} x_3\right] + F_3 U^{0(5)} \exp\left[\mathrm{j}kn_3^{(5)} x_3\right]\right\} \exp\left[\mathrm{j}k\left(x_1 - V_{BGM} t\right)\right] \qquad \text{(V.15)}$$

$$\varphi^{\Sigma} = \left\{-F_1 h \exp\left[kx_3\right] + F_2 \varphi^{0(3)} \exp\left[\mathrm{j}kn_3^{(3)} x_3\right] + F_3 \varphi^{0(5)} \exp\left[\mathrm{j}kn_3^{(5)} x_3\right]\right\} \exp\left[\mathrm{j}k\left(x_1 - V_{BGM} t\right)\right] \quad \text{(V.16)}$$

$$\psi^{\Sigma} = \left\{F_1 e \exp\left[kx_3\right] + F_2 \psi^{0(3)} \exp\left[\mathrm{j}kn_3^{(3)} x_3\right] + F_3 \psi^{0(5)} \exp\left[\mathrm{j}kn_3^{(5)} x_3\right]\right\} \exp\left[\mathrm{j}k\left(x_1 - V_{BGM} t\right)\right] \quad \text{(V.17)}$$

where $x_3 < 0$ (see figure II.1 in Chapter II) and V_{BGM} is defined by relation (V.8).

Because this chapter solidly obtained the explicit form for the SH-SAW velocity V_{BGM}, it is already possible to give sample calculations for the cubic piezoelectric composite materials listed in table III.3 introduced in Chapter III. Indeed, these calculations of the velocity V_{BGM} can be done utilizing formula (V.8). Table V.1 lists the calculated wave characteristics for the cubic piezoelectromagnetics introduced in Chapter III. In the table, the three different values of V_K, V_{tem}, and V_{BGM} are given due to three different values of the CMEMC K_{em}^2 given in table III.3. It is obvious that the value of the SH-BAW velocity V_{t4} defined by relation (II.18) does not depend on the value of the CMEMC K_{em}^2 defined by relation (II.19) in Chapter II. These three values of the CMEMC K_{em}^2 correspond to three various values of the electromagnetic constant α which dramatically differ from each other. However, the corresponding functions $K_{em}^2(\alpha)$ in table III.3 do not differ dramatically. As a result, the calculated three values of the velocity V_{BGM} listed in table V.1 do not differ dramatically. This is also true for the values of V_K and V_{tem}. The results of calculations given in table V.2 support this statement.

Table V.1. The wave characteristics (all in m/s) such as the SH-BAW velocities V_{t4} and V_{tem}, as well as the solution V_K and the SH-SAW velocity V_{BGM}.

PEM composite	V_{t4}	$(V_K)_1$ $(V_K)_2$ $(V_K)_3$	$(V_{tem})_1$ $(V_{tem})_2$ $(V_{tem})_3$	$(V_{BGM})_1$ $(V_{BGM})_2$ $(V_{BGM})_3$
Metglas–PZT-5H	2921.958806791	3678.447975787 3698.141918114 3700.266095928	3872.235689401 3926.252392852 3932.338930933	3494.876043793 3513.830745572 3515.911465808
Tl_3TaSe_4–Terfenol-D	822.4308925036	974.6381134971 982.5964255669 983.4411632428	977.9418053774 988.5645944468 989.7454829681	935.0971412344 940.5489993757 941.1423281090
Tl_3VS_4–Galfenol	3054.803058243	3614.077804857 3620.037327927 3620.990544603	3624.711880315 3632.275425946 3633.496860330	3469.235044605 3473.206940663 3473.845611497
Tl_3TaSe_4–Galfenol	2931.728242148	3470.652006748 3477.114881325 3478.100810794	3481.430690090 3489.693942470 3490.968207627	3330.913090240 3335.238062880 3335.901782658
Tl_3VS_4–Alfenol	3021.465479859	2815.130797809 2836.855262613 2839.407562615	3144.674241233 3149.939882162 3150.572818213	3135.380401976 3139.866866103 3140.404200088

Table V.2. The differences (all in m/s) between the corresponding values for the SH-BAW velocity V_{tem} and those for the SH-SAW velocity V_{BGM}. They correspond to three various values of the CMEMC $(K_{em}^2)_1$, $(K_{em}^2)_2$, and $(K_{em}^2)_3$ listed in table III.3.

PEM composite	$(V_{tem})_2 - (V_{tem})_1$	$(V_{tem})_3 - (V_{tem})_2$	$(V_{BGM})_2 - (V_{BGM})_1$	$(V_{BGM})_3 - (V_{BGM})_2$
Metglas–PZT-5H	54.02	6.09	18.95	2.08
Tl_3TaSe_4–Terfenol-D	10.62	1.18	5.45	0.59
Tl_3VS_4–Galfenol	7.56	1.22	3.97	0.64
Tl_3TaSe_4–Galfenol	8.26	1.27	4.32	0.66
Tl_3VS_4–Alfenol	5.27	0.63	4.49	0.54

Table V.2 lists the calculated differences between the corresponding values of the SH-BAW velocity V_{tem} and between the corresponding values of the SH-SAW velocity V_{BGM}. The reader can calculate the corresponding differences such as $(V_K)_2 - (V_K)_1$ and $(V_K)_3 - (V_K)_2$ in order to compare the obtained results with those obtained in table V.2. The calculations for the V_K are not given in the table, because this chapter has in interest in comparison of the corresponding values of the velocities V_{tem} and V_{BGM}. Over the all composites listed in table V.2, it is clearly seen that the dependencies of the velocities V_{tem} and V_{BGM} on the electromagnetic constant α are very complicated. The values of $(V_{tem})_2 - (V_{tem})_1$ are significantly larger than the values of $(V_{BGM})_2 - (V_{BGM})_1$. Also, the values of $(V_{tem})_3 - (V_{tem})_2$ are significantly larger than those of $(V_{BGM})_3 - (V_{BGM})_2$. This fact can mean that the sensitivity, i.e. the change of the SH-SAW velocity V_{BGM} with a dramatic change in the electromagnetic constant α is smaller than that for the SH-BAW velocity V_{tem}. This can mean that when researchers will experimentally investigate different piezoelectromagnetic composite materials (or the same composite under some different conditions) and their results will reveal an order change in the constant α and no significant change in the other material constants, it is possible that they can find only a slight change in the values of the velocities V_{tem} and V_{BGM}.

This chapter has obtained the analytical formula for the SH-SAW velocity concerning the case of SH-SAW propagation in cubic piezoelectromagnetics. Also, it was demonstrated in both the cases of the first and second sets of the eigenvector components that the obtained velocity represents the velocity V_{BGM} of the SH-SAW which also propagates in the transversely isotropic composite materials. It is also worth noting that the utilization of the first and second sets of the eigenvector components does not always lead to the same SH-SAW velocity like that obtained in this chapter. The following chapters treat the other possible electrical and magnetic boundary conditions. They serve for demonstration that the two different sets of the eigenvector components can lead to possible solutions for new SH-SAWs for the case of cubic piezoelectromagnetics.

CHAPTER VI. The Case of $D_3 = 0$ and $B_3 = 0$ at $x_3 = 0$

According to the theoretical results of recent book [89] obtained by the author of this work and paper [88] by A. Melkumyan for this case of the mechanically free, electrically open ($D_3 = 0$) and magnetically closed ($B_3 = 0$) surface, any SH-SAW solution cannot be found for both the sets of the eigenvector components in the case of SH-SAW propagation in the transversely isotropic piezoelectromagnetic (composite) materials. This is true because the single solution for the transversely isotropic case represents the SH-BAW velocity V_{tem}.

In order to obtain some results for the case of wave propagation in the cubic piezoelectromagnetics, it is necessary to analytically describe this case. Indeed, the following three homogeneous equations can be written in the matrix form as follows, using equation (V.1):

$$\begin{pmatrix} k_3^{(1)}\left[CU^{0(1)} + e\varphi^{0(1)} + h\psi^{0(1)}\right] & k_3^{(3)}\left[CU^{0(3)} + e\varphi^{0(3)} + h\psi^{0(3)}\right] & k_3^{(5)}\left[CU^{0(5)} + e\varphi^{0(5)} + h\psi^{0(5)}\right] \\ k_3^{(1)}\left[eU^{0(1)} - \varepsilon\varphi^{0(1)} - \alpha\psi^{0(1)}\right] & k_3^{(3)}\left[eU^{0(3)} - \varepsilon\varphi^{0(3)} - \alpha\psi^{0(3)}\right] & k_3^{(5)}\left[eU^{0(5)} - \varepsilon\varphi^{0(5)} - \alpha\psi^{0(5)}\right] \\ k_3^{(1)}\left[hU^{0(1)} - \alpha\varphi^{0(1)} - \mu\psi^{0(1)}\right] & k_3^{(3)}\left[hU^{0(3)} - \alpha\varphi^{0(3)} - \mu\psi^{0(3)}\right] & k_3^{(5)}\left[hU^{0(5)} - \alpha\varphi^{0(5)} - \mu\psi^{0(5)}\right] \end{pmatrix} \begin{pmatrix} F_1 \\ F_2 \\ F_3 \end{pmatrix} = \begin{pmatrix} 0 \\ 0 \\ 0 \end{pmatrix} \tag{VI.1}$$

It is clearly seen in equation (VI.1) that all the parameters $k_3^{(1,3,5)} = kn_3^{(1,3,5)}$ can be excluded for further analytical considerations.

Applying some transformations for equation (VI.1) and using equation (V.2), the third-order boundary-condition determinant called BCD3 for the coefficient matrix in equation (VI.1) can be reduced to the following form:

$$\begin{vmatrix} 0 & m^{(2)} & m^{(3)} \\ -1 & 2e\left(m^{(2)}-2\right) & 2e\left(m^{(3)}-2\right) \\ -(e\mu-h\alpha) & \begin{matrix} h(e\alpha-h\varepsilon)m^{(2)}\left(m^{(2)}-2\right) \\ -C\left(\varepsilon\mu-\alpha^2\right)m^{(2)}\left(m^{(2)}-\gamma_K^2\right) \\ -e(e\mu-h\alpha)\left(m^{(2)}-2\right)^2 \end{matrix} & \begin{matrix} h(e\alpha-h\varepsilon)m^{(3)}\left(m^{(3)}-2\right) \\ -C\left(\varepsilon\mu-\alpha^2\right)m^{(3)}\left(m^{(3)}-\gamma_K^2\right) \\ -e(e\mu-h\alpha)\left(m^{(3)}-2\right)^2 \end{matrix} \end{vmatrix} = 0 \qquad \text{(VI.2)}$$

In relation (VI.2), it is used the first set of the eigenvector components defined by relations (II.26), (II.61), and (II.62) for the eigenvalues defined by corresponding expressions (II.25) and (II.29) from Chapter II.

Expanding the matrix BCD3, the secular equation can be obtained in the following form:

$$\begin{aligned} &-2e(e\mu-h\alpha)m^{(2)}\left(m^{(3)}-2\right) \\ &-m^{(3)}\left[h(e\alpha-h\varepsilon)m^{(2)}\left(m^{(2)}-2\right)-C\left(\varepsilon\mu-\alpha^2\right)m^{(2)}\left(m^{(2)}-\gamma_K^2\right)-e(e\mu-h\alpha)\left(m^{(2)}-2\right)^2\right] \\ &+2e(e\mu-h\alpha)m^{(3)}\left(m^{(2)}-2\right) \\ &+m^{(2)}\left[h(e\alpha-h\varepsilon)m^{(3)}\left(m^{(3)}-2\right)-C\left(\varepsilon\mu-\alpha^2\right)m^{(3)}\left(m^{(3)}-\gamma_K^2\right)-e(e\mu-h\alpha)\left(m^{(3)}-2\right)^2\right]=0 \end{aligned} \qquad \text{(VI.3)}$$

It is obvious that the secular equation written above should be simplified. This mathematical procedure of simplification results in the following equation:

$$\begin{aligned} &-m^{(2)}m^{(3)}\left\{[h(e\alpha-h\varepsilon)-e(e\mu-h\alpha)]\left(m^{(2)}-2\right)-C\left(\varepsilon\mu-\alpha^2\right)\left(m^{(2)}-\gamma_K^2\right)\right\} \\ &+m^{(2)}m^{(3)}\left\{[h(e\alpha-h\varepsilon)-e(e\mu-h\alpha)]\left(m^{(3)}-2\right)-C\left(\varepsilon\mu-\alpha^2\right)\left(m^{(3)}-\gamma_K^2\right)\right\}=0 \end{aligned} \qquad \text{(VI.4)}$$

It is clearly seen that modified secular equation (VI.4) can be formed by two factors. The first factor is simple and can be written as follows, using relation (II.52) from Chapter II:

$$m^{(2)}m^{(3)} = \frac{4K_{em}^2}{1+K_{em}^2} = 0 \qquad \text{(VI.5)}$$

Using definition (II.19) for the CMEMC K_{em}^2, equation (VI.5) leads to the following solution:

$$K_{em}^2 = \frac{\mu e^2 + \varepsilon h^2 - 2\alpha eh}{C\left(\varepsilon\mu - \alpha^2\right)} = 0 \qquad \text{(VI.6)}$$

Equation (VI.6) overtly gives the following possible solution:

$$\mu e^2 + \varepsilon h^2 - 2\alpha eh = 0 \qquad \text{(VI.7)}$$

However, this solution defined by equations (VI.6) and (VI.7) does not depend on the SH-SAW phase velocity V_{ph}. This means that in this case one can choose any value for the phase velocity V_{ph} ($V_{ph} < V_{tem}$) because only suitable unique values of the material constants in equation (VI.7) can cause the case. So, this solution is inappropriate. It is possible to discuss the second factor in equation (VI.4).

It is obvious that the second factor in equation (VI.4) can be readily simplified. Therefore, it can be introduced in the following form:

$$\left(m^{(3)} - m^{(2)}\right)\times\left(1 + K_{em}^2\right) = 0 \qquad \text{(VI.8)}$$

Using definition (II.28) from Chapter II for the parameters $m^{(2)}$ and $m^{(3)}$ in equation (VI.8), it is feasible to receive equation (II.33). The latter equation soundly leads to the solution denoted by V_K in expression (II.34). This was discussed in Chapter II.

Using the second set of the eigenvector components defined by relations (II.26), (II.63), and (II.64) for equation (VI.1), the matrix BCD3 can be also reduced to the following form:

$$
\begin{vmatrix}
0 & m^{(2)} & m^{(3)} \\
-(e\alpha - h\varepsilon) & \begin{array}{l} e(e\mu - h\alpha)m^{(2)}\left(m^{(2)}-2\right) \\ +C\left(\varepsilon\mu-\alpha^2\right)m^{(2)}\left(m^{(2)}-\gamma_K^2\right) \\ -h(e\alpha - h\varepsilon)\left(m^{(2)}-2\right)^2 \end{array} & \begin{array}{l} e(e\mu - h\alpha)m^{(3)}\left(m^{(3)}-2\right) \\ +C\left(\varepsilon\mu-\alpha^2\right)m^{(3)}\left(m^{(3)}-\gamma_K^2\right) \\ -h(e\alpha - h\varepsilon)\left(m^{(3)}-2\right)^2 \end{array} \\
-1 & 2h\left(m^{(2)}-2\right) & 2h\left(m^{(3)}-2\right)
\end{vmatrix} = 0 \quad \text{(VI.9)}
$$

Therefore, the second secular equation can be written in the following form:

$$
\begin{aligned}
&-m^{(2)}\left[e(e\mu - h\alpha)m^{(3)}\left(m^{(3)}-2\right)+C\left(\varepsilon\mu-\alpha^2\right)m^{(3)}\left(m^{(3)}-\gamma_K^2\right)-h(e\alpha-h\varepsilon)\left(m^{(3)}-2\right)^2\right] \\
&-2h(e\alpha - h\varepsilon)m^{(3)}\left(m^{(2)}-2\right) \\
&+m^{(3)}\left[e(e\mu - h\alpha)m^{(2)}\left(m^{(2)}-2\right)+C\left(\varepsilon\mu-\alpha^2\right)m^{(2)}\left(m^{(2)}-\gamma_K^2\right)-h(e\alpha-h\varepsilon)\left(m^{(2)}-2\right)^2\right] \\
&+2h(e\alpha - h\varepsilon)m^{(2)}\left(m^{(3)}-2\right)=0
\end{aligned} \quad \text{(VI.10)}
$$

Indeed, secular equation (VI.10) can be then written in the simplified forms of two factors obtained earlier in equations (VI.5) and (VI.8). Therefore, in these two cases of two different sets of the eigenvector components, one can obtain the same solutions for both the sets. The first solution represents an inappropriate one defined by equation (VI.7) and the second solution represents the well-known solution denoted by V_K in expression (II.34) of Chapter II (see also the calculated values of V_K for all the cubic piezoelectromagnetics listed in table V.1). As a result, it is possible to state that any new SH-SAW velocities do not exist for this set of the electrical and magnetic boundary conditions. So, it is crucial to state that it is undoubting that the results of this chapter and the previous chapter for the cubic piezoelectromagnetics coincide with the results obtained in Refs. [88, 89] in which the transversely isotropic piezoelectromagnetic composite materials were theoretically investigated. It is expected that this excellent result can be true for the other sets of the electrical and magnetic boundary conditions that are treated in the following chapters.

CHAPTER VII. The Case of $B_3 = 0$ and $\varphi = 0$ at $x_3 = 0$

This chapter gives a theoretical study of SH-SAW propagation in cubic piezoelectromagnetics when the electrical boundary condition from Chapter V for the electrical potential such as $\varphi = 0$ is used together with the magnetic boundary condition from Chapter VI, namely $B_3 = 0$. The mechanical boundary condition is the mechanically free interface at $x_3 = 0$ between the solid surface and a vacuum. According to the theoretical results of the recent book cited in Ref. [89] concerning the study of the transversely isotropic piezoelectromagnetics, two different solutions for SH-SAWs can be found for the two different sets of the eigenvector components, namely one unique solution for either set. In the case of the transversely isotropic piezoelectromagnetics, one unique SH-SAW was discovered in 2007 by Arman Melkumyan in Ref. [88] and the second SH-SAW was discovered in 2010 by the author of this work in Ref. [89]. Their velocities are given by formulae (173) and (163) in book [89], respectively. It is expected that in the case of cubic piezoelectromagnetics, at least one SH-SAW solution can be also revealed because there are also two different sets of the eigenvector components.

According to the boundary conditions for the case of this chapter, the following three equations can be written down in the matrix form:

$$\begin{pmatrix} k_3^{(1)}\left[CU^{0(1)} + e\varphi^{0(1)} + h\psi^{0(1)}\right] & k_3^{(3)}\left[CU^{0(3)} + e\varphi^{0(3)} + h\psi^{0(3)}\right] & k_3^{(5)}\left[CU^{0(5)} + e\varphi^{0(5)} + h\psi^{0(5)}\right] \\ \varphi^{0(1)} & \varphi^{0(3)} & \varphi^{0(5)} \\ k_3^{(1)}\left[hU^{0(1)} - \alpha\varphi^{0(1)} - \mu\psi^{0(1)}\right] & k_3^{(3)}\left[hU^{0(3)} - \alpha\varphi^{0(3)} - \mu\psi^{0(3)}\right] & k_3^{(5)}\left[hU^{0(5)} - \alpha\varphi^{0(5)} - \mu\psi^{0(5)}\right] \end{pmatrix} \begin{pmatrix} F_1 \\ F_2 \\ F_3 \end{pmatrix} = \begin{pmatrix} 0 \\ 0 \\ 0 \end{pmatrix} \tag{VII.1}$$

where $k_3^{(1,3,5)} = kn_3^{(1,3,5)}$ is also used.

Using the first set of the eigenvector components defined by expressions (II.26), (II.61), and (II.62) for the eigenvalues defined by corresponding expressions (II.25) and (II.29), one can readily write the following corresponding determinant (BCD3) of the third order for the coefficient matrix in equation (VII.1):

$$\begin{vmatrix} 0 & n_3^{(3)}m^{(2)} & n_3^{(5)}m^{(3)} \\ h & \begin{array}{c} C\alpha m^{(2)}\left(m^{(2)}-\gamma_K^2\right) \\ +eh\left(m^{(2)}-2\right)^2 \end{array} & \begin{array}{c} C\alpha m^{(3)}\left(m^{(3)}-\gamma_K^2\right) \\ +eh\left(m^{(3)}-2\right)^2 \end{array} \\ -n_3^{(1)}(e\mu-h\alpha) & \begin{array}{c} n_3^{(3)}\left[h(e\alpha-h\varepsilon)m^{(2)}\left(m^{(2)}-2\right)\right. \\ -C\left(\varepsilon\mu-\alpha^2\right)m^{(2)}\left(m^{(2)}-\gamma_K^2\right) \\ \left.-e(e\mu-h\alpha)\left(m^{(2)}-2\right)^2\right] \end{array} & \begin{array}{c} n_3^{(5)}\left[h(e\alpha-h\varepsilon)m^{(3)}\left(m^{(3)}-2\right)\right. \\ -C\left(\varepsilon\mu-\alpha^2\right)m^{(3)}\left(m^{(3)}-\gamma_K^2\right) \\ \left.-e(e\mu-h\alpha)\left(m^{(3)}-2\right)^2\right] \end{array} \end{vmatrix} = 0 \quad \text{(VII.2)}$$

Using the well-known triangle rule for such determinants, it is feasible to transform determinant (VII.2) into a form of secular equation. Therefore, the following secular equation emerges as soon as determinant (VII.2) is expanded:

$$\begin{aligned} & hn_3^{(5)}n_3^{(3)}m^{(3)}\left[h(e\alpha-h\varepsilon)m^{(2)}\left(m^{(2)}-2\right)-C\left(\varepsilon\mu-\alpha^2\right)m^{(2)}\left(m^{(2)}-\gamma_K^2\right)-e(e\mu-h\alpha)\left(m^{(2)}-2\right)^2\right] \\ & -\mathrm{j}(e\mu-h\alpha)n_3^{(5)}m^{(3)}\left[C\alpha m^{(2)}\left(m^{(2)}-\gamma_K^2\right)+eh\left(m^{(2)}-2\right)^2\right] \\ & -hn_3^{(5)}n_3^{(3)}m^{(2)}\left[h(e\alpha-h\varepsilon)m^{(3)}\left(m^{(3)}-2\right)-C\left(\varepsilon\mu-\alpha^2\right)m^{(3)}\left(m^{(3)}-\gamma_K^2\right)-e(e\mu-h\alpha)\left(m^{(3)}-2\right)^2\right] \\ & +\mathrm{j}(e\mu-h\alpha)n_3^{(3)}m^{(2)}\left[C\alpha m^{(3)}\left(m^{(3)}-\gamma_K^2\right)+eh\left(m^{(3)}-2\right)^2\right]=0 \end{aligned} \quad \text{(VII.3)}$$

Utilizing expression (II.52) for $m^{(2)}m^{(3)}$ from Chapter II, equation (VII.3) can be led to the following simplified form:

$$\begin{aligned} & \frac{h(e\alpha-h\varepsilon)}{e(e\mu-h\alpha)}n_3^{(3)}n_3^{(5)}\left(m^{(3)}-m^{(2)}\right)-\mathrm{j}\frac{K_{em}^2\left(\gamma_K^2+4K_\alpha^2\right)}{K_\alpha^2\left(1+K_{em}^2\right)}\left(n_3^{(5)}-n_3^{(3)}\right) \\ & +\mathrm{j}\left(n_3^{(5)}m^{(3)}-n_3^{(3)}m^{(2)}\right)+\mathrm{j}\frac{K_{em}^2\left(1+K_\alpha^2\right)}{K_\alpha^2\left(1+K_{em}^2\right)}\left(n_3^{(5)}m^{(2)}-n_3^{(3)}m^{(3)}\right)=0 \end{aligned} \quad \text{(VII.4)}$$

where the non-dimensional parameters K_{em}^2 and γ_K^2 are defined by expressions (II.19) and (II.59) from Chapter II, respectively. Also, the non-dimensional parameter K_{e0}^2 in equation (VII.4) is defined as follows:

$$K_{\alpha}^2 = \frac{eh}{C\alpha} \tag{VII.5}$$

For the second set of the eigenvector components, one can also get the following form for the third-order BCD3 of the coefficient matrix in equation (VII.1):

$$\begin{vmatrix} 0 & n_3^{(3)} m^{(2)} & n_3^{(5)} m^{(3)} \\ h & C\mu m^{(2)}\left(m^{(2)} - \gamma_K^2\right) + h^2\left(m^{(2)} - 2\right)^2 & C\mu m^{(3)}\left(m^{(3)} - \gamma_K^2\right) + h^2\left(m^{(3)} - 2\right)^2 \\ -n_3^{(1)} & 2hn_3^{(3)}\left(m^{(2)} - 2\right) & 2hn_3^{(5)}\left(m^{(3)} - 2\right) \end{vmatrix} = 0 \tag{VII.6}$$

Therefore, the case of the second set of the eigenvector components provides the second secular equation written in the following form:

$$\begin{aligned} &- \mathrm{j} n_3^{(3)} m^{(2)} \left[C\mu m^{(3)}\left(m^{(3)} - \gamma_K^2\right) + h^2\left(m^{(3)} - 2\right)^2\right] + 4h^2 n_3^{(3)} n_3^{(5)} m^{(3)} \\ &+ \mathrm{j} n_3^{(5)} m^{(3)} \left[C\mu m^{(2)}\left(m^{(2)} - \gamma_K^2\right) + h^2\left(m^{(2)} - 2\right)^2\right] - 4h^2 n_3^{(3)} n_3^{(5)} m^{(2)} = 0 \end{aligned} \tag{VII.7}$$

Using expression (II.52) from Chapter II again, equation (VII.7) can be transformed into the following form:

$$\begin{aligned} &n_3^{(3)} n_3^{(5)}\left(m^{(3)} - m^{(2)}\right) - \mathrm{j}\frac{K_{em}^2\left(\gamma_K^2 + 4K_m^2\right)}{K_m^2\left(1 + K_{em}^2\right)}\left(n_3^{(5)} - n_3^{(3)}\right) \\ &+ \mathrm{j}\left(n_3^{(5)} m^{(3)} - n_3^{(3)} m^{(2)}\right) + \mathrm{j}\frac{K_{em}^2\left(1 + K_m^2\right)}{K_m^2\left(1 + K_{em}^2\right)}\left(n_3^{(5)} m^{(2)} - n_3^{(3)} m^{(3)}\right) = 0 \end{aligned} \tag{VII.8}$$

where the non-dimensional parameters K_m^2, K_{em}^2, and γ_K^2 are defined by expressions (II.22), (II.19), and (II.59) from Chapter II, respectively. Also, it is clearly seen in equations (VII.4) and (VII.8) that when $m^{(2)} = m^{(3)}$ and $n_3^{(3)} = n_3^{(5)}$ is fulfilled, the case of the solution denoted by the V_K in expression (II.34) from Chapter II is realized.

In formulae (VII.4) and (VII.8), the parameters $m^{(2)}$ and $m^{(3)}$ defined by relation (II.28) depend on the parameter B_t defined by relation (II.23) in Chapter II. Thus, it is possible to utilize the following substitutions, using relation (II.55) from Chapter II:

$$n_3^{(3)} n_3^{(5)} = \mp\sqrt{1-X} \tag{VII.9}$$

$$B_t = \gamma_K^2 + 4K_{em}^2 = \left(1+K_{em}^2\right)X + 4K_{em}^2 \tag{VII.10}$$

In expressions (VII.9) and (VII.10), the suitable phase velocity V_{ph}, which should be numerically found, is coupled with the parameter X defined below:

$$X = \left(\frac{V_{ph}}{V_{tem}}\right)^2 \tag{VII.11}$$

Indeed, it is possible to use recursive formulae in equations (VII.4) and (VII.8) for determination of suitable phase velocities $V_{c1new} = V_{ph1}(X_1)$ and $V_{c2new} = V_{ph2}(X_2)$ of new SH-SAWs. First of all, it is possible to write equations (VII.4) and (VII.8) by the following ways:

$$\left(n_3^{(3)} n_3^{(5)}\right)^2 = 1 - X_1 = f_1^2\left(n_3^{(3)}, n_3^{(5)}, m^{(2)}, m^{(3)}\right) = f_1^2\left(B_t\right) = f_1^2\left(X_1\right) \tag{VII.12}$$

$$\left(n_3^{(3)} n_3^{(5)}\right)^2 = 1 - X_2 = f_2^2\left(n_3^{(3)}, n_3^{(5)}, m^{(2)}, m^{(3)}\right) = f_2^2\left(B_t\right) = f_2^2\left(X_2\right) \tag{VII.13}$$

where X_1 and X_2 correspond to V_{ph1} and V_{ph2} in relation (VII.11).

It is clearly seen in equations (VII.12) and (VII.13) that these equations represent corresponding recursive formulae, in which the functions f_1 and f_2 can be obtained from equations (VII.4) and (VII.8), respectively. It is thought that it is necessary to introduce the obtained recursive solution in some used form which is also utilized in formula (V.9) for the SH-SAW velocity V_{BGM} (see Chapter V) as well as in all the explicit formulae for the SH-SAW velocities discovered in the recent book [89] by the author. It is obvious that either of equations (VII.12) and (VII.13) can give unique value of the SH-SAW phase velocity denoted by V_{c1new}. Note that it was numerically checked that either of equations (VII.4) and (VII.8) give the same value of the V_{c1new}. The calculated values of the new SH-SAW velocity V_{c1new} are listed in table VII.1 (see below) for several cubic piezoelectromagnetics.

The formula for the new SH-SAW velocity V_{c1new} can be then written in the following convenient and relatively simple form, following the other forms introduced in Ref. [89]:

$$V_{c1new} = V_{tem}\sqrt{1-\left(b_{c1}\left(X_1\right)\right)^2} \qquad \text{(VII.14)}$$

where the parameter b_{c1} depends on the phase velocity V_{c1new} of the new SH-SAW and represents very complicated function for recursive calculations. One can have attempts to obtain the solutions for the SH-SAW velocities in corresponding complicated analytical forms. However, it is thought that these analytical solutions can be more complicated than recursive formula (VII.14). Therefore, it is possible to state that to obtain SH-SAW solution in the case of cubic piezoelectromagnetics represents a significantly more complicated problem compared with the obtained explicit forms of the SH-SAW solutions in the case of the transversely isotropic piezoelectromagnetic materials [89].

It is flagrant that if the solution for the new velocity V_{c1new} for the SH-SAW propagating in the cubic piezoelectromagnetics exists, it should satisfy the following conditions:

$$0 < V_{c1new} < V_{tem} \qquad \text{(VII.15)}$$

$$0 < X_1 < 1 \qquad \text{(VII.16)}$$

It is critical to state that conditions (VII.15) and (VII.16) are true for the following CMEMC: $K_{em}^2 < 1/3$. For $K_{em}^2 > 1/3$, it is natural to apply the following conditions:

$$0 < V_{c1new} < V_K \tag{VII.17}$$

$$0 < X_1 < V_K / V_{tem} \tag{VII.18}$$

where $V_K < V_{tem}$.

Table VII.1. The calculated values of the new SH-SAW velocity V_{c1new} [m/s].

PEM composite	$(V_{c1new})_1$ $(V_{c1new})_2$ $(V_{c1new})_3$
Metglas–PZT-5H	3676.0613782111013 3693.6457478849274 3695.5206157506539
Tl_3TaSe_4–Terfenol-D	969.6324936892347 975.6663281671238 976.3080337919884
Tl_3VS_4–Galfenol	3614.0759713109963 3619.7803934618422 3620.6579725071904
Tl_3TaSe_4–Galfenol	3470.6470451921421 3476.7874762369843 3477.6865581211105
Tl_3VS_4–Alfenol	3144.6500708329990 3149.8423675715336 3150.4632207288199

Table VII.1 lists the calculated values of the new SH-SAW velocity V_{c1new} which can be obtained using either of equations (VII.4) and (VII.8). Three values of the velocity V_{c1new} were calculated because three values of the CMEMC $K_{em}{}^2$ corresponding to three values of the electromagnetic constant α exist for each cubic piezoelectromagnetics listed in table III.3, see Chapter III. It is clearly seen in table VII.1 that the values of the velocity V_{c1new} increase with the increase in the CMEMC $K_{em}{}^2$, i.e. with the decrease in the constant α. This is like the results for the velocity V_{BGM}. For Tl_3VS_4–Alfenol with $K_{em}{}^2 < 1/3$ in table VII.1, all the values of the velocity V_{c1new} are situated just below the value of the SH-BAW velocity V_{tem}. For the other cubic piezoelectromagnetics with $K_{em}{}^2 > 1/3$ in table VII.1, all the values of the velocity V_{c1new} lie just below the corresponding values of the solution symbolized as $V_K < V_{tem}$. Note that the values of V_{BGM}, V_{tem}, and V_K for all the cubic piezoelectromagnetics are listed in table V.1 from Chapter V. It is worth noticing that these calculations can be completed with a six-core processor (twelve ways) laptop.

Also, it is possible to use the found fact that both equations (VII.4) and (VII.8) reveal the same result, namely the new SH-SAW velocity V_{c1new}. This allows one to carry out some simplification. It is blatant that it is natural to subtract equation (VII.4) from equation (VII.8) (or vice versa) in order to cope with three terms instead of four terms. Therefore, the transformed equation reads:

$$\begin{aligned}&-K_m^2K_\alpha^2\left(1+K_{em}^2\right)\frac{C\left(\varepsilon\mu-\alpha^2\right)}{e\left(e\mu-h\alpha\right)}n_3^{(3)}n_3^{(5)}\left(m^{(3)}-m^{(2)}\right)\\&-\mathrm{j}\gamma_K^2\left(K_m^2-K_\alpha^2\right)\left(n_3^{(5)}-n_3^{(3)}\right)+\mathrm{j}\left(K_m^2-K_\alpha^2\right)\left(n_3^{(5)}m^{(2)}-n_3^{(3)}m^{(3)}\right)=0\end{aligned}\qquad\text{(VII.19)}$$

Three-term equation (VII.19) can be further regrouped to deal with only two terms for convenience. Consequently, one can get the following relatively compact form for the secular equation to calculate the new SH-SAW velocity V_{c1new}:

$$\begin{aligned}&-K_m^2K_\alpha^2\left(1+K_{em}^2\right)\frac{C\left(\varepsilon\mu-\alpha^2\right)}{e\left(e\mu-h\alpha\right)}n_3^{(3)}n_3^{(5)}\left(m^{(3)}-m^{(2)}\right)\\&+\mathrm{j}\left(K_m^2-K_\alpha^2\right)\left[n_3^{(5)}\left(m^{(2)}-\gamma_K^2\right)-n_3^{(3)}\left(m^{(3)}-\gamma_K^2\right)\right]=0\end{aligned}\qquad\text{(VII.20)}$$

This compact form can be used for numerical calculations of the velocity V_{c1new} instead of either of equations (VII.4) and (VII.8). It is also thought that the two-term form in equation (VII.20) is convenient to represent a compact form for the parameter b_{c1} introduced in equation (VII.14):

$$b_{c1} = n_3^{(3)} n_3^{(5)} = -\frac{K_m^2 - K_\alpha^2}{K_m^2 K_\alpha^2 \left(1 + K_{em}^2\right)} \frac{e(e\mu - h\alpha)}{C(\varepsilon\mu - \alpha^2)} \frac{\mathrm{j} n_3^{(5)} \left(m^{(2)} - \gamma_K^2\right) - \mathrm{j} n_3^{(3)} \left(m^{(3)} - \gamma_K^2\right)}{m^{(3)} - m^{(2)}} \quad \text{(VII.21)}$$

Also, it is possible to transform equation (VII.20) into a quadratic equation with the unknown variable such as $n_3^{(3)} n_3^{(5)}$. Indeed, it is realistic to write two-term equation (VII.20) as an equality between the first and the second terms and then to square the terms. Afterwards, the quadratic equation can be expressed as follows:

$$\begin{aligned} &\left[K_m^2 K_\alpha^2 \left(1 + K_{em}^2\right) \frac{C(\varepsilon\mu - \alpha^2)}{e(e\mu - h\alpha)}\right]^2 \left(m^{(3)} - m^{(2)}\right)^2 \left(n_3^{(3)} n_3^{(5)}\right)^2 \\ &- 2\left(K_m^2 - K_\alpha^2\right)^2 \left(m^{(2)} - \gamma_K^2\right)\left(m^{(3)} - \gamma_K^2\right) n_3^{(3)} n_3^{(5)} \\ &+ \left(K_m^2 - K_\alpha^2\right)^2 \left[\left(m^{(2)} - \gamma_K^2\right)\left(m^{(3)} - 1\right) - \left(m^{(3)} - \gamma_K^2\right)\left(m^{(2)} - 1\right)\right] = 0 \end{aligned} \quad \text{(VII.22)}$$

Finally, it is possible to move the second term with a negative sign in equation (VII.22) from the left side to the right side and to square both the sides. This is necessary procedure to have a polynomial with no square root. This will be a sixth-degree polynomial. Note that the author has read papers [201, 202] concerning the problems to express some solutions for quintic, sextic, and octic equations. Indeed, the analytical solutions are too complicated. It is thought that to obtain numerical solutions can be more suitable in this case.

The same analysis done in this chapter can be carried out in the following chapters. Chapter VIII describes the wave propagation in the cubic piezoelectromagnetics when the other set of the electrical and magnetic boundary conditions is exploited.

CHAPTER VIII. The Case of $D_3 = 0$ and $\psi = 0$ at $x_3 = 0$

This chapter provides the case of the electrically open surface ($D_3 = 0$) and the magnetically open surface ($\psi = 0$) of the corresponding boundary conditions at the suitable interface ($x_3 = 0$ in figure II.1 of Chapter II) between the surface of the cubic piezoelectromagnetics and a vacuum. It is necessary to mention that for the transversely isotropic piezoelectromagnetics and this set of the boundary conditions, only single independent solution for the SH-SAW velocity can be obtained in the explicit form given in Refs. [88, 89]. This SH-SAW velocity was also obtained by Arman Melkumyan in his recent theoretical work [88] and is defined by the explicit form in expression (156) written in book [89]. The second solution is not independent because it represents the SH-SAW velocity defined by equation (163) for the set of the boundary conditions relevant to the previous chapter. For the case of the study of cubic piezoelectromagnetics, it is necessary to show that one can also obtain some SH-SAW solution for this set of the boundary conditions.

Utilization of this set of the electrical ($D_3 = 0$) and magnetic ($\psi = 0$) boundary conditions gives the following three equations written in the matrix form:

$$\begin{pmatrix} k_3^{(1)}\left[CU^{0(1)} + e\varphi^{0(1)} + h\psi^{0(1)}\right] & k_3^{(3)}\left[CU^{0(3)} + e\varphi^{0(3)} + h\psi^{0(3)}\right] & k_3^{(5)}\left[CU^{0(5)} + e\varphi^{0(5)} + h\psi^{0(5)}\right] \\ k_3^{(1)}\left[eU^{0(1)} - \varepsilon\varphi^{0(1)} - \alpha\psi^{0(1)}\right] & k_3^{(3)}\left[eU^{0(3)} - \varepsilon\varphi^{0(3)} - \alpha\psi^{0(3)}\right] & k_3^{(5)}\left[eU^{0(5)} - \varepsilon\varphi^{0(5)} - \alpha\psi^{0(5)}\right] \\ \psi^{0(1)} & \psi^{0(3)} & \psi^{0(5)} \end{pmatrix}\begin{pmatrix} F_1 \\ F_2 \\ F_3 \end{pmatrix} = \begin{pmatrix} 0 \\ 0 \\ 0 \end{pmatrix} \tag{VIII.1}$$

For the first set of the eigenvector components, one can obtain the following BCD3 of the coefficient matrix in equation (VIII.1):

$$\begin{vmatrix} 0 & n_3^{(3)} m^{(2)} & n_3^{(5)} m^{(3)} \\ -n_3^{(1)} & 2en_3^{(3)}\left(m^{(2)}-2\right) & 2en_3^{(5)}\left(m^{(3)}-2\right) \\ e & C\varepsilon m^{(2)}\left(m^{(2)}-\gamma_K^2\right)+e^2\left(m^{(2)}-2\right)^2 & C\varepsilon m^{(3)}\left(m^{(3)}-\gamma_K^2\right)+e^2\left(m^{(3)}-2\right)^2 \end{vmatrix} = 0 \quad \text{(VIII.2)}$$

It is noted that any boundary-condition determinant represents a number. In this case, the BCD3 in equation (VIII.2) must vanish. It is natural to introduce the following secular equation obtained by the expansion of determinant (VIII.2):

$$\begin{aligned} &n_3^{(3)} n_3^{(5)}\left(m^{(3)}-m^{(2)}\right)-\mathrm{j}\frac{K_{em}^2\left(\gamma_K^2+4K_e^2\right)}{K_e^2\left(1+K_{em}^2\right)}\left(n_3^{(5)}-n_3^{(3)}\right) \\ &+\mathrm{j}\left(n_3^{(5)} m^{(3)}-n_3^{(3)} m^{(2)}\right)+\mathrm{j}\frac{K_{em}^2\left(1+K_e^2\right)}{K_e^2\left(1+K_{em}^2\right)}\left(n_3^{(5)} m^{(2)}-n_3^{(3)} m^{(3)}\right)=0 \end{aligned} \quad \text{(VIII.3)}$$

It is worth noting that it is convenient to use in equation (VIII.3) such parameters from Chapter II as the CMEMC K_{em}^2 and the CEMC K_e^2 defined by expressions (II.19) and (II.21), respectively, in order to cope with non-dimensional values. Also, the non-dimensional value of γ_K^2 is defined by relation (II.59).

Equation (VIII.3) for the first set of the eigenvector components looks like equation (VII.8) for the second set of the eigenvector components from the previous chapter. However, there is the significant difference. It is as follows: the CEMC K_e^2 is used instead of the CMMC K_m^2. Therefore, the calculated two new SH-SAW velocities for equations (VIII.3) and (VII.8) cannot coincide. In the transversely isotropic case, they coincide. Therefore, it is possible to state that this fact demonstrates some dissimilarity of wave propagation in the transversely isotropic and cubic piezoelectromagnetics. Indeed, to study cubic piezoelectromagnetics is more complicated busyness.

For the second set of the eigenvector components, it is doable to demonstrate the following simplified BCD3 of the coefficient matrix in equation (VIII.1):

$$\begin{vmatrix} 0 & n_3^{(3)}m^{(2)} & n_3^{(5)}m^{(3)} \\ -(e\alpha - h\varepsilon)n_3^{(1)} & \begin{matrix} n_3^{(3)}\Big[e(e\mu - h\alpha)m^{(2)}\left(m^{(2)}-2\right) \\ +C\left(\varepsilon\mu-\alpha^2\right)m^{(2)}\left(m^{(2)}-\gamma_K^2\right) \\ -h(e\alpha-h\varepsilon)\left(m^{(2)}-2\right)^2\Big] \end{matrix} & \begin{matrix} n_3^{(5)}\Big[e(e\mu - h\alpha)m^{(3)}\left(m^{(3)}-2\right) \\ +C\left(\varepsilon\mu-\alpha^2\right)m^{(3)}\left(m^{(3)}-\gamma_K^2\right) \\ -h(e\alpha-h\varepsilon)\left(m^{(3)}-2\right)^2\Big] \end{matrix} \\ e & \begin{matrix} C\alpha m^{(2)}\left(m^{(2)}-\gamma_K^2\right) \\ +eh\left(m^{(2)}-2\right)^2 \end{matrix} & \begin{matrix} C\alpha m^{(3)}\left(m^{(3)}-\gamma_K^2\right) \\ +eh\left(m^{(3)}-2\right)^2 \end{matrix} \end{vmatrix} = 0 \quad \text{(VIII.4)}$$

The following secular equation can be readily written after expansion of the determinant in equation (VIII.4):

$$\begin{aligned} &en_3^{(5)}n_3^{(3)}m^{(3)}\left[e(e\mu-h\alpha)m^{(2)}\left(m^{(2)}-2\right)+C\left(\varepsilon\mu-\alpha^2\right)m^{(2)}\left(m^{(2)}-\gamma_K^2\right)-h(e\alpha-h\varepsilon)\left(m^{(2)}-2\right)^2\right] \\ &-\mathrm{j}(e\alpha-h\varepsilon)n_3^{(5)}m^{(3)}\left[C\alpha m^{(2)}\left(m^{(2)}-\gamma_K^2\right)+eh\left(m^{(2)}-2\right)^2\right] \\ &-en_3^{(5)}n_3^{(3)}m^{(2)}\left[e(e\mu-h\alpha)m^{(3)}\left(m^{(3)}-2\right)+C\left(\varepsilon\mu-\alpha^2\right)m^{(3)}\left(m^{(3)}-\gamma_K^2\right)-h(e\alpha-h\varepsilon)\left(m^{(3)}-2\right)^2\right] \\ &+\mathrm{j}(e\alpha-h\varepsilon)n_3^{(3)}m^{(2)}\left[C\alpha m^{(3)}\left(m^{(3)}-\gamma_K^2\right)+eh\left(m^{(3)}-2\right)^2\right]=0 \end{aligned} \quad \text{(VIII.5)}$$

Indeed, secular equation (VIII.5) can be also simplified. After some transformations, it is natural to write down the simplified equation in the following convenient form:

$$\begin{aligned} &\frac{e(e\mu-h\alpha)}{h(e\alpha-h\varepsilon)}n_3^{(3)}n_3^{(5)}\left(m^{(3)}-m^{(2)}\right)-\mathrm{j}\frac{K_{em}^2\left(\gamma_K^2+4K_\alpha^2\right)}{K_\alpha^2\left(1+K_{em}^2\right)}\left(n_3^{(5)}-n_3^{(3)}\right) \\ &+\mathrm{j}\left(n_3^{(5)}m^{(3)}-n_3^{(3)}m^{(2)}\right)+\mathrm{j}\frac{K_{em}^2\left(1+K_\alpha^2\right)}{K_\alpha^2\left(1+K_{em}^2\right)}\left(n_3^{(5)}m^{(2)}-n_3^{(3)}m^{(3)}\right)=0 \end{aligned} \quad \text{(VIII.6)}$$

where the non-dimensional parameters K_α^2, K_{em}^2, and γ_K^2 are defined by expressions (VII.5), (II.19), and (II.59), respectively. Note that the form of equation (VIII.6) is convenient for comparison with those in equations (VIII.3), (VII.4), and (VII.8).

Equation (VIII.6) for the second set of the eigenvector components looks like equation (VII.4) from the previous chapter for the first set. However, there is the significant difference only in the first terms of equations (VIII.6) and (VII.4). The difference is as follows: the first factor of the first term in equation (VIII.6), namely $e(e\mu - h\alpha)/[h(e\alpha - h\varepsilon)]$, is reverse to that in equation (VII.4). Also, it is clearly seen in equations (VIII.3) and (VIII.6) that the solution denoted by V_K (see the calculated values of V_K in table V.1 from Chapter V) exists as soon as $n_3^{(5)} = n_3^{(3)}$ and $m^{(3)} = m^{(2)}$.

Following the form in expression (VII.14) from the previous chapter, it is natural to write the expression for the new SH-SAW velocity denoted by V_{c2new}. It reads:

$$V_{c2new} = V_{tem}\sqrt{1-\left(b_{c2}\left(X_2\right)\right)^2} \tag{VIII.7}$$

Equation (VIII.7) also represents the recursive formula obtained from expression (VIII.3) or (VIII.6). The reader must read the previous chapter to obtain the complicated form of the parameter $b_{c2}(X_2)$ in expression (VIII.7). Indeed, it can be obtained from equation (VIII.3) or (VIII.6).

The calculated values of the second new SH-SAW velocity V_{c2new} for the case of the wave propagation in the cubic piezoelectromagnetics are listed in table VIII.1. They can be obtained using either of equations (VIII.3) and (VIII.6). Three values of the velocity V_{c2new} correspond to three values of the CMEMC K_{em}^2 (three values of the electromagnetic constant α) for each cubic piezoelectromagnetics listed in table III.3, see Chapter III. Table VIII.1 demonstrates the natural results that the values of the velocity V_{c2new} increase with the increase in the CMEMC K_{em}^2 that is to say with the decrease in α. This is like the results for the other SH-SAW velocities such as V_{BGM} and V_{c1new}. For the single composite with the small value of the CMEMC (K_{em}^2 < 1/3) listed in table VIII.1 such as Tl_3VS_4–Alfenol, one can find that there occurs the following: $V_{c2new} < V_{tem}$. For the other cubic piezoelectromagnetics with $K_{em}^2 > 1/3$ listed in table VIII.1, the values of the velocity V_{c2new} are positioned just below the corresponding values of V_K, where $V_K < V_{tem}$. It is also noted that the values of V_{BGM}, V_{tem}, and V_K for all the studied cubic piezoelectromagnetic composite materials are listed in table V.1, see Chapter V.

Table VIII.1. The calculated values of the new SH-SAW velocity V_{c2new} [m/s].

PEM composite	$(V_{c2new})_1$ $(V_{c2new})_2$ $(V_{c2new})_3$
Metglas–PZT-5H	3554.3878716718497 3572.6821740374885 3574.6835747917829
Tl_3TaSe_4–Terfenol-D	947.6264163156739 953.2374174241880 953.8455078350671
Tl_3VS_4–Galfenol	3472.4265705829890 3476.4066678095341 3477.0466261355771
Tl_3TaSe_4–Galfenol	3334.5037870085563 3338.8390415231202 3339.5042963396260
Tl_3VS_4–Alfenol	3136.8115385787345 3141.3468370027921 3141.8899674581957

Following the simplifications carried out in the previous chapter, it is convenient to cope with a two-term secular equation instead of either of four-term equations (VIII.3) and (VIII.6). First of all, it is natural to receive a three-term equation from one of two four-term equations by subtraction of equation (VIII.3) from equation (VIII.6), or vice versa. This procedure excludes the third term in one of the four-term equations. Next, the second and third terms in the resulting three-term equation can be regrouped to form only one term of them. So, the following two-term equation can be obtained to compare with that from the previous chapter:

$$K_e^2 K_\alpha^2 \left(1+K_{em}^2\right)\frac{C\left(\varepsilon\mu-\alpha^2\right)}{h\left(e\alpha-h\varepsilon\right)} n_3^{(3)} n_3^{(5)}\left(m^{(3)}-m^{(2)}\right)$$
$$+\mathrm{j}\left(K_e^2-K_\alpha^2\right)\left[n_3^{(5)}\left(m^{(2)}-\gamma_K^2\right)-n_3^{(3)}\left(m^{(3)}-\gamma_K^2\right)\right]=0 \tag{VIII.8}$$

This relatively compact form in equation (VIII.8) already allows demonstration of the following compact form for the parameter b_{c2} introduced in equation (VIII.7):

$$b_{c2}=n_3^{(3)} n_3^{(5)}=\frac{K_e^2-K_\alpha^2}{K_e^2 K_\alpha^2\left(1+K_{em}^2\right)}\frac{h\left(e\alpha-h\varepsilon\right)}{C\left(\varepsilon\mu-\alpha^2\right)}\frac{\mathrm{j}n_3^{(5)}\left(m^{(2)}-\gamma_K^2\right)-\mathrm{j}n_3^{(3)}\left(m^{(3)}-\gamma_K^2\right)}{m^{(3)}-m^{(2)}} \tag{VIII.9}$$

Indeed, equation (VIII.8) can be also transformed into the form of the sixth-degree polynomial. However, to compare complicated forms of sixth-degree polynomials with each other can be less informative than to compare the two-term compact forms given in equations (VII.20) and (VIII.8). Therefore, these two-term compact forms can be also compared with those obtained in the following chapters for the other possible sets of the electrical and magnetic boundary conditions.

This chapter and the previous three chapters coped with the theoretical investigations of SH-SAW propagation characteristics in cubic piezoelectromagnetics when there is no dependence on the material constants of the free space (vacuum) such as ε_0 and μ_0. The following five chapters use the electrical and magnetic boundary conditions, with which the vacuum material constants can be accounted in formulae for the calculations of new SH-SAW velocities.

CHAPTER IX. The Case of $B_3 = 0$ and Continuity of D_3 at $x_3 = 0$

In the case of magnetically closed surface ($B_3 = 0$ at $x_3 = 0$) and the continuity of the electrical displacement component D_3, one can also investigate wave propagation in cubic piezoelectromagnetics. It is also possible to compare this case of the cubic piezoelectromagnetics with the case of the transversely isotropic ones. According to the results of book [89] for the transversely isotropic piezoelectromagnetics, the discovered first SH-SAW velocity is defined by equation (163) for the first set of the eigenvector components and the discovered second one is defined by equation (194) for the second set of the components. Indeed, two possible sets of the eigenvector components are also used below for the case of the cubic piezoelectromagnetics.

Applying this set of the electrical and magnetic boundary condition, three equations for determination of the weight factors F_1, F_2, and F_3 can be written as follows:

$$\begin{pmatrix} k_3^{(1)}\left[CU^{0(1)} + e\varphi^{0(1)} + h\psi^{0(1)}\right] & k_3^{(3)}\left[CU^{0(3)} + e\varphi^{0(3)} + h\psi^{0(3)}\right] & k_3^{(5)}\left[CU^{0(5)} + e\varphi^{0(5)} + h\psi^{0(5)}\right] \\ ek_3^{(1)}U^{0(1)} - \left(\varepsilon k_3^{(1)} - \mathrm{j}\varepsilon_0 k_1\right)\varphi^{0(1)} - \alpha k_3^{(1)}\psi^{0(1)} & ek_3^{(3)}U^{0(3)} - \left(\varepsilon k_3^{(3)} - \mathrm{j}\varepsilon_0 k_1\right)\varphi^{0(3)} - \alpha k_3^{(3)}\psi^{0(3)} & ek_3^{(5)}U^{0(5)} - \left(\varepsilon k_3^{(5)} - \mathrm{j}\varepsilon_0 k_1\right)\varphi^{0(5)} - \alpha k_3^{(5)}\psi^{0(5)} \\ k_3^{(1)}\left[hU^{0(1)} - \alpha\varphi^{0(1)} - \mu\psi^{0(1)}\right] & k_3^{(3)}\left[hU^{0(3)} - \alpha\varphi^{0(3)} - \mu\psi^{0(3)}\right] & k_3^{(5)}\left[hU^{0(5)} - \alpha\varphi^{0(5)} - \mu\psi^{0(5)}\right] \end{pmatrix} \begin{pmatrix} F_1 \\ F_2 \\ F_3 \end{pmatrix} = \begin{pmatrix} 0 \\ 0 \\ 0 \end{pmatrix} \tag{IX.1}$$

Choosing the first set of the eigenvector components defined by expressions (II.26), (II.61), and (II.62) for the eigenvalues defined by corresponding expressions (II.25) and (II.29) from Chapter II, one can get the following BCD3 of the coefficient matrix in equation (IX.1):

$$
\begin{vmatrix}
0 & n_3^{(3)} m^{(2)} & n_3^{(5)} m^{(3)} \\
e\alpha - h(\varepsilon+\varepsilon_0) & \begin{matrix} -4e(e\alpha - h\varepsilon) n_3^{(3)} \\ -\mathrm{j}\varepsilon_0 \Big[C\alpha m^{(2)} \left(m^{(2)} - \gamma_K^2 \right) \\ + eh\left(m^{(2)} - 2 \right)^2 \Big] \end{matrix} & \begin{matrix} -4e(e\alpha - h\varepsilon) n_3^{(5)} \\ -\mathrm{j}\varepsilon_0 \Big[C\alpha m^{(3)} \left(m^{(3)} - \gamma_K^2 \right) \\ + eh\left(m^{(3)} - 2 \right)^2 \Big] \end{matrix} \\
e\mu - h\alpha & \begin{matrix} n_3^{(3)} \Big[h(e\alpha - h\varepsilon) m^{(2)} \left(m^{(2)} - 2 \right) \\ - C\left(\varepsilon\mu - \alpha^2 \right) m^{(2)} \left(m^{(2)} - \gamma_K^2 \right) \\ - e(e\mu - h\alpha)\left(m^{(2)} - 2 \right)^2 \Big] \end{matrix} & \begin{matrix} n_3^{(5)} \Big[h(e\alpha - h\varepsilon) m^{(3)} \left(m^{(3)} - 2 \right) \\ - C\left(\varepsilon\mu - \alpha^2 \right) m^{(3)} \left(m^{(3)} - \gamma_K^2 \right) \\ - e(e\mu - h\alpha)\left(m^{(3)} - 2 \right)^2 \Big] \end{matrix}
\end{vmatrix} = 0 \quad \text{(IX.2)}
$$

This boundary-condition determinant (BCD3) of the coefficient matrix in equation (IX.2) looks like a very complicated one compared with those from the previous chapters for the other electrical and magnetic boundary conditions. However, the reader can have attempts to transform it. First of all, it is necessary to expand it. Exploiting the well-known triangle rule for such determinants, the mathematical procedure of expansion of the BCD3 in equation (IX.2) results in the following complicated secular equation:

$$
\begin{aligned}
& -\mathrm{j}\varepsilon_0 (e\mu - h\alpha) n_3^{(3)} m^{(2)} \left[C\alpha m^{(3)} \left(m^{(3)} - \gamma_K^2 \right) + eh\left(m^{(3)} - 2 \right)^2 \right] \\
& + \left[e\alpha - h(\varepsilon + \varepsilon_0) \right] n_3^{(5)} n_3^{(3)} m^{(3)} \\
& \times \left[h(e\alpha - h\varepsilon) m^{(2)} \left(m^{(2)} - 2 \right) - C\left(\varepsilon\mu - \alpha^2 \right) m^{(2)} \left(m^{(2)} - \gamma_K^2 \right) - e(e\mu - h\alpha)\left(m^{(2)} - 2 \right)^2 \right] \\
& - 4e(e\mu - h\alpha)(e\alpha - h\varepsilon) n_3^{(5)} n_3^{(3)} m^{(2)} \\
& + \mathrm{j}\varepsilon_0 (e\mu - h\alpha) n_3^{(5)} m^{(3)} \left[C\alpha m^{(2)} \left(m^{(2)} - \gamma_K^2 \right) + eh\left(m^{(2)} - 2 \right)^2 \right] \\
& - \left[e\alpha - h(\varepsilon + \varepsilon_0) \right] n_3^{(5)} n_3^{(3)} m^{(2)} \\
& \times \left[h(e\alpha - h\varepsilon) m^{(3)} \left(m^{(3)} - 2 \right) - C\left(\varepsilon\mu - \alpha^2 \right) m^{(3)} \left(m^{(3)} - \gamma_K^2 \right) - e(e\mu - h\alpha)\left(m^{(3)} - 2 \right)^2 \right] \\
& + 4e(e\mu - h\alpha)(e\alpha - h\varepsilon) n_3^{(5)} n_3^{(3)} m^{(3)} = 0
\end{aligned} \quad \text{(IX.3)}
$$

All the terms of this complicated secular equation can be readily regrouped with the purpose of simplification. As a result, one can get the following form of secular equation (IX.3):

$$\frac{h(e\alpha-h\varepsilon)}{e(e\mu-h\alpha)}\left[1+\frac{\varepsilon}{\varepsilon_0}\frac{K_{em}^2}{K_m^2}\left(1-\frac{\alpha^2}{\varepsilon\mu}\right)\right]n_3^{(3)}n_3^{(5)}\left(m^{(3)}-m^{(2)}\right)-\mathrm{j}\frac{K_{em}^2\left(\gamma_K^2+4K_\alpha^2\right)}{K_\alpha^2\left(1+K_{em}^2\right)}\left(n_3^{(5)}-n_3^{(3)}\right)$$
$$+\mathrm{j}\left(n_3^{(5)}m^{(3)}-n_3^{(3)}m^{(2)}\right)+\mathrm{j}\frac{K_{em}^2\left(1+K_\alpha^2\right)}{K_\alpha^2\left(1+K_{em}^2\right)}\left(n_3^{(5)}m^{(2)}-n_3^{(3)}m^{(3)}\right)=0 \qquad \text{(IX.4)}$$

In equation (IX.4), the parameters such as K_α^2, K_{em}^2, K_m^2, and γ_K^2 are those used in equations (VII.4), (VII.8), and (VIII.6). These equations (IX.4), (VII.4), and (VIII.6) are represented in such convenient mathematical forms that one can compare them with each other. One can soundly find that each of these three obtained equations for determination of the corresponding phase velocities of the new SH-SAWs has its own unique first term. The other three terms are the same in the equations. Indeed, the first term in each equation has its own unique factor. These unique factors solidly demonstrate that the solutions for the SH-SAWs are independent.

The selection of the second set of the components defined by expressions (II.26), (II.63), and (II.64) for the same eigenvalues allows one to introduce the second BCD3 of the coefficient matrix in equation (IX.1). This BCD3 reads:

$$\begin{vmatrix} 0 & n_3^{(3)}m^{(2)} & n_3^{(5)}m^{(3)} \\ e\alpha-h(\varepsilon+\varepsilon_0) & \begin{matrix} n_3^{(3)}\left[e(e\mu-h\alpha)m^{(2)}\left(m^{(2)}-2\right)\right. \\ +C\left(\varepsilon\mu-\alpha^2\right)m^{(2)}\left(m^{(2)}-\gamma_K^2\right) \\ \left.-h(e\alpha-h\varepsilon)\left(m^{(2)}-2\right)^2\right] \\ -\mathrm{j}\varepsilon_0\left[C\mu m^{(2)}\left(m^{(2)}-\gamma_K^2\right)\right. \\ \left.+h^2\left(m^{(2)}-2\right)^2\right] \end{matrix} & \begin{matrix} n_3^{(5)}\left[e(e\mu-h\alpha)m^{(3)}\left(m^{(3)}-2\right)\right. \\ +C\left(\varepsilon\mu-\alpha^2\right)m^{(3)}\left(m^{(3)}-\gamma_K^2\right) \\ \left.-h(e\alpha-h\varepsilon)\left(m^{(3)}-2\right)^2\right] \\ -\mathrm{j}\varepsilon_0\left[C\mu m^{(3)}\left(m^{(3)}-\gamma_K^2\right)\right. \\ \left.+h^2\left(m^{(3)}-2\right)^2\right] \end{matrix} \\ 1 & -4hn_3^{(3)} & -4hn_3^{(5)} \end{vmatrix}=0 \qquad \text{(IX.5)}$$

The result of the expansion of this matrix BCD3 can be inscribed as follows:

$$
\begin{aligned}
&-4hn_3^{(3)}n_3^{(5)}m^{(3)}\left[e\alpha - h(\varepsilon+\varepsilon_0)\right] \\
&+n_3^{(3)}n_3^{(5)}m^{(2)}\left[e(e\mu - h\alpha)m^{(3)}\left(m^{(3)}-2\right)+C\left(\varepsilon\mu-\alpha^2\right)m^{(3)}\left(m^{(3)}-\gamma_K^2\right)-h(e\alpha-h\varepsilon)\left(m^{(3)}-2\right)^2\right] \\
&-\mathrm{j}\varepsilon_0 n_3^{(3)}m^{(2)}\left[C\mu m^{(3)}\left(m^{(3)}-\gamma_K^2\right)+h^2\left(m^{(3)}-2\right)^2\right] \\
&+4hn_3^{(3)}n_3^{(5)}m^{(2)}\left[e\alpha - h(\varepsilon+\varepsilon_0)\right] \\
&-n_3^{(3)}n_3^{(5)}m^{(3)}\left[e(e\mu - h\alpha)m^{(2)}\left(m^{(2)}-2\right)+C\left(\varepsilon\mu-\alpha^2\right)m^{(2)}\left(m^{(2)}-\gamma_K^2\right)-h(e\alpha-h\varepsilon)\left(m^{(2)}-2\right)^2\right] \\
&+\mathrm{j}\varepsilon_0 n_3^{(5)}m^{(3)}\left[C\mu m^{(2)}\left(m^{(2)}-\gamma_K^2\right)+h^2\left(m^{(2)}-2\right)^2\right]=0
\end{aligned}
\tag{IX.6}
$$

Indeed, the second secular equation given above in expression (IX.6) can be also transformed. The transformed form already consists of four terms. The final secular equation is as follows:

$$
\begin{aligned}
&\left[1+\frac{\varepsilon}{\varepsilon_0}\frac{K_{em}^2}{K_m^2}\left(1-\frac{\alpha^2}{\varepsilon\mu}\right)\right]n_3^{(3)}n_3^{(5)}\left(m^{(3)}-m^{(2)}\right)-\mathrm{j}\frac{K_{em}^2\left(\gamma_K^2+4K_m^2\right)}{K_m^2\left(1+K_{em}^2\right)}\left(n_3^{(5)}-n_3^{(3)}\right) \\
&+\mathrm{j}\left(n_3^{(5)}m^{(3)}-n_3^{(3)}m^{(2)}\right)+\mathrm{j}\frac{K_{em}^2\left(1+K_m^2\right)}{K_m^2\left(1+K_{em}^2\right)}\left(n_3^{(5)}m^{(2)}-n_3^{(3)}m^{(3)}\right)=0
\end{aligned}
\tag{IX.7}
$$

where the non-dimensional parameters K_m^2, K_{em}^2, and γ_K^2 are those used in expression (VII.8) and defined by expressions (II.22), (II.19), and (II.59) from Chapter II, respectively. Comparing the first term in equations (IX.7) with that in equation (VII.8), one can find the additional factor for the first term in equations (IX.7). This factor is always larger than unity for $K_{em}^2 > 1$.

Following the main purpose of the theoretical investigations described in the previous chapters, either of two secular equations (IX.4) and (IX.7) can reveal the new SH-SAW velocity, V_{c3new}. It can be written in the following recursive form:

$$
V_{c3new}=V_{tem}\sqrt{1-\left(b_{c3}(X_3)\right)^2}
\tag{IX.8}
$$

where the complicated form of the parameter b_{c3} is written using equation (IX.4) or (IX.7). This form is also significantly complicated when corresponding definitions for $n_3^{(3)}$, $n_3^{(5)}$, $m^{(2)}$, and $m^{(3)}$ in expressions (II.28) and (II.29) from the second chapter are substituted.

The theoretical study of wave propagation in the cubic piezoelectromagnetics carried out in this chapter provides the calculated values of the third new SH-SAW velocity V_{c3new}. The results of the computation are listed in table IX.1. These values of the velocity V_{c3new} can be calculated utilizing equation (IX.4) or (IX.7). In the table, three values of the velocity V_{c3new} correspond to three values of the CMEMC K_{em}^2. The values of K_{em}^2 in dependence on the electromagnetic constant α for each cubic piezoelectromagnetics are listed in table III.3 from the third chapter.

Table IX.1. The calculated values of the new SH-SAW velocity V_{c3new} [m/s].

PEM composite	$(V_{c3new})_1$ $(V_{c3new})_2$ $(V_{c3new})_3$
Metglas–PZT-5H	3678.4479731124811 3698.1419136252568 3700.2660912402382
Tl_3TaSe_4–Terfenol-D	974.3649294881972 982.2704558628170 983.1103176265559
Tl_3VS_4–Galfenol	3614.0777993502521 3620.0365742033507 3620.9895675434407
Tl_3TaSe_4–Galfenol	3470.6518693370964 3477.1059650032712 3478.0895042154676
Tl_3VS_4–Alfenol	3144.6741670471829 3149.9395825708184 3150.5724807593158

According to the results given in table IX.1, the value of V_{c3new} increases as soon as the value of K_{em}^2 increases. This is likely the results for the other SH-SAW velocities V_{BGM} , V_{c1new}, and V_{c2new}. In table IX.1, Tl_3VS_4–Alfenol with $K_{em}^2 < 1/3$ has the values of the velocity $V_{c3new} < V_{tem}$ and the others have the following condition for the SH-SAW velocity: $V_{c3new} < V_K < V_{tem}$. The reader can find the values of V_{BGM}, V_{tem}, and V_K in table V.1 (Chapter V) calculated for all the cubic composites.

It is also practicable to simplify equations (IX.4) and (IX.7). For this purpose, it is indispensable to exploit the mathematical procedures from the previous two chapters. Indeed, a subtraction of equation (IX.7) from equation (IX.4) can give a three-term equation which can be then reduced to the following two-term equation:

$$\begin{aligned}&-K_m^2K_\alpha^2\left(1+K_{em}^2\right)\frac{C\left(\varepsilon\mu-\alpha^2\right)}{e\left(e\mu-h\alpha\right)}\left[1+\frac{\varepsilon}{\varepsilon_0}\frac{K_{em}^2}{K_m^2}\left(1-\frac{\alpha^2}{\varepsilon\mu}\right)\right]n_3^{(3)}n_3^{(5)}\left(m^{(3)}-m^{(2)}\right)\\&+\mathrm{j}\left(K_m^2-K_\alpha^2\right)\left[n_3^{(5)}\left(m^{(2)}-\gamma_K^2\right)-n_3^{(3)}\left(m^{(3)}-\gamma_K^2\right)\right]=0\end{aligned}\qquad \text{(IX.9)}$$

This compact form is convenient for comparison with those given in equations (VII.20) and (VIII.8).

Equation (IX.9) can be readily used for demonstration of the following compact form for the parameter b_{c3} originated in expression (IX.8):

$$\begin{aligned}b_{c3}=n_3^{(3)}n_3^{(5)}&=-\frac{K_m^2-K_\alpha^2}{K_m^2K_\alpha^2\left(1+K_{em}^2\right)}\frac{e\left(e\mu-h\alpha\right)}{C\left(\varepsilon\mu-\alpha^2\right)}\frac{1}{1+\frac{\varepsilon}{\varepsilon_0}\frac{K_{em}^2}{K_m^2}\left(1-\frac{\alpha^2}{\varepsilon\mu}\right)}\\&\times\frac{\mathrm{j}n_3^{(5)}\left(m^{(2)}-\gamma_K^2\right)-\mathrm{j}n_3^{(3)}\left(m^{(3)}-\gamma_K^2\right)}{m^{(3)}-m^{(2)}}\end{aligned}\qquad \text{(IX.10)}$$

The following chapter also provides the theory for wave propagation in the cubic piezoelectromagnetics. It treats the case of the other set of the electrical and magnetic boundary conditions such as the electrically open surface ($D_3 = 0$) and the continuity of the magnetic flux component B_3.

CHAPTER X. The Case of $D_3 = 0$ and Continuity of B_3 at $x_3 = 0$

This chapter describes the wave propagation in the cubic piezoelectromagnetics in the case of the electrically open surface ($D_3 = 0$) and the continuity of the magnetic flux component B_3 above the crystal surface toward the free space, see figure II.1 from Chapter II. For the transversely isotropic piezoelectromagnetics studied in book [89], the discovered two SH-SAW velocities for the first and second sets of the eigenvector components are defined by expressions (180) and (163), respectively. For the case of the cubic piezoelectromagnetics studied in this chapter, two different sets of the eigenvector components defined by expression (II.26) and expressions from (II.61) to (II.64) also exist. They will be also used below. However, it is not possible to surely say that employment of these two sets can lead to two different solutions. In order to verify it, these two sets will be used below.

The utilisation of the electrically open surface ($D_3 = 0$) and the continuity of the component B_3 results in the following homogeneous equations written in a matrix form for convenience:

$$\begin{pmatrix} k_3^{(1)}\left[CU^{0(1)} + e\varphi^{0(1)} + h\psi^{0(1)}\right] & k_3^{(3)}\left[CU^{0(3)} + e\varphi^{0(3)} + h\psi^{0(3)}\right] & k_3^{(5)}\left[CU^{0(5)} + e\varphi^{0(5)} + h\psi^{0(5)}\right] \\ k_3^{(1)}\left[eU^{0(1)} - \varepsilon\varphi^{0(1)} - \alpha\psi^{0(1)}\right] & k_3^{(3)}\left[eU^{0(3)} - \varepsilon\varphi^{0(3)} - \alpha\psi^{0(3)}\right] & k_3^{(5)}\left[eU^{0(5)} - \varepsilon\varphi^{0(5)} - \alpha\psi^{0(5)}\right] \\ hk_3^{(1)}U^{0(1)} - \alpha k_3^{(1)}\varphi^{0(1)} - \left(\mu k_3^{(1)} - \mathrm{j}\mu_0 k_1\right)\psi^{0(1)} & hk_3^{(3)}U^{0(3)} - \alpha k_3^{(3)}\varphi^{0(3)} - \left(\mu k_3^{(3)} - \mathrm{j}\mu_0 k_1\right)\psi^{0(3)} & hk_3^{(5)}U^{0(5)} - \alpha k_3^{(5)}\varphi^{0(5)} - \left(\mu k_3^{(5)} - \mathrm{j}\mu_0 k_1\right)\psi^{0(5)} \end{pmatrix} \begin{pmatrix} F_1 \\ F_2 \\ F_3 \end{pmatrix} = \begin{pmatrix} 0 \\ 0 \\ 0 \end{pmatrix} \quad \text{(X.1)}$$

Therefore, the coefficient matrix in equation (X.1) possesses its own boundary-condition determinant (BCD3) which can be written as follows, using the first set of the eigenvector components:

$$\begin{vmatrix} 0 & n_3^{(3)} m^{(2)} & n_3^{(5)} m^{(3)} \\ 1 & -4e n_3^{(3)} & -4e n_3^{(5)} \\ e(\mu+\mu_0)-h\alpha & \begin{array}{l} n_3^{(3)}\Big[h(e\alpha-h\varepsilon)m^{(2)}\left(m^{(2)}-2\right) \\ -C\left(\varepsilon\mu-\alpha^2\right)m^{(2)}\left(m^{(2)}-\gamma_K^2\right) \\ -e(e\mu-h\alpha)\left(m^{(2)}-2\right)^2\Big] \\ +\mathrm{j}\mu_0\Big[C\varepsilon m^{(2)}\left(m^{(2)}-\gamma_K^2\right) \\ +e^2\left(m^{(2)}-2\right)^2\Big] \end{array} & \begin{array}{l} n_3^{(5)}\Big[h(e\alpha-h\varepsilon)m^{(3)}\left(m^{(3)}-2\right) \\ -C\left(\varepsilon\mu-\alpha^2\right)m^{(3)}\left(m^{(3)}-\gamma_K^2\right) \\ -e(e\mu-h\alpha)\left(m^{(3)}-2\right)^2\Big] \\ +\mathrm{j}\mu_0\Big[C\varepsilon m^{(3)}\left(m^{(3)}-\gamma_K^2\right) \\ +e^2\left(m^{(3)}-2\right)^2\Big] \end{array} \end{vmatrix} = 0 \tag{X.2}$$

To expand the BCD3 in equation (X.2), it is essential to use the well-known triangle rule for such determinants. Therefore, the following complicated secular equation can be obtained after expansion of this BCD3 in equation (X.2):

$$\begin{aligned} &-4e\left[e(\mu+\mu_0)-h\alpha\right]n_3^{(3)}n_3^{(5)}m^{(2)} \\ &+n_3^{(3)}n_3^{(5)}m^{(3)}\Big[h(e\alpha-h\varepsilon)m^{(2)}\left(m^{(2)}-2\right)-C\left(\varepsilon\mu-\alpha^2\right)m^{(2)}\left(m^{(2)}-\gamma_K^2\right)-e(e\mu-h\alpha)\left(m^{(2)}-2\right)^2\Big] \\ &+\mathrm{j}\mu_0 n_3^{(5)}m^{(3)}\Big[C\varepsilon m^{(2)}\left(m^{(2)}-\gamma_K^2\right)+e^2\left(m^{(2)}-2\right)^2\Big] \\ &+4e\left[e(\mu+\mu_0)-h\alpha\right]n_3^{(3)}n_3^{(5)}m^{(3)} \\ &-n_3^{(3)}n_3^{(5)}m^{(2)}\Big[h(e\alpha-h\varepsilon)m^{(3)}\left(m^{(3)}-2\right)-C\left(\varepsilon\mu-\alpha^2\right)m^{(3)}\left(m^{(3)}-\gamma_K^2\right)-e(e\mu-h\alpha)\left(m^{(3)}-2\right)^2\Big] \\ &-\mathrm{j}\mu_0 n_3^{(3)}m^{(2)}\Big[C\varepsilon m^{(3)}\left(m^{(3)}-\gamma_K^2\right)+e^2\left(m^{(3)}-2\right)^2\Big]=0 \end{aligned} \tag{X.3}$$

It is necessary to state that this complicated equation needs to be simplified. After, some transformation, it is possible to give a relatively simple form for the secular equation. This simplified form is written below in equation (X.4). Indeed, the following form is ideal for comparison with equation (VIII.3 from Chapter VIII:

$$\left[1+\frac{\mu}{\mu_0}\frac{K_{em}^2}{K_e^2}\left(1-\frac{\alpha^2}{\varepsilon\mu}\right)\right]n_3^{(3)}n_3^{(5)}\left(m^{(3)}-m^{(2)}\right)-\mathrm{j}\frac{K_{em}^2\left(\gamma_K^2+4K_e^2\right)}{K_e^2\left(1+K_{em}^2\right)}\left(n_3^{(5)}-n_3^{(3)}\right)$$
$$+\mathrm{j}\left(n_3^{(5)}m^{(3)}-n_3^{(3)}m^{(2)}\right)+\mathrm{j}\frac{K_{em}^2\left(1+K_e^2\right)}{K_e^2\left(1+K_{em}^2\right)}\left(n_3^{(5)}m^{(2)}-n_3^{(3)}m^{(3)}\right)=0 \quad \text{(X.4)}$$

where all the parameters such as K_e^2, K_{em}^2, and γ_K^2 are defined by expressions (II.21), (II.19), and (II.59) from Chapter II, respectively, and represent the non-dimensional values for convenience.

It is also possible to discuss the comparison of equation (X.4) with equation (VIII.3) from Chapter VIII. It is clearly seen that equation (X.4) looks like equation (VIII.3). However, the single difference occurs. The first term in equation (X.4) has the additional factor which is deficient in the first term of equation (VIII.3). It is obvious that this factor must always be larger than unity for the CMEMC $K_{em}^2 > 0$. However, the situation when $K_{em}^2 = 0$ can also occur. This is the particular and very interesting case when $V_{tem} = V_{t4}$.

Exploiting the second set of the eigenvector components for equation (X.1), the corresponding BCD3 reads:

$$\begin{vmatrix} 0 & n_3^{(3)}m^{(2)} & n_3^{(5)}m^{(3)} \\ e\alpha-h\varepsilon & \begin{gathered} n_3^{(3)}\Big[e(e\mu-h\alpha)m^{(2)}\left(m^{(2)}-2\right) \\ +C\left(\varepsilon\mu-\alpha^2\right)m^{(2)}\left(m^{(2)}-\gamma_K^2\right) \\ -h(e\alpha-h\varepsilon)\left(m^{(2)}-2\right)^2\Big] \end{gathered} & \begin{gathered} n_3^{(5)}\Big[e(e\mu-h\alpha)m^{(3)}\left(m^{(3)}-2\right) \\ +C\left(\varepsilon\mu-\alpha^2\right)m^{(3)}\left(m^{(3)}-\gamma_K^2\right) \\ -h(e\alpha-h\varepsilon)\left(m^{(3)}-2\right)^2\Big] \end{gathered} \\ e(\mu+\mu_0)-h\alpha & \begin{gathered} -4h(e\mu-h\alpha)n_3^{(3)} \\ +\mathrm{j}\mu_0\Big[C\alpha m^{(2)}\left(m^{(2)}-\gamma_K^2\right) \\ +eh\left(m^{(2)}-2\right)^2\Big] \end{gathered} & \begin{gathered} -4h(e\mu-h\alpha)n_3^{(5)} \\ +\mathrm{j}\mu_0\Big[C\alpha m^{(3)}\left(m^{(3)}-\gamma_K^2\right) \\ +eh\left(m^{(3)}-2\right)^2\Big] \end{gathered} \end{vmatrix}=0 \quad \text{(X.5)}$$

This BCD3 written above can be also expanded by the same way using the well-known triangle rule. As the result, one can obtain the second possible secular equation for this case of the electrical and magnetic boundary conditions. This secular equation reads:

$$
\begin{aligned}
&-4h(e\alpha-h\varepsilon)(e\mu-h\alpha)n_3^{(3)}n_3^{(5)}m^{(3)}+\\
&\mathrm{j}\mu_0(e\alpha-h\varepsilon)n_3^{(5)}m^{(3)}\left[C\alpha m^{(2)}\left(m^{(2)}-\gamma_K^2\right)+eh\left(m^{(2)}-2\right)^2\right]+\\
&\left[e(\mu+\mu_0)-h\alpha\right]n_3^{(3)}n_3^{(5)}m^{(2)}\times\\
&\left[e(e\mu-h\alpha)m^{(3)}\left(m^{(3)}-2\right)+C\left(\varepsilon\mu-\alpha^2\right)m^{(3)}\left(m^{(3)}-\gamma_K^2\right)-h(e\alpha-h\varepsilon)\left(m^{(3)}-2\right)^2\right]+\\
&4h(e\alpha-h\varepsilon)(e\mu-h\alpha)n_3^{(3)}n_3^{(5)}m^{(2)}-\\
&\mathrm{j}\mu_0(e\alpha-h\varepsilon)n_3^{(3)}m^{(2)}\left[C\alpha m^{(3)}\left(m^{(3)}-\gamma_K^2\right)+eh\left(m^{(3)}-2\right)^2\right]-\\
&\left[e(\mu+\mu_0)-h\alpha\right]n_3^{(3)}n_3^{(5)}m^{(3)}\times\\
&\left[e(e\mu-h\alpha)m^{(2)}\left(m^{(2)}-2\right)+C\left(\varepsilon\mu-\alpha^2\right)m^{(2)}\left(m^{(2)}-\gamma_K^2\right)-h(e\alpha-h\varepsilon)\left(m^{(2)}-2\right)^2\right]=0
\end{aligned}
\tag{X.6}
$$

Several suitable transformations applied to complicated equation (X.6) can lead to the following simplified and convenient form:

$$
\begin{aligned}
&\frac{e(e\mu-h\alpha)}{h(e\alpha-h\varepsilon)}\left[1+\frac{\mu}{\mu_0}\frac{K_{em}^2}{K_e^2}\left(1-\frac{\alpha^2}{\varepsilon\mu}\right)\right]n_3^{(3)}n_3^{(5)}\left(m^{(3)}-m^{(2)}\right)-\mathrm{j}\frac{K_{em}^2\left(\gamma_K^2+4K_\alpha^2\right)}{K_\alpha^2\left(1+K_{em}^2\right)}\left(n_3^{(5)}-n_3^{(3)}\right)\\
&+\mathrm{j}\left(n_3^{(5)}m^{(3)}-n_3^{(3)}m^{(2)}\right)+\mathrm{j}\frac{K_{em}^2\left(1+K_\alpha^2\right)}{K_\alpha^2\left(1+K_{em}^2\right)}\left(n_3^{(5)}m^{(2)}-n_3^{(3)}m^{(3)}\right)=0
\end{aligned}
\tag{X.7}
$$

where the non-dimensional parameters $K_{em}{}^2$, $K_e{}^2$, and $\gamma_K{}^2$ are those used in equation (X.4). Also, the non-dimensional parameter $K_\alpha{}^2$ is defined by relation (VII.5) from Chapter VII.

Comparing the results of this chapter given in equations (X.4) and (X.7) with the results obtained in Chapters from VII to IX, the reader can find that two secular equations (IX.4) and (IX.7) can also reveal the new SH-SAW velocity, V_{c4new}. Indeed, it can be also written in the recursive form given below:

$$
V_{c4new}=V_{tem}\sqrt{1-\left(b_{c4}(X_4)\right)^2}
\tag{X.8}
$$

where the complicated parameter b_{c4} can be found, for instance, from equation (X.4) or (X.7).

Utilizing equation (X.4) or (X.7), it is possible to compute the values of the fourth new SH-SAW velocity V_{c4new}. These values are listed in table X.1 for all the studied cubic piezoelectromagnetics. Similar to the results obtained in the previous chapters, the application of both the sets of the eigenvector components leads to the same phase velocity denoted by V_{c4new}. It was already mentioned that this fact is the main difference between the wave propagation in the cubic piezoelectromagnetics and that in the transversely isotropic composite materials. In table X.1, three values of the velocity V_{c4new} correspond to three values of K_{em}^2 which depend on the different values of the electromagnetic constant α, see table III.3 from the third chapter.

Table X.1. The calculated values of the new SH-SAW velocity V_{c4new} [m/s].

PEM composite	$(V_{c4new})_1$ $(V_{c4new})_2$ $(V_{c4new})_3$
Metglas–PZT-5H	3678.4479703684924 3698.1419135014436 3700.2660913871003
Tl_3TaSe_4–Terfenol-D	963.5122839970316 971.0154599165743 971.8214867922123
Tl_3VS_4–Galfenol	3613.9118960143485 3619.8874296985671 3620.8425795290979
Tl_3TaSe_4–Galfenol	3470.4987153452582 3476.9776066953124 3477.9654008755682
Tl_3VS_4–Alfenol	3144.6597055299464 3149.9240289840432 3150.5567694878639

Table X.1 soundly demonstrates that the values of the fourth new SH-SAW velocity V_{c4new} are increased as soon as any increase in the value of the CMEMC K_{em}^2 occurs. This behavior is analogical to those of the other SH-SAW velocities V_{BGM} , V_{c1new}, V_{c2new}, and V_{c3new}, for which the values can be found in the previous chapters. It is worth noticing that the single cubic piezoelectromagnetics with $K_{em}^2 < 1/3$ in table X.1 such as Tl_3VS_4–Alfenol possesses the values of the velocity V_{c4new} positioned just below the corresponding values of the SH-BAW velocity V_{tem}. The other cubic piezoelectromagnetics listed in the table possess their corresponding values of the velocity $V_{c4new} < V_K < V_{tem}$. Table V.1 from Chapter V lists all the values of V_{BGM}, V_{tem}, and V_K calculated for all the cubic piezoelectromagnetics.

The two-term secular equation can be also received in this case by the same transformations described in the previous chapters. A subtraction of equation (X.4) from equation (X.7) and then regrouping the last terms can result in the following expression:

$$\begin{aligned} &K_e^2 K_\alpha^2\left(1+K_{em}^2\right)\frac{C\left(\varepsilon\mu-\alpha^2\right)}{h\left(e\alpha-h\varepsilon\right)}\left[1+\frac{\mu}{\mu_0}\frac{K_{em}^2}{K_e^2}\left(1-\frac{\alpha^2}{\varepsilon\mu}\right)\right]n_3^{(3)}n_3^{(5)}\left(m^{(3)}-m^{(2)}\right) \\ &+\mathrm{j}\left(K_e^2-K_\alpha^2\right)\left[n_3^{(5)}\left(m^{(2)}-\gamma_K^2\right)-n_3^{(3)}\left(m^{(3)}-\gamma_K^2\right)\right]=0 \end{aligned} \quad \text{(X.9)}$$

Equation (X.9) is also convenient for comparison with the compact forms of the other secular equations given in expressions (VII.20), (VIII.8), and (IX.9) from the previous three chapters.

The parameter b_{c4} from expression (X.8) can be expressed using equation (X.9). For this set of the electrical and magnetic boundary conditions, it reads as follows:

$$\begin{aligned} b_{c4}=n_3^{(3)}n_3^{(5)}=&\frac{K_e^2-K_\alpha^2}{K_e^2K_\alpha^2\left(1+K_{em}^2\right)}\frac{h\left(e\alpha-h\varepsilon\right)}{C\left(\varepsilon\mu-\alpha^2\right)}\frac{1}{1+\dfrac{\mu}{\mu_0}\dfrac{K_{em}^2}{K_e^2}\left(1-\dfrac{\alpha^2}{\varepsilon\mu}\right)} \\ &\times\frac{\mathrm{j}n_3^{(5)}\left(m^{(2)}-\gamma_K^2\right)-\mathrm{j}n_3^{(3)}\left(m^{(3)}-\gamma_K^2\right)}{m^{(3)}-m^{(2)}} \end{aligned} \quad \text{(X.10)}$$

It is thought that the last three chapters can reveal more complicated solutions. However, they can be represented following the results obtained in this chapter and the previous several chapters.

CHAPTER XI. The Case of $\psi = 0$ and Continuity of D_3 at $x_3 = 0$

It is natural to also treat the case of the magnetically open surface ($\psi = 0$) and the continuity of the electrical displacement component D_3 when the wave propagation in the cubic piezoelectromagnetics is studied. First of all, it is indispensable to give the results of the study concerning the wave propagation in the transversely isotropic piezoelectromagnetics when the same boundary conditions were applied in book [89]. This recently published book cited in Ref. [89] provides two SH-SAW velocities defined by expressions (148) and (120) for the first and second sets of the eigenvector components, respectively. It is thought that exploitation of two possible sets of the eigenvector components in the case of the cubic piezoelectromagnetics can also reveal some new result.

Focusing of attention on the boundary conditions such as $\sigma_{23} = 0$, the continuity of the component D_3, and $\psi = 0$ leads to the following three equations written in the matrix form which must be resolved:

$$\begin{pmatrix} k_3^{(1)}\left[CU^{0(1)} + e\varphi^{0(1)} + h\psi^{0(1)}\right] & k_3^{(3)}\left[CU^{0(3)} + e\varphi^{0(3)} + h\psi^{0(3)}\right] & k_3^{(5)}\left[CU^{0(5)} + e\varphi^{0(5)} + h\psi^{0(5)}\right] \\ ek_3^{(1)}U^{0(1)} - \left(\varepsilon k_3^{(1)} - \mathrm{j}\varepsilon_0 k_1\right)\varphi^{0(1)} - \alpha k_3^{(1)}\psi^{0(1)} & ek_3^{(3)}U^{0(3)} - \left(\varepsilon k_3^{(3)} - \mathrm{j}\varepsilon_0 k_1\right)\varphi^{0(3)} - \alpha k_3^{(3)}\psi^{0(3)} & ek_3^{(5)}U^{0(5)} - \left(\varepsilon k_3^{(5)} - \mathrm{j}\varepsilon_0 k_1\right)\varphi^{0(5)} - \alpha k_3^{(5)}\psi^{0(5)} \\ \psi^{0(1)} & \psi^{0(3)} & \psi^{0(5)} \end{pmatrix} \begin{pmatrix} F_1 \\ F_2 \\ F_3 \end{pmatrix} = \begin{pmatrix} 0 \\ 0 \\ 0 \end{pmatrix} \tag{XI.1}$$

In order to resolve the system of three homogeneous equations written above, it is necessary to find such solution for the phase velocity V_{ph} which changes the sign of the determinant BCD3 of the coefficient matrix in equation (XI.1). Therefore, it is necessary to require for the BCD3 corresponding to the first set of the eigenvector components to satisfy the following equality:

$$
\begin{vmatrix}
0 & n_3^{(3)}m^{(2)} & n_3^{(5)}m^{(3)} \\
\mathrm{j}[e\alpha - h(\varepsilon+\varepsilon_0)] & \begin{array}{l} -4e(e\alpha - h\varepsilon)n_3^{(3)} \\ -\mathrm{j}\varepsilon_0\Big[C\alpha m^{(2)}\left(m^{(2)}-\gamma_K^2\right) \\ +eh\left(m^{(2)}-2\right)^2\Big] \end{array} & \begin{array}{l} -4e(e\alpha - h\varepsilon)n_3^{(5)} \\ -\mathrm{j}\varepsilon_0\Big[C\alpha m^{(3)}\left(m^{(3)}-\gamma_K^2\right) \\ +eh\left(m^{(3)}-2\right)^2\Big] \end{array} \\
e & \begin{array}{l} C\varepsilon m^{(2)}\left(m^{(2)}-\gamma_K^2\right) \\ +e^2\left(m^{(2)}-2\right)^2 \end{array} & \begin{array}{l} C\varepsilon m^{(3)}\left(m^{(3)}-\gamma_K^2\right) \\ +e^2\left(m^{(3)}-2\right)^2 \end{array}
\end{vmatrix} = 0 \quad \text{(XI.2)}
$$

This equality can be written in the form of secular equation by means of expansion of the BCD3 in equation (XI.2). Therefore, it is possible to obtain the following complex secular equation for the first set of the eigenvector components:

$$
\begin{aligned}
&-4e(e\alpha - h\varepsilon)n_3^{(3)}n_3^{(5)}m^{(2)} \\
&-\mathrm{j}\varepsilon_0 e n_3^{(3)}m^{(2)}\Big[C\alpha m^{(3)}\left(m^{(3)}-\gamma_K^2\right)+eh\left(m^{(3)}-2\right)^2\Big] \\
&+\mathrm{j}[e\alpha - h(\varepsilon+\varepsilon_0)]n_3^{(5)}m^{(3)}\Big[C\varepsilon m^{(2)}\left(m^{(2)}-\gamma_K^2\right)+e^2\left(m^{(2)}-2\right)^2\Big] \\
&+4e(e\alpha - h\varepsilon)n_3^{(3)}n_3^{(5)}m^{(3)} \\
&+\mathrm{j}\varepsilon_0 e n_3^{(5)}m^{(3)}\Big[C\alpha m^{(2)}\left(m^{(2)}-\gamma_K^2\right)+eh\left(m^{(2)}-2\right)^2\Big] \\
&-\mathrm{j}[e\alpha - h(\varepsilon+\varepsilon_0)]n_3^{(3)}m^{(2)}\Big[C\varepsilon m^{(3)}\left(m^{(3)}-\gamma_K^2\right)+e^2\left(m^{(3)}-2\right)^2\Big]=0
\end{aligned} \quad \text{(XI.3)}
$$

Secular equation (XI.3) can be also led to the mathematical form consisting of four terms. This four-term form is used in this work for the case of cubic piezoelectromagnetics, because such form is convenient for comparison of all the obtained solutions with each other. Therefore, the ninth four-term form which represents the unique equation is as follows:

$$
\begin{aligned}
&n_3^{(3)}n_3^{(5)}\left(m^{(3)}-m^{(2)}\right)-\mathrm{j}\frac{K_{em}^2}{K_e^2\left(1+K_{em}^2\right)}\left(\gamma_K^2+\gamma_K^2\frac{\varepsilon_0}{\varepsilon}+4K_e^2\right)\left(n_3^{(5)}-n_3^{(3)}\right) \\
&+\mathrm{j}\left(n_3^{(5)}m^{(3)}-n_3^{(3)}m^{(2)}\right)+\mathrm{j}\frac{K_{em}^2}{K_e^2\left(1+K_{em}^2\right)}\left(1+\frac{\varepsilon_0}{\varepsilon}+K_e^2\right)\left(n_3^{(5)}m^{(2)}-n_3^{(3)}m^{(3)}\right)=0
\end{aligned} \quad \text{(XI.4)}
$$

where the non-dimensional parameters such as the CMEMC $K_{em}{}^2$, CEMC $K_e{}^2$, and $\gamma_K{}^2$ are those used in equations (X.4) and (X.7).

As soon as the second set of the eigenvector components is used instead of the first one, the following BCD3 must also equal to zero:

$$
\begin{vmatrix}
0 & n_3^{(3)} m^{(2)} & n_3^{(5)} m^{(3)} \\
\mathrm{j}[e\alpha - h(\varepsilon + \varepsilon_0)] &
\begin{array}{l}
n_3^{(3)}\Big[e(e\mu - h\alpha)m^{(2)}\left(m^{(2)} - 2\right) \\
+ C\left(\varepsilon\mu - \alpha^2\right)m^{(2)}\left(m^{(2)} - \gamma_K^2\right) \\
- h(e\alpha - h\varepsilon)\left(m^{(2)} - 2\right)^2\Big] \\
- \mathrm{j}\varepsilon_0\Big[C\mu m^{(2)}\left(m^{(2)} - \gamma_K^2\right) \\
+ h^2\left(m^{(2)} - 2\right)^2\Big]
\end{array} &
\begin{array}{l}
n_3^{(5)}\Big[e(e\mu - h\alpha)m^{(3)}\left(m^{(3)} - 2\right) \\
+ C\left(\varepsilon\mu - \alpha^2\right)m^{(3)}\left(m^{(3)} - \gamma_K^2\right) \\
- h(e\alpha - h\varepsilon)\left(m^{(3)} - 2\right)^2\Big] \\
- \mathrm{j}\varepsilon_0\Big[C\mu m^{(3)}\left(m^{(3)} - \gamma_K^2\right) \\
+ h^2\left(m^{(3)} - 2\right)^2\Big]
\end{array} \\
e &
\begin{array}{l}
C\alpha m^{(2)}\left(m^{(2)} - \gamma_K^2\right) \\
+ eh\left(m^{(2)} - 2\right)^2
\end{array} &
\begin{array}{l}
C\alpha m^{(3)}\left(m^{(3)} - \gamma_K^2\right) \\
+ eh\left(m^{(3)} - 2\right)^2
\end{array}
\end{vmatrix} = 0 \tag{XI.5}
$$

Note that a determinant represents a number and the BCD3 in equation (XI.5) must vanish because expression (XI.1) corresponds to three homogeneous equations. Expanding the boundary-condition determinant (BCD3) in equation (XI.5), one can obtain the following secular equation:

$$
\begin{aligned}
& e n_3^{(3)} n_3^{(5)} m^{(2)} \\
& \times \Big[e(e\mu - h\alpha)m^{(3)}\left(m^{(3)} - 2\right) + C\left(\varepsilon\mu - \alpha^2\right)m^{(3)}\left(m^{(3)} - \gamma_K^2\right) - h(e\alpha - h\varepsilon)\left(m^{(3)} - 2\right)^2\Big] \\
& - \mathrm{j}e\varepsilon_0 n_3^{(3)} m^{(2)}\Big[C\mu m^{(3)}\left(m^{(3)} - \gamma_K^2\right) + h^2\left(m^{(3)} - 2\right)^2\Big] \\
& + \mathrm{j}[e\alpha - h(\varepsilon + \varepsilon_0)] n_3^{(5)} m^{(3)}\Big[C\alpha m^{(2)}\left(m^{(2)} - \gamma_K^2\right) + eh\left(m^{(2)} - 2\right)^2\Big] \\
& - e n_3^{(3)} n_3^{(5)} m^{(3)} \\
& \times \Big[e(e\mu - h\alpha)m^{(2)}\left(m^{(2)} - 2\right) + C\left(\varepsilon\mu - \alpha^2\right)m^{(2)}\left(m^{(2)} - \gamma_K^2\right) - h(e\alpha - h\varepsilon)\left(m^{(2)} - 2\right)^2\Big] \\
& + \mathrm{j}e\varepsilon_0 n_3^{(5)} m^{(3)}\Big[C\mu m^{(2)}\left(m^{(2)} - \gamma_K^2\right) + h^2\left(m^{(2)} - 2\right)^2\Big] \\
& - \mathrm{j}[e\alpha - h(\varepsilon + \varepsilon_0)] n_3^{(3)} m^{(2)}\Big[C\alpha m^{(3)}\left(m^{(3)} - \gamma_K^2\right) + eh\left(m^{(3)} - 2\right)^2\Big] = 0
\end{aligned} \tag{XI.6}
$$

The terms in equation (XI.6) can be also regrouped. After regrouping and some simplifications, secular equation (XI.6) transforms into the following non-dimensional expression formed by four terms:

$$
\begin{aligned}
&\frac{e(e\mu - h\alpha)}{h(e\alpha - h\varepsilon)} n_3^{(3)} n_3^{(5)} \left(m^{(3)} - m^{(2)}\right) \\
&- \mathrm{j}\frac{K_{em}^2}{K_\alpha^2\left(1+K_{em}^2\right)}\left(\gamma_K^2 + \gamma_K^2 \frac{\varepsilon_0}{\varepsilon}\frac{K_\alpha^2}{K_e^2}\frac{e(e\mu - h\alpha)}{h(e\alpha - h\varepsilon)} + 4K_\alpha^2\right)\left(n_3^{(5)} - n_3^{(3)}\right) \\
&+ \mathrm{j}\left(n_3^{(5)} m^{(3)} - n_3^{(3)} m^{(2)}\right) \\
&+ \mathrm{j}\frac{K_{em}^2}{K_\alpha^2\left(1+K_{em}^2\right)}\left(1 + \frac{\varepsilon_0}{\varepsilon}\frac{K_\alpha^2}{K_e^2}\frac{e(e\mu - h\alpha)}{h(e\alpha - h\varepsilon)} + K_\alpha^2\right)\left(n_3^{(5)} m^{(2)} - n_3^{(3)} m^{(3)}\right) = 0
\end{aligned}
\tag{XI.7}
$$

where the non-dimensional parameters such as K_{em}^2, K_e^2, and γ_K^2 are those used in equations (XI.4), (X.4), and (X.7). Also, the parameter K_α^2 is defined by relation (VII.5) from Chapter VII.

It is obvious that equations (XI.4) and (XI.7) are also unique. Therefore, either of them can numerically reveal the fifth new SH-SAW velocity for the case of wave propagation in the cubic piezoelectromagnetics. It is natural to denote the velocity by V_{c5new}. Following the forms for the other new SH-SAW velocities obtained in the previous chapters, it is possible to write the following recursive relation for determination of this new velocity denoted by V_{c5new}:

$$
V_{c5new} = V_{tem}\sqrt{1 - \left(b_{c5}\left(X_5\right)\right)^2} \tag{XI.8}
$$

where the complicated parameter b_{c5} under the square root is found from equation (XI.4) or (XI.7).

For this set of the electrical and magnetic boundary conditions applied to the free surface of the cubic piezoelectromagnetics, the values of the fifth new SH-SAW velocity, V_{c5new}, were computed and they are listed in table XI.1. Indeed, it is also possible to compare the values of the velocity V_{c5new} with those of the following SH-

SAW velocities (see the previous chapters): V_{BGM} , V_{c1new}, V_{c2new}, V_{c3new}, and V_{c4new}. It is natural that the values of the velocity V_{c5new} are located below either the SH-BAW velocity V_{tem} for the cubic piezoelectromagnetics with $K_{em}^2 < 1/3$ or the solution V_K for the ones with $K_{em}^2 > 1/3$. In table XI.1, three values of the velocity V_{c5new} correspond to three values of K_{em}^2 (see table III.3 in Chapter III). Also, it is necessary to mention that table V.1 from Chapter V lists all the values of V_{BGM}, V_{tem}, and V_K calculated for all the cubic piezoelectromagnetics.

Table XI.1. The calculated values of the new SH-SAW velocity V_{c5new} [m/s].

PEM composite	$(V_{c5new})_1$ $(V_{c5new})_2$ $(V_{c5new})_3$
Metglas–PZT-5H	3554.3222801970332 3572.6175241654119 3574.6190358400683
Tl_3TaSe_4–Terfenol-D	945.6208035378705 951.2038035564396 951.8093548193600
Tl_3VS_4–Galfenol	3472.2535215223269 3476.2331705701350 3476.8730585515777
Tl_3TaSe_4–Galfenol	3333.9117323014363 3338.2452779669583 3338.9102777224558
Tl_3VS_4–Alfenol	3136.7360251425249 3141.2685996043768 3141.8114067959477

A subtraction of equation (XI.4) from equation (XI.7) and then regrouping the last terms can result in the convenient simplifications. As a result, the two-term secular equation can be also obtained for this set of the boundary conditions. After the applied simplifications, the resulting two-term expression reads:

$$
\begin{aligned}
&K_e^2 K_\alpha^2 \left(1 + K_{em}^2\right) \frac{C\left(\varepsilon\mu - \alpha^2\right)}{h(e\alpha - h\varepsilon)} n_3^{(3)} n_3^{(5)} \left(m^{(3)} - m^{(2)}\right) \\
&+ \mathrm{j}\left[K_e^2 - K_\alpha^2 + \frac{\varepsilon_0}{\varepsilon} K_\alpha^2 K_{em}^2 \frac{C\left(\varepsilon\mu - \alpha^2\right)}{h(e\alpha - h\varepsilon)}\right]\left[n_3^{(5)}\left(m^{(2)} - \gamma_K^2\right) - n_3^{(3)}\left(m^{(3)} - \gamma_K^2\right)\right] = 0
\end{aligned}
\tag{XI.9}
$$

Equation (XI.9) is written in the convenient compact form which is actually suitable for comparison with those given in expressions (VII.20), (VIII.8), (IX.9), and (X.9) from the previous chapters.

Using equation (XI.9), the parameter b_{c5} from expression (XI.8) can be also expressed in the following compact form:

$$
\begin{aligned}
b_{c5} = n_3^{(3)} n_3^{(5)} = &\left[\frac{K_e^2 - K_\alpha^2}{K_e^2 K_\alpha^2 \left(1 + K_{em}^2\right)} \frac{h(e\alpha - h\varepsilon)}{C\left(\varepsilon\mu - \alpha^2\right)} + \frac{\varepsilon_0}{\varepsilon} \frac{K_{em}^2}{K_e^2 \left(1 + K_{em}^2\right)}\right] \\
&\times \frac{\mathrm{j} n_3^{(5)}\left(m^{(2)} - \gamma_K^2\right) - \mathrm{j} n_3^{(3)}\left(m^{(3)} - \gamma_K^2\right)}{m^{(3)} - m^{(2)}}
\end{aligned}
\tag{XI.10}
$$

The study of the cubic piezoelectromagnetics is continued in the following chapter. Chapter XII uses the case of the electrically closed surface ($\varphi = 0$) and the continuity of the magnetic flux component B_3 of the boundary conditions. Therefore, it is expected that the reader can find in the following chapter that the wave characteristics, namely the SH-SAW velocity can be also different from those discovered in this chapter and the previous chapters.

CHAPTER XII. The Case of $\varphi = 0$ and Continuity of B_3 at $x_3 = 0$

For the case of the electrically closed surface ($\varphi = 0$ at $x_3 = 0$) and the continuity of the magnetic flux component B_3, the acoustic waves guided by the free surface shown in figure II.1 can also propagate along direction [101] in the cubic piezoelectromagnetics. Utilizing the same boundary conditions for the problem of wave propagation in the transversely isotropic piezoelectromagnetics, two SH-SAW velocities can exist. They are defined by the explicit forms of equations (108) and (133) obtained in Ref. [89], respectively. These forms correspond to the first and second sets of the eigenvector components. Indeed, it is fundamental to treat the both sets of the corresponding eigenvector components for the problem of wave propagation in the cubic piezoelectromagnetics.

So, it is essential to write down three equations which correspond to three boundary conditions: one mechanical such as $\sigma_{23} = 0$, one electrical ($\varphi = 0$), and one magnetic (continuity of the component B_3) conditions. Indeed, they can be written in the following matrix form:

$$\begin{pmatrix} k_3^{(1)}\left[CU^{0(1)} + e\varphi^{0(1)} + h\psi^{0(1)}\right] & k_3^{(3)}\left[CU^{0(3)} + e\varphi^{0(3)} + h\psi^{0(3)}\right] & k_3^{(5)}\left[CU^{0(5)} + e\varphi^{0(5)} + h\psi^{0(5)}\right] \\ \varphi^{0(1)} & \varphi^{0(3)} & \varphi^{0(5)} \\ hk_3^{(1)}U^{0(1)} - \alpha k_3^{(1)}\varphi^{0(1)} - \left(\mu k_3^{(1)} - \mathrm{j}\mu_0 k_1\right)\psi^{0(1)} & hk_3^{(3)}U^{0(3)} - \alpha k_3^{(3)}\varphi^{0(3)} - \left(\mu k_3^{(3)} - \mathrm{j}\mu_0 k_1\right)\psi^{0(3)} & hk_3^{(5)}U^{0(5)} - \alpha k_3^{(5)}\varphi^{0(5)} - \left(\mu k_3^{(5)} - \mathrm{j}\mu_0 k_1\right)\psi^{0(5)} \end{pmatrix} \begin{pmatrix} F_1 \\ F_2 \\ F_3 \end{pmatrix} = \begin{pmatrix} 0 \\ 0 \\ 0 \end{pmatrix} \tag{XII.1}$$

To resolve these three homogeneous equations in expression (XII.1), one also has to deal with the boundary-condition determinant (BCD3) of the coefficient matrix. This means that the following equation can be introduced by means of the use of the first set of the eigenvector components:

$$\begin{vmatrix} 0 & n_3^{(3)}m^{(2)} & n_3^{(5)}m^{(3)} \\ h & \begin{matrix} C\alpha m^{(2)}\left(m^{(2)}-\gamma_K^2\right) \\ +eh\left(m^{(2)}-2\right)^2 \end{matrix} & \begin{matrix} C\alpha m^{(3)}\left(m^{(3)}-\gamma_K^2\right) \\ +eh\left(m^{(3)}-2\right)^2 \end{matrix} \\ \mathrm{j}\left[e(\mu+\mu_0)-h\alpha\right] & \begin{matrix} n_3^{(3)}\Big[h(e\alpha-h\varepsilon)m^{(2)}\left(m^{(2)}-2\right) \\ -C\left(\varepsilon\mu-\alpha^2\right)m^{(2)}\left(m^{(2)}-\gamma_K^2\right) \\ -e(e\mu-h\alpha)\left(m^{(2)}-2\right)^2\Big] \\ +\mathrm{j}\mu_0\Big[C\varepsilon m^{(2)}\left(m^{(2)}-\gamma_K^2\right) \\ +e^2\left(m^{(2)}-2\right)^2\Big] \end{matrix} & \begin{matrix} n_3^{(5)}\Big[h(e\alpha-h\varepsilon)m^{(3)}\left(m^{(3)}-2\right) \\ -C\left(\varepsilon\mu-\alpha^2\right)m^{(3)}\left(m^{(3)}-\gamma_K^2\right) \\ -e(e\mu-h\alpha)\left(m^{(3)}-2\right)^2\Big] \\ +\mathrm{j}\mu_0\Big[C\varepsilon m^{(3)}\left(m^{(3)}-\gamma_K^2\right) \\ +e^2\left(m^{(3)}-2\right)^2\Big] \end{matrix} \end{vmatrix} = 0 \tag{XII.2}$$

For these electrical and magnetic boundary conditions and the first set of the eigenvector components, one has to deal with the following complex secular equation obtained after expansion of the BCD3 in equation (XII.2):

$$\begin{aligned} &-\mathrm{j}\left[e(\mu+\mu_0)-h\alpha\right]n_3^{(5)}m^{(3)}\left[C\alpha m^{(2)}\left(m^{(2)}-\gamma_K^2\right)+eh\left(m^{(2)}-2\right)^2\right] \\ &-hn_3^{(3)}n_3^{(5)}m^{(2)} \\ &\times\left[h(e\alpha-h\varepsilon)m^{(3)}\left(m^{(3)}-2\right)-C\left(\varepsilon\mu-\alpha^2\right)m^{(3)}\left(m^{(3)}-\gamma_K^2\right)-e(e\mu-h\alpha)\left(m^{(3)}-2\right)^2\right] \\ &-\mathrm{j}h\mu_0 n_3^{(3)}m^{(2)}\left[C\varepsilon m^{(3)}\left(m^{(3)}-\gamma_K^2\right)+e^2\left(m^{(3)}-2\right)^2\right] \\ &+\mathrm{j}\left[e(\mu+\mu_0)-h\alpha\right]n_3^{(3)}m^{(2)}\left[C\alpha m^{(3)}\left(m^{(3)}-\gamma_K^2\right)+eh\left(m^{(3)}-2\right)^2\right] \\ &+hn_3^{(3)}n_3^{(5)}m^{(3)} \\ &\times\left[h(e\alpha-h\varepsilon)m^{(2)}\left(m^{(2)}-2\right)-C\left(\varepsilon\mu-\alpha^2\right)m^{(2)}\left(m^{(2)}-\gamma_K^2\right)-e(e\mu-h\alpha)\left(m^{(2)}-2\right)^2\right] \\ &+\mathrm{j}h\mu_0 n_3^{(5)}m^{(3)}\left[C\varepsilon m^{(2)}\left(m^{(2)}-\gamma_K^2\right)+e^2\left(m^{(2)}-2\right)^2\right]=0 \end{aligned} \tag{XII.3}$$

To simplify equation (XII.3), it is possible to regroup all the terms in the equation. The result of this complicated procedure can be readily written in the following four-term final form which can be used for determination of the phase velocity V_{ph} of propagating waves:

$$\begin{aligned}&\frac{h(e\alpha-h\varepsilon)}{e(e\mu-h\alpha)}n_3^{(3)}n_3^{(5)}\left(m^{(3)}-m^{(2)}\right)\\&-\mathrm{j}\frac{K_{em}^2}{K_\alpha^2\left(1+K_{em}^2\right)}\left(\gamma_K^2+\gamma_K^2\frac{\mu_0}{\mu}\frac{K_\alpha^2}{K_m^2}\frac{h(e\alpha-h\varepsilon)}{e(e\mu-h\alpha)}+4K_\alpha^2\right)\left(n_3^{(5)}-n_3^{(3)}\right)\\&+\mathrm{j}\left(n_3^{(5)}m^{(3)}-n_3^{(3)}m^{(2)}\right)\\&+\mathrm{j}\frac{K_{em}^2}{K_\alpha^2\left(1+K_{em}^2\right)}\left(1+\frac{\mu_0}{\mu}\frac{K_\alpha^2}{K_m^2}\frac{h(e\alpha-h\varepsilon)}{e(e\mu-h\alpha)}+K_\alpha^2\right)\left(n_3^{(5)}m^{(2)}-n_3^{(3)}m^{(3)}\right)=0\end{aligned} \qquad \text{(XII.4)}$$

where the parameters such as $K_{em}{}^2$, $K_m{}^2$, $K_\alpha{}^2$, and $\gamma_K{}^2$ are defined by relations (II.19), (II.22), (VII.5), and (II.59), respectively.

Next, it is also possible to exploit the second set of the eigenvector components. As the result, here the following BCD3 equals to zero:

$$\begin{vmatrix} 0 & n_3^{(3)}m^{(2)} & n_3^{(5)}m^{(3)} \\ h & \begin{matrix} C\mu m^{(2)}\left(m^{(2)}-\gamma_K^2\right) \\ +h^2\left(m^{(2)}-2\right)^2 \end{matrix} & \begin{matrix} C\mu m^{(3)}\left(m^{(3)}-\gamma_K^2\right) \\ +h^2\left(m^{(3)}-2\right)^2 \end{matrix} \\ \mathrm{j}\left[e(\mu+\mu_0)-h\alpha\right] & \begin{matrix} -4h(e\mu-h\alpha)n_3^{(3)} \\ +\mathrm{j}\mu_0\left[C\alpha m^{(2)}\left(m^{(2)}-\gamma_K^2\right)\right. \\ \left.+eh\left(m^{(2)}-2\right)^2\right] \end{matrix} & \begin{matrix} -4h(e\mu-h\alpha)n_3^{(5)} \\ +\mathrm{j}\mu_0\left[C\alpha m^{(3)}\left(m^{(3)}-\gamma_K^2\right)\right. \\ \left.+eh\left(m^{(3)}-2\right)^2\right] \end{matrix} \end{vmatrix}=0 \qquad \text{(XII.5)}$$

The result of expansion of the BCD3 in equation (XII.5) can reveal a secular equation. This secular equation must be further transformed in order to get an appropriate form. Utilizing the well-known triangle rule for such determinant, the original form for the secular equation is as follows:

$$
\begin{aligned}
&\mathrm{j}\left[e(\mu+\mu_0)-h\alpha\right]n_3^{(3)}m^{(2)}\left[C\mu m^{(3)}\left(m^{(3)}-\gamma_K^2\right)+h^2\left(m^{(3)}-2\right)^2\right]\\
&-4h^2(e\mu-h\alpha)n_3^{(3)}n_3^{(5)}m^{(3)}\\
&+\mathrm{j}h\mu_0 n_3^{(5)}m^{(3)}\left[C\alpha m^{(2)}\left(m^{(2)}-\gamma_K^2\right)+eh\left(m^{(2)}-2\right)^2\right]\\
&-\mathrm{j}\left[e(\mu+\mu_0)-h\alpha\right]n_3^{(5)}m^{(3)}\left[C\mu m^{(2)}\left(m^{(2)}-\gamma_K^2\right)+h^2\left(m^{(2)}-2\right)^2\right]\\
&+4h^2(e\mu-h\alpha)n_3^{(3)}n_3^{(5)}m^{(2)}\\
&-\mathrm{j}h\mu_0 n_3^{(3)}m^{(2)}\left[C\alpha m^{(3)}\left(m^{(3)}-\gamma_K^2\right)+eh\left(m^{(3)}-2\right)^2\right]=0
\end{aligned}
\tag{XII.6}
$$

The final non-dimensional form for secular equation (XII.6) can be also introduced as the following four terms:

$$
\begin{aligned}
&n_3^{(3)}n_3^{(5)}\left(m^{(3)}-m^{(2)}\right)-\mathrm{j}\frac{K_{em}^2}{K_m^2\left(1+K_{em}^2\right)}\left(\gamma_K^2+\gamma_K^2\frac{\mu_0}{\mu}+4K_m^2\right)\left(n_3^{(5)}-n_3^{(3)}\right)\\
&+\mathrm{j}\left(n_3^{(5)}m^{(3)}-n_3^{(3)}m^{(2)}\right)+\mathrm{j}\frac{K_{em}^2}{K_m^2\left(1+K_{em}^2\right)}\left(1+\frac{\mu_0}{\mu}+K_m^2\right)\left(n_3^{(5)}m^{(2)}-n_3^{(3)}m^{(3)}\right)=0
\end{aligned}
\tag{XII.7}
$$

where the parameters such as K_{em}^2, K_m^2, and γ_K^2 are those used in formula (XII.4).

Formulae (XII.4) and (XII.7) can be utilized for determinations of the phase velocity of the new SH-SAW. The velocity represents already the sixth new SH-SAWs which can propagate in the cubic piezoelectromagnetics. It can be denoted by V_{c6new}. Therefore, the recursive formula can be given in the following form, following the results of the previous chapters:

$$
V_{c6new}=V_{tem}\sqrt{1-\left(b_{c6}\left(X_6\right)\right)^2}
\tag{XII.8}
$$

where the form for the complicated parameter b_{c6} under the square root can be obtained from equation (XII.4) or (XII.7).

Table XII.1 lists the values of the sixth new SH-SAW velocity denoted by V_{c6new}. These values were calculated using equation (XII.4) for the first set of the eigenvector components. Using the second set of the components, the second four-term expression (XII.7) reveals the same SH-SAW velocity V_{c6new}. Note that the values of the velocity V_{c6new} were calculated with a high precision (see table XII.1) in order to solidly demonstrate that both equations (XII.4) and (XII.7) give the same result. Indeed, these two different secular equations reveal the same result given in table XII.1 and to give the second values which will duplicate the values of the velocity V_{c6new} is not suitable here. The reader can readily check it.

Table XII.1. The calculated values of the new SH-SAW velocity V_{c6new} [m/s].

PEM composite	$(V_{c6new})_1$ $(V_{c6new})_2$ $(V_{c6new})_3$
Metglas–PZT-5H	3676.0517581168012 3693.6334035320207 3695.5080278692763
Tl_3TaSe_4–Terfenol-D	954.2906962032965 960.0035674321671 960.6206352126536
Tl_3VS_4–Galfenol	3613.8726250313773 3619.2533363340318 3620.0887165010403
Tl_3TaSe_4–Galfenol	3470.4353273590005 3476.2441457548700 3477.1029658424587
Tl_3VS_4–Alfenol	3144.5964923241957 3149.7515911845775 3150.3680586102008

Also, the high precision calculations are suitable in the case of study of surface acoustic waves. This is true due to the fact that the SH-SAWs represent the corresponding instabilities of the SH-BAW characterised by the velocity V_{tem} under application of the different electrical and magnetic boundary conditions. Therefore, the values of the SH-SAW velocities should be situated below or in many cases just below the value of the velocity V_{tem}. This is the condition for all the transversely isotropic piezoelectromagnetics as well as for the cubic piezoelectromagnetics with $K_{em}^2 < 1/3$, see the results for Tl_3VS_4–Alfenol listed in table XII.1. For the other cubic piezoelectromagnetics with $K_{em}^2 > 1/3$ listed in table XII.1, the values of the velocity V_{c6new} lie below the value of the solution V_K. It is thought that this solution denoted by V_K must be unstable. Also, this solution was never studied and experimentally checked. However, it is very important parameter for cubic piezoelectromagnetics. The calculated values of the sixth new SH-SAW velocity denoted by V_{c6new} can be compares with the values of V_{BGM}, V_{tem}, and V_K (see table V.1 from Chapter V for the purpose).

The number of the terms in four-term secular equation (XII.4) or (XII.7) can be also reduced. It is clearly seen that these two equations have the same thir term. Hence, it is natural to subtract one equation from the other to get a three-term secular equation. The terms of the latter equation can be further regrouped, and one can express the following simplified two-term equation:

$$\begin{aligned} & -K_m^2 K_\alpha^2 \left(1+K_{em}^2\right) \frac{C\left(\varepsilon\mu-\alpha^2\right)}{e\left(e\mu-h\alpha\right)} n_3^{(3)} n_3^{(5)} \left(m^{(3)}-m^{(2)}\right) \\ & +\mathrm{j}\left[K_m^2 - K_\alpha^2 - \frac{\mu_0}{\mu} K_\alpha^2 K_{em}^2 \frac{C\left(\varepsilon\mu-\alpha^2\right)}{e\left(e\mu-h\alpha\right)}\right]\left[n_3^{(5)}\left(m^{(2)}-\gamma_K^2\right)-n_3^{(3)}\left(m^{(3)}-\gamma_K^2\right)\right]=0 \end{aligned} \tag{XII.9}$$

Using secular equation (XII.9), all the values of the new SH-SAW velocity V_{c6new} can be readily calculated.

The definition of the parameter b_{c6} introduced in equation (XII.8) can be also written using equation (XII.9). This parameter is convenient to compare the theoretical results obtained in this work for the cubic piezoelectromagnetics with those for the transversely-isotropic composite materials described in book [89]. So, the parameter b_{c6} reads:

$$b_{c6}=n_3^{(3)}n_3^{(5)}=-\left[\frac{K_m^2-K_\alpha^2}{K_m^2K_\alpha^2\left(1+K_{em}^2\right)}\frac{e(e\mu-h\alpha)}{C\left(\varepsilon\mu-\alpha^2\right)}-\frac{\mu_0}{\mu}\frac{K_{em}^2}{K_m^2\left(1+K_{em}^2\right)}\right]$$
$$\times\frac{\mathrm{j}n_3^{(5)}\left(m^{(2)}-\gamma_K^2\right)-\mathrm{j}n_3^{(3)}\left(m^{(3)}-\gamma_K^2\right)}{m^{(3)}-m^{(2)}} \quad \text{(XII.10)}$$

The following chapter describes the case of the last possible set of the electrical and magnetic boundary conditions. It is thought that this is the most complicated case compared with the obtained results in this chapter and in the previous chapter. However, the results can be also represented in some convenient forms in order to compare them with those obtained in this work and in book [89].

CHAPTER XIII. The Case of Continuity of both D_3 and B_3 at $x_3 = 0$

This chapter describes the wave propagation in the cubic piezoelectromagnetics when the last possible set of the boundary conditions is used. This case represents the continuity of both the electrical displacement component D_3 and the magnetic flux component B_3 for the mechanically free surface, $\sigma_{23} = 0$. The wave propagation in the transversely isotropic piezoelectromagnetics was also theoretically investigated in book [89]. The SH-SAW velocities for the transversely isotropic case are expressed by formulae (110) and (120) in the explicit forms for the first and second sets of the eigenvector components, respectively. Concerning the cubic piezoelectromagnetics, it is thought that two sets of the eigenvector components can also make known at least one new SH-SAW velocity. This is the main purpose for this chapter.

Therefore, based on the boundary conditions, one can write the following matrix form of three equations:

$$\begin{pmatrix} k_3^{(1)}\left[CU^{0(1)} + e\varphi^{0(1)} + h\psi^{0(1)}\right] & k_3^{(3)}\left[CU^{0(3)} + e\varphi^{0(3)} + h\psi^{0(3)}\right] & k_3^{(5)}\left[CU^{0(5)} + e\varphi^{0(5)} + h\psi^{0(5)}\right] \\ ek_3^{(1)}U^{0(1)} - \left(\varepsilon k_3^{(1)} - \mathrm{j}\varepsilon_0 k_1\right)\varphi^{0(1)} - \alpha k_3^{(1)}\psi^{0(1)} & ek_3^{(3)}U^{0(3)} - \left(\varepsilon k_3^{(3)} - \mathrm{j}\varepsilon_0 k_1\right)\varphi^{0(3)} - \alpha k_3^{(3)}\psi^{0(3)} & ek_3^{(5)}U^{0(5)} - \left(\varepsilon k_3^{(5)} - \mathrm{j}\varepsilon_0 k_1\right)\varphi^{0(5)} - \alpha k_3^{(5)}\psi^{0(5)} \\ hk_3^{(1)}U^{0(1)} - \alpha k_3^{(1)}\varphi^{0(1)} - \left(\mu k_3^{(1)} - \mathrm{j}\mu_0 k_1\right)\psi^{0(1)} & hk_3^{(3)}U^{0(3)} - \alpha k_3^{(3)}\varphi^{0(3)} - \left(\mu k_3^{(3)} - \mathrm{j}\mu_0 k_1\right)\psi^{0(3)} & hk_3^{(5)}U^{0(5)} - \alpha k_3^{(5)}\varphi^{0(5)} - \left(\mu k_3^{(5)} - \mathrm{j}\mu_0 k_1\right)\psi^{0(5)} \end{pmatrix} \begin{pmatrix} F_1 \\ F_2 \\ F_3 \end{pmatrix} = \begin{pmatrix} 0 \\ 0 \\ 0 \end{pmatrix} \quad \text{(XIII.1)}$$

The determinant BCD3 of the coefficient matrix in equation (XIII.1) must vanish because one copes here with the homogeneous equations. Using the first set of the eigenvector components, it is possible to write the matrix BCD3 in the following convenient form:

$$
\left|
\begin{array}{ccc}
0 & n_3^{(3)} m^{(2)} & n_3^{(5)} m^{(3)} \\
 & & \\
e\alpha - h(\varepsilon + \varepsilon_0) & \begin{array}{l} -4e(e\alpha - h\varepsilon)n_3^{(3)} \\ -\mathrm{j}\varepsilon_0\Big[C\alpha m^{(2)}\left(m^{(2)} - \gamma_K^2\right) \\ +eh\left(m^{(2)} - 2\right)^2\Big] \end{array} & \begin{array}{l} -4e(e\alpha - h\varepsilon)n_3^{(5)} \\ -\mathrm{j}\varepsilon_0\Big[C\alpha m^{(3)}\left(m^{(3)} - \gamma_K^2\right) \\ +eh\left(m^{(3)} - 2\right)^2\Big] \end{array} \\
 & & \\
e(\mu + \mu_0) - h\alpha & \begin{array}{l} n_3^{(3)}\Big[h(e\alpha - h\varepsilon)m^{(2)}\left(m^{(2)} - 2\right) \\ -C\left(\varepsilon\mu - \alpha^2\right)m^{(2)}\left(m^{(2)} - \gamma_K^2\right) \\ -e(e\mu - h\alpha)\left(m^{(2)} - 2\right)^2\Big] \\ +\mathrm{j}\mu_0\Big[C\varepsilon m^{(2)}\left(m^{(2)} - \gamma_K^2\right) \\ +e^2\left(m^{(2)} - 2\right)^2\Big] \end{array} & \begin{array}{l} n_3^{(5)}\Big[h(e\alpha - h\varepsilon)m^{(3)}\left(m^{(3)} - 2\right) \\ -C\left(\varepsilon\mu - \alpha^2\right)m^{(3)}\left(m^{(3)} - \gamma_K^2\right) \\ -e(e\mu - h\alpha)\left(m^{(3)} - 2\right)^2\Big] \\ +\mathrm{j}\mu_0\Big[C\varepsilon m^{(3)}\left(m^{(3)} - \gamma_K^2\right) \\ +e^2\left(m^{(3)} - 2\right)^2\Big] \end{array}
\end{array}
\right| = 0 \tag{XIII.2}
$$

It is thought that this is the most complicated case comparing with the studies carried out in the previous chapters from Chapter V. However, the simplifications must be also applied for secular equations in the case. Expanding the boundary-condition determinant (BCD3) in equation (XIII.2), the reader can find that the most complicated secular equation for the first set of the eigenvector components is as follows:

$$
\begin{aligned}
& -4e(e\alpha - h\varepsilon)[e(\mu + \mu_0) - h\alpha]n_3^{(3)}n_3^{(5)}m^{(2)} \\
& -\mathrm{j}\varepsilon_0[e(\mu + \mu_0) - h\alpha]n_3^{(3)}m^{(2)}\left[C\alpha m^{(3)}\left(m^{(3)} - \gamma_K^2\right) + eh\left(m^{(3)} - 2\right)^2\right] \\
& +[e\alpha - h(\varepsilon + \varepsilon_0)]n_3^{(3)}n_3^{(5)}m^{(3)} \\
& \times\left[h(e\alpha - h\varepsilon)m^{(2)}\left(m^{(2)} - 2\right) - C\left(\varepsilon\mu - \alpha^2\right)m^{(2)}\left(m^{(2)} - \gamma_K^2\right) - e(e\mu - h\alpha)\left(m^{(2)} - 2\right)^2\right] \\
& +\mathrm{j}\mu_0[e\alpha - h(\varepsilon + \varepsilon_0)]n_3^{(5)}m^{(3)}\left[C\varepsilon m^{(2)}\left(m^{(2)} - \gamma_K^2\right) + e^2\left(m^{(2)} - 2\right)^2\right] \\
& +4e(e\alpha - h\varepsilon)[e(\mu + \mu_0) - h\alpha]n_3^{(3)}n_3^{(5)}m^{(3)} \\
& +\mathrm{j}\varepsilon_0[e(\mu + \mu_0) - h\alpha]n_3^{(5)}m^{(3)}\left[C\alpha m^{(2)}\left(m^{(2)} - \gamma_K^2\right) + eh\left(m^{(2)} - 2\right)^2\right] \\
& -[e\alpha - h(\varepsilon + \varepsilon_0)]n_3^{(3)}n_3^{(5)}m^{(2)} \\
& \times\left[h(e\alpha - h\varepsilon)m^{(3)}\left(m^{(3)} - 2\right) - C\left(\varepsilon\mu - \alpha^2\right)m^{(3)}\left(m^{(3)} - \gamma_K^2\right) - e(e\mu - h\alpha)\left(m^{(3)} - 2\right)^2\right] \\
& -\mathrm{j}\mu_0[e\alpha - h(\varepsilon + \varepsilon_0)]n_3^{(3)}m^{(2)}\left[C\varepsilon m^{(3)}\left(m^{(3)} - \gamma_K^2\right) + e^2\left(m^{(3)} - 2\right)^2\right] = 0
\end{aligned} \tag{XIII.3}
$$

Using the same transformations to regroup all the terms in equation (XIII.3), the final form of the secular equation can be also written as the following equation, in which the left side consists of four terms:

$$\begin{aligned}
&\left[K_{em}^2\left(1-\frac{\alpha^2}{\varepsilon\mu}\right)+K_e^2\frac{\mu_0}{\mu}+K_m^2\frac{\varepsilon_0}{\varepsilon}\right]n_3^{(3)}n_3^{(5)}\left(m^{(3)}-m^{(2)}\right)\\
&-\mathrm{j}\frac{K_{em}^2}{1+K_{em}^2}\left[\gamma_K^2\frac{\varepsilon_0\mu_0}{\varepsilon\mu}+\frac{\varepsilon_0}{\varepsilon}\frac{K_m^2}{K_\alpha^2}\frac{e(e\mu-h\alpha)}{h(e\alpha-h\varepsilon)}\left(\gamma_K^2+4K_\alpha^2\right)+\frac{\mu_0}{\mu}\left(\gamma_K^2+4K_e^2\right)\right]\left(n_3^{(5)}-n_3^{(3)}\right)\\
&+\mathrm{j}\left[K_m^2\frac{\varepsilon_0}{\varepsilon}\frac{e(e\mu-h\alpha)}{h(e\alpha-h\varepsilon)}+K_e^2\frac{\mu_0}{\mu}\right]\left(n_3^{(5)}m^{(3)}-n_3^{(3)}m^{(2)}\right)\\
&+\mathrm{j}\frac{K_{em}^2}{1+K_{em}^2}\left[\frac{\varepsilon_0\mu_0}{\varepsilon\mu}+\frac{\varepsilon_0}{\varepsilon}\frac{K_m^2}{K_\alpha^2}\frac{e(e\mu-h\alpha)}{h(e\alpha-h\varepsilon)}\left(1+K_\alpha^2\right)+\frac{\mu_0}{\mu}\left(1+K_e^2\right)\right]\left(n_3^{(5)}m^{(2)}-n_3^{(3)}m^{(3)}\right)=0
\end{aligned}\tag{XIII.4}$$

where all the material constants for a cubic piezoelectromagnetics and the free space (vacuum) are combined in such ways in order to deal with the non-dimensional expression. In equation (XIII.4), the value of the speed of light in a vacuum, C_L = 1/sqrt($\varepsilon_0\mu_0$), is given in the beginning of Chapter IV. Also, the speed of the electromagnetic waves in a solid is defined by the following formula: V_L = 1/sqrt($\varepsilon\mu$). The other non-dimensional parameters such as K_{em}^2, K_e^2, K_m^2, K_α^2, and γ_K^2 are defined by relations (II.19), (II.21), (II.22), (VII.5), and (II.59), respectively. It is clearly seen in equation (XIII.4) that the following relation $e(e\mu - h\alpha)/[h(e\alpha - h\varepsilon)] = - e(e\mu - h\alpha)/[h(h\varepsilon - e\alpha)]$ is also non-dimensional and looks like the relation of the corresponding terms of the CMEMC K_{em}^2. Indeed, the CMEMC K_{em}^2 can be represented as a sum of four terms, see the definition of K_{em}^2 in relation (II.19).

To complete the mathematical analysis, the final step is the utilization of the second set of the eigenvector components. This allows formation of the second boundary-condition determinant (BCD3). After some useful simplifications and transformations, it can be then introduced as follows:

$$
\begin{vmatrix}
0 & n_3^{(3)} m^{(2)} & n_3^{(5)} m^{(3)} \\
e\alpha - h(\varepsilon + \varepsilon_0) & \begin{array}{l} n_3^{(3)}\Big[e(e\mu - h\alpha)m^{(2)}\big(m^{(2)} - 2\big) \\ + C\big(\varepsilon\mu - \alpha^2\big)m^{(2)}\big(m^{(2)} - \gamma_K^2\big) \\ - h(e\alpha - h\varepsilon)\big(m^{(2)} - 2\big)^2\Big] \\ - \mathrm{j}\varepsilon_0\Big[C\mu m^{(2)}\big(m^{(2)} - \gamma_K^2\big) \\ + h^2\big(m^{(2)} - 2\big)^2\Big] \end{array} & \begin{array}{l} n_3^{(5)}\Big[e(e\mu - h\alpha)m^{(3)}\big(m^{(3)} - 2\big) \\ + C\big(\varepsilon\mu - \alpha^2\big)m^{(3)}\big(m^{(3)} - \gamma_K^2\big) \\ - h(e\alpha - h\varepsilon)\big(m^{(3)} - 2\big)^2\Big] \\ - \mathrm{j}\varepsilon_0\Big[C\mu m^{(3)}\big(m^{(3)} - \gamma_K^2\big) \\ + h^2\big(m^{(3)} - 2\big)^2\Big] \end{array} \\
e(\mu + \mu_0) - h\alpha & \begin{array}{l} -4h(e\mu - h\alpha)n_3^{(3)} \\ + \mathrm{j}\mu_0\Big[C\alpha m^{(2)}\big(m^{(2)} - \gamma_K^2\big) \\ + eh\big(m^{(2)} - 2\big)^2\Big] \end{array} & \begin{array}{l} -4h(e\mu - h\alpha)n_3^{(5)} \\ + \mathrm{j}\mu_0\Big[C\alpha m^{(3)}\big(m^{(3)} - \gamma_K^2\big) \\ + eh\big(m^{(3)} - 2\big)^2\Big] \end{array}
\end{vmatrix} = 0 \qquad \text{(XIII.5)}
$$

For the second set of the eigenvector components, it is also expected that the second secular equation will be different from the first one, for which the final simplified form is given in expression (XIII.4). Expanding the second BCD3 in equation (XIII.5), the reader can also obtain the following secular equation in the original form which can be further transformed:

$$
\begin{aligned}
& -4h(e\mu - h\alpha)[e\alpha - h(\varepsilon + \varepsilon_0)]n_3^{(3)} n_3^{(5)} m^{(3)} \\
& + \mathrm{j}\mu_0[e\alpha - h(\varepsilon + \varepsilon_0)]n_3^{(5)} m^{(3)}\Big[C\alpha m^{(2)}\big(m^{(2)} - \gamma_K^2\big) + eh\big(m^{(2)} - 2\big)^2\Big] \\
& + [e(\mu + \mu_0) - h\alpha]n_3^{(3)} n_3^{(5)} m^{(2)} \\
& \times\Big[e(e\mu - h\alpha)m^{(3)}\big(m^{(3)} - 2\big) + C\big(\varepsilon\mu - \alpha^2\big)m^{(3)}\big(m^{(3)} - \gamma_K^2\big) - h(e\alpha - h\varepsilon)\big(m^{(3)} - 2\big)^2\Big] \\
& - \mathrm{j}\varepsilon_0[e(\mu + \mu_0) - h\alpha]n_3^{(3)} m^{(2)}\Big[C\mu m^{(3)}\big(m^{(3)} - \gamma_K^2\big) + h^2\big(m^{(3)} - 2\big)^2\Big] \\
& + 4h(e\mu - h\alpha)[e\alpha - h(\varepsilon + \varepsilon_0)]n_3^{(3)} n_3^{(5)} m^{(2)} \\
& - \mathrm{j}\mu_0[e\alpha - h(\varepsilon + \varepsilon_0)]n_3^{(3)} m^{(2)}\Big[C\alpha m^{(3)}\big(m^{(3)} - \gamma_K^2\big) + eh\big(m^{(3)} - 2\big)^2\Big] \\
& - [e(\mu + \mu_0) - h\alpha]n_3^{(3)} n_3^{(5)} m^{(3)} \\
& \times\Big[e(e\mu - h\alpha)m^{(2)}\big(m^{(2)} - 2\big) + C\big(\varepsilon\mu - \alpha^2\big)m^{(2)}\big(m^{(2)} - \gamma_K^2\big) - h(e\alpha - h\varepsilon)\big(m^{(2)} - 2\big)^2\Big] \\
& + \mathrm{j}\varepsilon_0[e(\mu + \mu_0) - h\alpha]n_3^{(5)} m^{(3)}\Big[C\mu m^{(2)}\big(m^{(2)} - \gamma_K^2\big) + h^2\big(m^{(2)} - 2\big)^2\Big] = 0
\end{aligned} \qquad \text{(XIII.6)}
$$

Finally, application of the simplification procedure results in the following last secular equation written in the convenient form consisting of four terms:

$$\begin{aligned}
&\left[K_{em}^2\left(1-\frac{\alpha^2}{\varepsilon\mu}\right)+K_e^2\frac{\mu_0}{\mu}+K_m^2\frac{\varepsilon_0}{\varepsilon}\right]n_3^{(3)}n_3^{(5)}\left(m^{(3)}-m^{(2)}\right)\\
&-\mathrm{j}\frac{K_{em}^2}{1+K_{em}^2}\left[\gamma_K^2\frac{\varepsilon_0\mu_0}{\varepsilon\mu}+\frac{\mu_0}{\mu}\frac{K_e^2}{K_\alpha^2}\frac{h(e\alpha-h\varepsilon)}{e(e\mu-h\alpha)}\left(\gamma_K^2+4K_\alpha^2\right)+\frac{\varepsilon_0}{\varepsilon}\left(\gamma_K^2+4K_m^2\right)\right]\left(n_3^{(5)}-n_3^{(3)}\right)\\
&+\mathrm{j}\left[K_e^2\frac{\mu_0}{\mu}\frac{h(e\alpha-h\varepsilon)}{e(e\mu-h\alpha)}+K_m^2\frac{\varepsilon_0}{\varepsilon}\right]\left(n_3^{(5)}m^{(3)}-n_3^{(3)}m^{(2)}\right)\\
&+\mathrm{j}\frac{K_{em}^2}{1+K_{em}^2}\left[\frac{\varepsilon_0\mu_0}{\varepsilon\mu}+\frac{\mu_0}{\mu}\frac{K_e^2}{K_\alpha^2}\frac{h(e\alpha-h\varepsilon)}{e(e\mu-h\alpha)}\left(1+K_\alpha^2\right)+\frac{\varepsilon_0}{\varepsilon}\left(1+K_m^2\right)\right]\left(n_3^{(5)}m^{(2)}-n_3^{(3)}m^{(3)}\right)=0
\end{aligned} \quad \text{(XIII.7)}$$

The new SH-SAW velocity can be calculated with formula (XIII.4) or (XIII.7). It is obvious that these formulae are the most complicated. This velocity denoted by V_{c7new} represents already the seventh new SH-SAW velocity. For the cubic piezoelectromagnetics, the value of the velocity V_{c7new} can be obtained using the following recursive formula:

$$V_{c7new}=V_{tem}\sqrt{1-\left(b_{c7}(X_7)\right)^2} \quad \text{(XIII.8)}$$

where the parameter b_{c7} is defined below.

Using this set of the electrical and magnetic boundary conditions, one can also calculate the values of the seventh new SH-SAW velocity V_{c7new} for the studied cubic piezoelectromagnetics. The results of the calculations are listed in table XIII.1. Like for the other new SH-SAW velocities calculated in the previous chapters, three values of V_{c7new} are calculated with a high precision for each studied material listed in the table. One can compare the calculated values of V_{c7new} with those of the other six new SH-SAW velocities and velocity V_{BGM}. For the cubic piezoelectromagnetics with K_{em}^2 < 1/3, the values of all the seven new SH-SAW velocities lie in the phase velocity range between the values of the SH-SAW velocity V_{BGM} and the value of the SH-

BAW velocity V_{tem} given in table V.1 from Chapter V. For those with $K_{em}^2 > 1/3$, it is apt to use the value of the solution V_K instead of that of the SH-BAW velocity V_{tem}.

Table XIII.1. The calculated values of the new SH-SAW velocity V_{c7new} [m/s].

PEM composite	$(V_{c7new})_1$ $(V_{c7new})_2$ $(V_{c7new})_3$
Metglas–PZT-5H	3678.4479600723056 3698.1418999052634 3700.2660774646043
Tl_3TaSe_4–Terfenol-D	962.0331923300526 969.2665702898084 970.0440338220781
Tl_3VS_4–Galfenol	3613.9098468606157 3619.8653101138586 3620.8174665209454
Tl_3TaSe_4–Galfenol	3470.4888929721035 3476.8984274315751 3477.8756515991725
Tl_3VS_4–Alfenol	3144.6575150817353 3149.9194411326577 3150.5518653562942

The complicated four-term formulae given in expressions (XIII.4) and (XIII.7) can be also transformed into the form of two-term expression. It is clearly seen in the equations that their first terms are equal. However, these equations have to be transformed to the suitable forms when they should have equal third terms, but not the first ones, to apply the subtraction procedure. After this procedure, one can obtain a three-term expression which can be then written in the following compact form used in this work for all the cases of the wave propagation in the cubic piezoelectromagnetics:

$$An_3^{(3)}n_3^{(5)}\left(m^{(3)}-m^{(2)}\right)+\mathrm{j}B\left[n_3^{(5)}\left(m^{(2)}-\gamma_K^2\right)-n_3^{(3)}\left(m^{(3)}-\gamma_K^2\right)\right]=0 \qquad \text{(XIII.9)}$$

where the complicated parameters A and B are defined as follows:

$$A=-\left[K_{em}^2\left(1-\frac{\alpha^2}{\varepsilon\mu}\right)+K_e^2\frac{\mu_0}{\mu}+K_m^2\frac{\varepsilon_0}{\varepsilon}\right]\times\left[K_e^2\frac{\mu_0}{\mu}\frac{C\left(\varepsilon\mu-\alpha^2\right)}{e\left(e\mu-h\alpha\right)}+K_m^2\frac{\varepsilon_0}{\varepsilon}\frac{C\left(\varepsilon\mu-\alpha^2\right)}{h\left(e\alpha-h\varepsilon\right)}\right] \qquad \text{(XIII.10)}$$

and

$$\begin{aligned}B=&-\frac{K_{em}^2}{1+K_{em}^2}\frac{\varepsilon_0\mu_0}{\varepsilon\mu}\left[K_e^2\frac{\mu_0}{\mu}\frac{C\left(\varepsilon\mu-\alpha^2\right)}{e\left(e\mu-h\alpha\right)}+K_m^2\frac{\varepsilon_0}{\varepsilon}\frac{C\left(\varepsilon\mu-\alpha^2\right)}{h\left(e\alpha-h\varepsilon\right)}\right]+\frac{\varepsilon_0\mu_0}{\varepsilon\mu}\frac{K_m^2-K_e^2}{1+K_{em}^2}\\&+\frac{K_m^2}{K_\alpha^2}\left(\frac{\varepsilon_0}{\varepsilon}\right)^2\frac{e\left(e\mu-h\alpha\right)}{h\left(e\alpha-h\varepsilon\right)}\frac{K_m^2-K_\alpha^2}{1+K_{em}^2}-\frac{K_e^2}{K_\alpha^2}\left(\frac{\mu_0}{\mu}\right)^2\frac{h\left(e\alpha-h\varepsilon\right)}{e\left(e\mu-h\alpha\right)}\frac{K_e^2-K_\alpha^2}{1+K_{em}^2}\end{aligned} \qquad \text{(XIII.11)}$$

The parameters A and B are quite complicated. Using them, the parameter b_{c7} introduced in expression (XIII.8) can be defined as follows:

$$\begin{aligned}b_{c7}=n_3^{(3)}n_3^{(5)}=&\frac{\mathrm{j}n_3^{(5)}\left(m^{(2)}-\gamma_K^2\right)-\mathrm{j}n_3^{(3)}\left(m^{(3)}-\gamma_K^2\right)}{m^{(3)}-m^{(2)}}\times\left[\frac{\dfrac{K_{em}^2}{1+K_{em}^2}\dfrac{\varepsilon_0\mu_0}{\varepsilon\mu}}{K_{em}^2\left(1-\dfrac{\alpha^2}{\varepsilon\mu}\right)+K_e^2\dfrac{\mu_0}{\mu}+K_m^2\dfrac{\varepsilon_0}{\varepsilon}}\right.\\&\left.-\frac{\dfrac{\varepsilon_0\mu_0}{\varepsilon\mu}\dfrac{K_m^2-K_e^2}{1+K_{em}^2}+\dfrac{K_m^2}{K_\alpha^2}\left(\dfrac{\varepsilon_0}{\varepsilon}\right)^2\dfrac{e\left(e\mu-h\alpha\right)}{h\left(e\alpha-h\varepsilon\right)}\dfrac{K_m^2-K_\alpha^2}{1+K_{em}^2}-\dfrac{K_e^2}{K_\alpha^2}\left(\dfrac{\mu_0}{\mu}\right)^2\dfrac{h\left(e\alpha-h\varepsilon\right)}{e\left(e\mu-h\alpha\right)}\dfrac{K_e^2-K_\alpha^2}{1+K_{em}^2}}{\left[K_{em}^2\left(1-\dfrac{\alpha^2}{\varepsilon\mu}\right)+K_e^2\dfrac{\mu_0}{\mu}+K_m^2\dfrac{\varepsilon_0}{\varepsilon}\right]\times\left[K_e^2\dfrac{\mu_0}{\mu}\dfrac{C\left(\varepsilon\mu-\alpha^2\right)}{e\left(e\mu-h\alpha\right)}+K_m^2\dfrac{\varepsilon_0}{\varepsilon}\dfrac{C\left(\varepsilon\mu-\alpha^2\right)}{h\left(e\alpha-h\varepsilon\right)}\right]}\right]\end{aligned} \qquad \text{(XIII.12)}$$

This chapter finalizes the theoretical analysis of the problem of wave propagation in the cubic piezoelectromagnetics. The ninth set of the possible electrical and magnetic boundary conditions was used here, and the values of the seventh new SH-SAW velocity V_{c7new} were calculated. However, it is thought that it also is indispensable to discuss this problem and to do some conclusive notes in the following chapters.

CHAPTER XIV. Discussion

All the solutions for the SH-SAWs obtained in this work can be naturally divided into two groups. The first group is for those without the material constants of the free space (vacuum), namely the dielectric permittivity constant ε_0 and the magnetic permeability constant μ_0. The obtained new SH-SAW velocities such as V_{c1new} and V_{c2new} studied in Chapters VII and VIII, respectively, pertain to the first group. Also, it was soundly shown in Chapter V that the SH-SAW with the velocity V_{BGM} can also propagate in the cubic piezoelectromagnetics. This SH-SAW velocity is also valid for the first group. The second group is for those with the vacuum material constants. The new SH-SAW velocities such as V_{c3new}, V_{c4new}, V_{c5new}, V_{c6new}, and V_{c7new} studied in Chapters from IX to XIII relate to this second group.

It is thought that it can be convenient for the reader to analyse some results combined together. This is realised in table XIV.1. This table lists all the velocity values for the SH-SAWs which can propagate in the cubic piezoelectromagnetics. In the table, Tl_3TaSe_4–Galfenol is the material with $K_{em}^2 > 1/3$ and Tl_3VS_4–Alfenol is that with $K_{em}^2 < 1/3$. The values of the SH-BAW velocities V_{t4} and V_{tem} and the solution V_K are also given in the table for comparison. It is clearly seen in the table that all the values of the new SH-SAW velocities are positioned between the values of V_{BGM} and V_K for Tl_3TaSe_4–Galfenol with $K_{em}^2 > 1/3$. For Tl_3VS_4–Alfenol with $K_{em}^2 < 1/3$, they are situated between the values of V_{BGM} and V_{tem}. Also, it is possible to focus the attention to the values of the velocity V_{c3new}, for which the values are very close to the value of V_{tem} for Tl_3VS_4–Alfenol and quite close to the value of V_K for Tl_3TaSe_4–Galfenol. One can also found that all the values of the seven new SH-SAW velocities are different from the other SH-SAW velocities obtained for the transversely isotropic piezoelectromagnetic composite materials [88, 89]. In order to compare, one can treat the transversely isotropic symmetry for the studied piezoelectromagnetics instead of the cubic symmetry. However, this difference is blatant because the transversely isotropic piezoelectromagnetics have no such very important wave characteristic as the solution V_K.

Table XIV.1. The calculated values of all the new SH-SAW velocities from V_{c1new} to V_{c7new} as well as the velocities V_{t4}, V_{tem}, and V_{BGM} [all only for $(K_{em}^2)_3$] for two cubic piezoelectromagnetics.

Velocity [m/s]	Tl_3TaSe_4–Galfenol	Tl_3VS_4–Alfenol
V_{t4}	2931.7282421476365	3021.4654798594457
V_K	3478.1008107942868	2839.4075626150029
V_{tem}	3490.9682076269390	3150.5728182133777
V_{BGM}	3335.9017826581493	3140.4042000875146
V_{c1new}	3477.6865581211105	3150.4632207288199
V_{c2new}	3339.5042963396260	3141.8899674581957
V_{c3new}	3478.0895042154676	3150.5724807593158
V_{c4new}	3477.9654008755682	3150.5567694878639
V_{c5new}	3338.9102777224558	3141.8114067959477
V_{c6new}	3477.1029658424587	3150.3680586102008
V_{c7new}	3477.8756515991725	3150.5518653562942

It is also possible to compare the seven forms of the secular equations which can be used for the calculations of the seven new SH-SAW velocities listed in table XIV.1. It is natural to compare the corresponding two-term forms. Indeed, each of the seven two-term forms can be written in the common form given in formula (XIII.9) from the previous chapter. This common form is convenient because it allows one to compare only the differences in the material parameters such as A and B. These parameters explicitly depend on the material constants of the cubic piezoelectromagnetics. Note that each case of the boundary conditions has its own set of the parameters A and B and any difference in these parameters solidly defines the uniqueness of each new SH-SAW velocity. These unique parameters A and B are listed in table XIV.2 for each of the seven new SH-SAWs which can propagate in the cubic piezoelectromagnetics. The explicit forms of the parameters A and B are relatively simple, but the forms for the last case studied in the previous chapter. Formulae (XIII.10) and (XIII.11) for the A and B are quite complicated because both the vacuum constants such as ε_0 and μ_0 are here coupled with all the material constants of the cubic piezoelectromagnetics. This is the most complicated case because in the other cases either the vacuum constant ε_0 or μ_0, or none is coupled with those.

It is thought that the theoretical results obtained in this work can be also useful for the other very interesting studies concerning the wave propagation in cubic piezoelectromagnetics. For example, there is a great current interest in various investigations of left-handed artificial materials called the metamaterials. It is expected that some of the piezoelectromagnetic metamaterials can possess the transversely isotropic symmetry and some of them can have the cubic symmetry. These solid metamaterials are characterized by the dielectric permittivity constant ε and the magnetic permeability constant μ with negative signs. So, $\varepsilon < 0$ and $\mu < 0$ surely give $\varepsilon\mu > 0$. However, the opposite sign of the material constants ε and μ can always result in the following condition for the CMEMC defined by expression (II.19) in Chapter II: $K_{em}^2 < 0$. It is expected that the negative sign of K_{em}^2 can be true for the following cases: (1) $\varepsilon < 0$, $\mu < 0$, and $\alpha < 0$ as well as (2) $\varepsilon < 0$, $\mu < 0$, and $\alpha > 0$. This can be true because the value of the electromagnetic constant α is very small in the main for almost all piezoelectromagnetic composites. Also, this unique situation when $K_{em}^2 < 0$ results in unusual correlation between the SH-BAW velocities such as V_{tem} and V_{t4}, see formulae (II.24) and (II.18) from Chapter II, namely $V_{tem} < V_{t4}$. For usual materials, one has to have $V_{tem} > V_{t4}$. The problem is that no answer can be received on the following question: $V_{tem} < V_{t4}$ is true for the metamaterials or not? This problem exists due to absence of any experimental data on SH-BAW propagation in bulk metamaterials. It is still not clear about the preference for experimentalists to cope with bulk metamaterials or thin-film ones. It is thought that as soon as one can measure the SH-BAW velocities V_{tem} and V_{t4} for metamaterials, one can state that the metamaterials with the bulk acoustic wave (BAW) properties were fabricated.

Table XIV.2. The explicit forms of the material parameters A and B in dependence on the electrical and magnetic boundary conditions.

Boundary conditions (Chapter)	Material parameter A	Material parameter B
$B_3 = 0$ and $\varphi = 0$ (VII)	$-K_m^2 K_\alpha^2 (1+K_{em}^2)\frac{C(\varepsilon\mu-\alpha^2)}{e(e\mu-h\alpha)}$	$K_m^2 - K_\alpha^2$
$D_3 = 0$ and $\psi = 0$ (VIII)	$K_e^2 K_\alpha^2 (1+K_{em}^2)\frac{C(\varepsilon\mu-\alpha^2)}{h(e\alpha-h\varepsilon)}$	$K_e^2 - K_\alpha^2$
$B_3 = 0$ and continuity of D_3 (IX)	$-K_m^2 K_\alpha^2 (1+K_{em}^2)\frac{C(\varepsilon\mu-\alpha^2)}{e(e\mu-h\alpha)} \times\left[1+\frac{\varepsilon}{\varepsilon_0}\frac{K_{em}^2}{K_m^2}\left(1-\frac{\alpha^2}{\varepsilon\mu}\right)\right]$	$K_m^2 - K_\alpha^2$
$D_3 = 0$ and continuity of B_3 (X)	$K_e^2 K_\alpha^2 (1+K_{em}^2)\frac{C(\varepsilon\mu-\alpha^2)}{h(e\alpha-h\varepsilon)} \times\left[1+\frac{\mu}{\mu_0}\frac{K_{em}^2}{K_e^2}\left(1-\frac{\alpha^2}{\varepsilon\mu}\right)\right]$	$K_e^2 - K_\alpha^2$
$\psi = 0$ and continuity of D_3 (XI)	$K_e^2 K_\alpha^2 (1+K_{em}^2)\frac{C(\varepsilon\mu-\alpha^2)}{h(e\alpha-h\varepsilon)}$	$K_e^2 - K_\alpha^2 + \frac{\varepsilon_0}{\varepsilon}K_\alpha^2 K_{em}^2 \frac{C(\varepsilon\mu-\alpha^2)}{h(e\alpha-h\varepsilon)}$
$\varphi = 0$ and continuity of B_3 (XII)	$-K_m^2 K_\alpha^2 (1+K_{em}^2)\frac{C(\varepsilon\mu-\alpha^2)}{e(e\mu-h\alpha)}$	$K_m^2 - K_\alpha^2 - \frac{\mu_0}{\mu}K_\alpha^2 K_{em}^2 \frac{C(\varepsilon\mu-\alpha^2)}{e(e\mu-h\alpha)}$
continuity of both D_3 and B_3 (XIII)	See equation (XIII.10)	See equation (XIII.11)

It is possible to review some recent papers concerning various investigations of the metamaterials. Refs. [203, 204] reported their studies of left-handed artificial materials (metamaterials) in the frequency region from 1 THz to 100 THz, and even above [203]. The main problem of the experimental reports in Refs. [203, 204, 205] is that they do not provide the complete set of material constants for investigated unique composites. Ref. [206] reported a study of piezoelectric-piezomagnetic multilayer with $\varepsilon < 0$ and $\mu < 0$ in which dielectric polariton and magnetic polariton can be simultaneously created. Also, it was recently stated that phonon-polaritons in a form of a band-like structure can exist in piezomagnetic superlattices (PMSL) with periodically up and down polarized domain structures [207] in which the piezomagnetic coefficients are periodically modulated. It is worth noticing that some theoretical approaches exist which use complex material constants to describe wave propagation in multi-layered structures [208]. Some latterly works concerning the investigations of different metamaterials can be also found in Refs. [209-218], of which Ref. [210] copes with three-dimensional bulk metamaterial.

This work is written for seasoned theoreticians and experimentalists in the research arena of the wave propagation in solids. However, it is thought that young researchers can also grasp the problems of wave propagation studied in this work. Indeed, it is thought that undergraduate, graduate, and postgraduate students can improve their skills when they additionally study the well-known classical books about the wave propagation and wave phenomena in crystals cited in Refs. [167-177]. It is also recommended for the reader to read the recent review papers concerning magnetoelectric materials cited in Refs. [219-226]. The additional literature is cited in Refs. [227-231] which also study the coupling between magnetic and ferroelectric properties. Indeed, outside the problem of wave propagation in the cubic and transversely isotropic piezoelectromagnetics there exist many others which are of a great interest for practical devices.

Also, the recent Nobel lectures on spintronics, its origin, and development for the future can be found in Refs. [232, 233] written by A. Fert. Also, Chappert and Kim [234] discussed developments of electronics in the future (metal spintronics) which will be free of charges. It is well-known that the magnetoelectric materials sre used to resolve problems of spintronics and magnetic recording. The future of the magnetic memory is coupled with the computer memory called magnetic random access memory (MRAM) which will be as fast as the modern random access memory (RAM) and energetically independent in contrast to RAM. According to work [235] by Bibes and Barthélémy, creative studies of multiferroics are also directed towards creation of magnetoelectric memories.

It is also possible to mention about a promising proposal for a novel storage-class memory described in some the United States patents, for instance, see Refs. [236, 237]. In the novel memory, magnetic domains are used to store information in a "magnetic race-track". The magnetic race-track technology promises a solid state memory with storage capacities and low cost comparable with those of magnetic disk drives, but with much improved performance and reliability. This can be called as follows: "hard disk on a chip". The current induced resonant excitation and motion of domain walls in permalloy nanowires were discussed in papers [238, 239]. According to work [240], the injection of spin polarized current below a threshold value through a domain wall confined to a pinning potential results in its precessional motion within the potential well. Using a short train of current pulses, whose length and spacing are tuned to this precession frequency and oscillations of the domain walls can be resonantly amplified [241]. As a result, the motion of domain walls can be feasible with much reduced spin polarized currents, more than five times smaller than in the absence of resonant amplification.

It is also well-known that different dispersive SH-SAWs guided by the suitable surfaces of piezoelectrics, piezomagnetics, and piezoelectromagnetics are multi-promising candidates for non-destructive testing and sensor applications. It is expected that using some apt piezoelectromagnetic materials, it is possible to create various sensors. They can be quite cheap and revolutionize our life. For example, modern dwellings can be built with smart electronics interacting with thousands cheap sensors working at room temperatures. Indeed, a room-temperature magnetoelectric sensor as cheap as one cent has already been proposed by Israel, Mathur, and Scott [242]. The utilization of magnetoelectric materials for sensors is also discussed in Refs. [243, 244]. Also, Srinivasan and Fetisov [245] have written their collaborative work concerning signal processing devices and microwave magnetoelectric effects. It is worth stating that theoretical investigations of dispersive SH-SAWs propagating in layered systems, when one piezoelectromagnetic material is in a solid contact with the other, are very complicated and, therefore, are still not carried out. It is possible that they can be analytically performed for the transversely isotropic layered structures. It is thought that any analytical analysis is very impotent for complete understanding of wave processes in very complicated layered systems.

There are many interesting applications of the magnetoelectric effect. For instance, magnetized liquid crystals and electronic paper (e-paper) are some of them. In 2008, Lin *et al*. [246] studied the composite consisting of liquid crystals and ferromagnetic nanorods and the possibility of electrical manipulation of magnetic anisotropy in it. It is not possible to mention about all applications of two-phase (composite) materials possessing the magnetoelectric effect. It is also necessary to include much work concerning creation and characterization of new composites possessing the magnetoelectric effect. One can find thousand works on the subjects and the number of applications increases from year to year. The reader can find them, for example, in Internet. To help the reader, it is possible to give some additional works [247-255] which can be also read to receive some broaden knowledges in these subjects.

CONCLUSION

To perform numerical calculations of the SH-SAW characteristics, several piezoelectromagnetic composite materials possessing both the piezoelectric and piezomagnetic phases were propounded in this theoretical work. It was also assumed that they can have the cubic symmetry. The piezomagnetic phase in the proposed piezoelectromagnetic composites can be formed by the following very popular piezomagnetics: Metglas, Terfenol-D, Galfenol, and Alfenol. These piezomagnetics have the cubic symmetry and only Terfenol-D can also have the hexagonal symmetry. The piezoelectric phase can be obtained with the following strongly piezoelectric materials: Tl_3TaSe_4, Tl_3VS_4, PZT. The first two of them possess the cubic symmetry and the third is the transversely isotropic material (hexagonal symmetry). Indeed, for the resulting cubic piezoelectromagnetics, the average material properties were used. Also, it was discussed that some lead-free piezoelectrics can be utilized instead of any of the PZT-family.

This theoretical work predicted the existence of the seven new SH-SAWs propagating in the cubic piezoelectromagnetics with both the CMEMC $K_{em}^2 < 1/3$ and $K_{em}^2 > 1/3$. These new SH-SAWs can propagate in direction [101] on the surface of cubic piezoelectromagnetic (composite) material. These seven new SH-SAWs correspond to the seven sets of the electrical and magnetic boundary conditions. The solutions for the seven new SH-SAW velocities were given in the convenient forms for comparison with each other. It was also shown in this work that the eighth SH-SAW called the surface Bleustein-Gulyaev-Melkumyan (BGM) wave can propagate in the cubic piezoelectromagnetics. Therefore, in the cubic piezoelectromagnetics, only eight SH-SAWs including the surface BGM-wave can exist. This number of the SH-SAWs is smaller than that for the transversely isotropic materials in which as many as ten SH-SAWs including the surface BGM-wave can propagate.

Only eight SH-SAWs can exist in the cubic piezoelectromagnetics due to the found fact that only single SH-SAW solution can be revealed in each case of eight for both the sets of the eigenvector components. This is true for both groups of the cubic piezoelectromagnetics, namely for those with the CMEMC $K_{em}^2 < 1/3$ and $K_{em}^2 > 1/3$. This is one of the main differences between the problems of wave propagation in the cubic piezoelectromagnetics and the transversely isotropic composite materials. For the cubic piezoelectromagnetics with $K_{em}^2 < 1/3$, the SH-SAWs can propagate with the velocities higher than the SH-SAW velocity V_{BGM} and slower than the SH-BAW velocity V_{tem}. For those with $K_{em}^2 > 1/3$, the SH-SAWs can propagate with the velocities when their values are situated above the value of the SH-SAW velocity V_{BGM} and just below the value of V_K. Note that the existence of the solution denoted by V_K, which always presents and does not depend on the boundary conditions, also represents the feature of cubic piezoelectromagnetics which does not exist foe the transversely isotropic piezoelectromagnetics.

Like the transversely isotropic materials, the dependence on the speed of light in a vacuum was also revealed in the cubic piezoelectromagnetics for the suitable boundary conditions. It is flagrant that the obtained results can be useful for complete grasping of the problem of wave propagation in two-phase and laminated composite materials with both the cubic and hexagonal symmetries. This can be relevant to the following quite wide subjects: acoustoelectronics, acoustooptics, and optoelectronics. It is expected that the obtained results can be utilized in fabricating smart materials in the microwave technology. It is thought that employment of the electromagnetic acoustic transducers (EMATs) can allow one to carry out measurements of all the new SH-SAW velocities for the cubic piezoelectromagnetics and the transversely isotropic piezoelectromagnetic composites.

REFERENCES

[1] G. Srinivasan, "Magnetoelectric composites" *Annual Review of Materials Research* **40**, 153 – 178 (2010).

[2] Ü. Özgür, Ya. Alivov, H. Morkoç, "Microwave ferrites, part 2: passive components and electrical tuning" *Journal of Materials Science: Materials in Electronics* **20** (10) 911 – 952 (2009).

[3] J. Zhai, Z.-P. Xing, Sh.-X. Dong, J.-F. Li, D. Viehland, "Magnetoelectric laminate composites: an overview" *Journal of the American Ceramic Society* **91** (2) 351 – 358 (2008).

[4] M. Fiebig, "Revival of the magnetoelectric effect" *Journal of Physics D: Applied Physics* **38** (8) R123 – R152 (2005).

[5] W. Eerenstein, N.D. Mathur, J.F. Scott, "Multiferroic and magnetoelectric materials" *Nature* **442**, 759 – 765 (2006).

[6] J.-P. Rivera, "The linear magnetoelectric effect in $LiCoPO_4$ revisited" *Ferroelectrics* **161** (1) 147 – 164 (1994).

[7] G.T. Rado, J.M. Ferrari, W.G. Maisch, "Magnetoelectric susceptibility and magnetic symmetry of magnetoelectrically annealed $TbPO_4$" *Physical Review B* **29** (7) 4041 – 4048 (1984).

[8] J. Ryu, Sh. Priya, K. Uchino, H.-E. Kim, "Magnetoelectric effect in composites of magnetostrictive and piezoelectric materials" *Journal of Electroceramics* **8**, 107 – 119 (2002).

[9] C.L. Zhang, W.Q. Chen, J.Y. Li, J.S. Yang, "Two-dimensional analysis of magnetoelectric effects in multiferroic laminated plates" *IEEE Transactions on Ultrasonics, Ferroelectrics, and Frequency Control* **56** (5) 1046 – 1053 (2009).

[10] M. Zeng, S.W. Or, H.L.W. Chan, "Magnetic field-induced strain and magnetoelectric effects in sandwich composite of ferromagnetic shape memory Ni-

Mn-Ga crystal and piezoelectric PVDF polymer" *The IEEE Transactions on Ultrasonics, Ferroelectrics, and Frequency Control* **57** (10) 2147 – 2153 (2010).

[11] Sh.-X. Dong, J.-F. Li, D. Viehland, "Longitudinal and transverse magnetoelectric voltage coefficients of magnetostrictive/piezoelectric laminate composite: experiments" *The IEEE Transactions on Ultrasonics, Ferroelectrics, and Frequency Control* **51** (7) 793 – 798 (2004).

[12] M. Avellaneda, G. Harshe, "Magnetoelectric Effect in Piezoelectric/Magnetostrictive Multilayer (2-2) Composites" *Journal of Intelligent Material Systems and Structures* **5**, 501 – 513 (1994).

[13] M.J. Dapino, "Nonlinear and hysteretic magnetomechanical model for magnetostrictive transducers" PhD thesis, Iowa State University, 1999.

[14] A.A. Zakharenko, "First evidence of surface SH-wave propagation in cubic piezomagnetics" *Journal of Electromagnetic Analysis and Applications* (Scientific Research Publishing, California, USA) **2** (5) 287 – 296 (2010).

[15] L. Sandlund, M. Fahlander, T. Cedell, A.E. Clark, J.B. Restorff, M. Wun-Fogle, "Magnetostriction, elastic moduli and coupling factors of composite Terfenol-D" *Journal of Applied Physics* **75**, 5656 (1994).

[16] A.E. Clark, J.B. Restorff, M. Wun-Fogle, Th.A. Lograsso, D.L. Schlagel, "Magnetostrictive properties of body-centered cubic Fe-Ga and Fe-Ga-Al alloys" *The IEEE Transaction on Magnetics* **36** (5) 3238 – 3240 (2000).

[17] H.M. Schurter, Y. Zhang, R. Wu, A.B. Flatau, "Mechanical behavior and auxetic properties of Galfenol" in: Behavior and Mechanics of Multifunctional Materials and Composites (Edited by Z. Ounaies, J. Li) *Proceedings of the SPIE*, **Vol. 7289**, 72891Y – 72891Y-12 (2009).

[18] Z. Kaczkowski, "Effect of a magnetic field on the piezomagnetic parameters of some magnetostrictive materials" *Ultrasonics* **8** (4) 239 – 242 (1970).

[19] R.C. Hall, "Single crystal anisotropy and magnetostriction constants of several ferromagnetic materials including alloys of NiFe, SiFe, AlFe, CoNi, and CoFe " *Journal of Applied Physics* **30** (6) 816 – 819 (1959).

[20] H.J. Leamy, E.D. Gibson, F.X. Kayser, "The elastic stiffness constants of iron-aluminum alloys. I. Experimental results and thermodynamic analysis" *Acta Metallurgica Materialica* **15**, 1827 – 1838 (1967).

[21] I.J. Busch-Vishniac, *Electromechanical sensors and actuators*, Springer-Verlag Publishers, New York (1999) page 186 of 347.

[22] A.B. Flatau, "USA Magnetostrictive materials" in *Encyclopedia of Vibrations*, three-volume set, Academic Press Inc. Publisher, pp. 753 – 762 of 1645 pages (2001); ISBN: 0122270851; DOI: 10.1006/rwvb.2001.0079.

[23] M.J. Dapino, "On magnetostrictive materials and their use in adaptive structures" *International Journal of Structural Engineering and Mechanics* **17** (3-4) 303 – 329 (2004).

[24] M.J. Dapino, F.T. Calkins, A.B. Flatau, "Magnetostrictive devices" *Wiley Encyclopedia of Electrical and Electronics Engineering*, J.G. Webster, Ed., John Wiley and Sons, Inc., New York, **Vol. 12**, 278 – 305, 1999.

[25] J.B. Restorff, "Magnetostrictive materials and devices" *Encyclopedia of Applied Physics* **9** 229 – 244 (1994).

[26] R. Chung, R. Weber, D. Jiles, "A Terfenol-D based magnetostrictive diode laser magnetometer" *IEEE Transactions on Magnetics* **27** (6) 5358 – 5243 (1991).

[27] M.J. Dapino, R.C. Smith, A.B. Flatau, "Structural-magnetic strain model for magnetostrictive transducers" *IEEE Transactions on Magnetics* **36** (3) 545 – 556 (2000).

[28] P.R. Downey, A.B. Flatau, "Magnetoelastic bending of Galfenol for sensor applications" *Journal of Applied Physics* **97** (10) 10R505, Part 3 (2005).

[29] J. Atulasimha, A.B. Flatau, R.A. Kellogg, "Sensing behavior of varied stoichiometry single crystal Fe-Ga" *Journal of Intelligent Material Systems and Structures* **17** (2) 97 – 105 (2006).

[30] D. Fang, Yo-P. Wan, X. Feng, A.K. Soh, "Deformation and fracture of functional ferromagnetics" *ASME Applied Mechanics Review* **61**, 020803-1 – 020803-23 (2008).

[31] M. Wun-Fogle, J.B. Restorff, K. Leung, J.R. Cullen, "Magnetostriction of Terfenol-D heat treated under compressive stress" *IEEE Transactions on Magnetics* **35** (5) 3817 – 3819 (1999).

[32] R.A. Kellogg, A.M. Russell, Th.A. Lograsso, A.B. Flatau, A.E. Clark, M. Wun-Fogle, "Mechanical properties of magnetostrictive Iron-Gallium alloys" *Proceedings of the SPIE's 10th Annual International Symposium on Smart Structures and Materials*, San Diego, CA, Paper #5053-70, **vol. 5053**, 534 – 543 (2003).

[33] M. Letcher, G.A. Jones, D.G. Lord, M. Wun-Fogle, H.T. Savage, "Domain structure of As-cast and annealed FeSiB amorphous wires" *Journal of Applied Physics* **69** (8) 5331 – 5333 (1991).

[34] M. Wun-Fogle, J.B. Restorff, A.E. Clark, E. Dreyer, E. Summers, "Stress annealing of Fe-Ga transduction alloys for operation under tension and compression" *Journal of Applied Physics* **97** (10) 10M301-1 – 10M301-3 (2005).

[35] G. Petculescu, K.B. Hathaway, T.A. Lograsso, M. Wun-Fogle, A.E. Clark, "Magnetic field dependence of Galfenol elastic properties" *Journal of Applied Physics* **97** (10) 10M315-1 – 10M315-3 (2005).

[36] A.E. Clark, M. Wun-Fogle, J.B. Restorff, K.W. Dennis, Th.A. Lograsso, R.W. McCallum, "Temperature dependence of the magnetic anisotropy and magnetostriction of $Fe_{100-x}Ga_x$ (x = 8.6, 16.6, 28.5)" *Journal of Applied Physics* **97** (10) 10M316-1 – 10M316-3 (2005).

[37] S.F. Cheng, B.N. Das, M. Wun-Fogle, P. Lubitz, A.E. Clark, "Structure of melt-spun Fe-Ga-based magnetostrictive alloys" *IEEE Transactions on Magnetics* **38** (5) 2838 – 2840 (2002).

[38] J.B. Restorff, M. Wun-Fogle, A.E. Clark, "Temperature and stress dependencies of the magnetostriction in ternary and quaternary Terfenol alloys" *Journal of Applied Physics* **87** (9) 5786 – 5788 (2000).

[39] J.R. Dullen, M. Wun-Fogle, J.P. Teter, J.B. Restorff, A.E. Clark, "Magnetization and magnetostriction of $Tb_{1-x}Dy_xZn$ single crystals" *Journal of Applied Physics* **85** (8) 6250 – 6252 (1999).

[40] M. Wun-Fogle, J.B. Restorff, A.E. Clark, “Hysteresis and magnetostriction of $Tb_xDy_yHo_{1-x-y}Fe_{1.95}$ [112] dendritic rods” *Journal of Applied Physics* **85** (8) 6253 – 6255 (1999).

[41] M. Wun-Fogle, J.B. Restorff, A.E. Clark, “Magnetostriction of stress annealed Fe-Ga-Al and Fe-Ga alloys under compressive and tensile stress” *The SPIE Eleventh Annual International Symposium on Smart Structures and Materials* (San Diego, California) *Proceedings of the SPIE* **5387**, 468 – 475 (2004).

[42] R.A. Kellogg, A.B. Flatau, A.E. Clark, M. Wun-Fogle, Th.A. Lograsso, “Quasi-static transduction characterization of Galfenol” *Proceedings of IMECE 2003* (2003 ASME International Mechanical Engineering Congress, Washington, D.C.) 1 – 8 (2003).

[43] S. Guruswamy, N. Srisukhumbowornchai, A.E. Clark, J.B. Restorff, M. Wun-Fogle, “Strong, ductile, and low-field-magnetostrictive alloys based on Fe-Ga” *Scripta Materialia* **43** (3) 239 – 244 (2000).

[44] A.E. Clark, M. Wun-Fogle, J.B. Restorff, Th.A. Lograsso, D.L. Schlagel, “Magnetostrictive Galfenol/Alfenol single crystal alloys under large compressive stresses” *Proceedings of Actuator 2000*, *7th International Conference on New Actuators*, Bremen, Germany, pp. 111 – 115 (2000).

[45] R.A. Kellogg, “Development and modeling of Iron-Gallium alloys” PhD thesis, Iowa State University, 117 pages, 2003.

[46] J.R. Cullen, A.E. Clark, M. Wun-Fogle, J.B. Restorff, Th.A. Lograsso, “Magnetoelasticity of Fe-Ga and Fe-Al alloys” *Journal of Magnetism and Magnetic Materials* **226-230** (part 1) 948 – 949 (2001).

[47] A.E. Clark, M. Wun-Fogle, J.B. Restorff, Th.A. Lograsso, A.R. Ross, J.R. Cullen, “Effect of quenching on the magnetostriction of $Fe_{1-x}Ga_x$ ($0.13 < x < 0.21$)” *The 8th Joint MMM-Intermag Conference* (San Antonio, Texas) *IEEE Transactions on Magnetics* **37** (4) 2678 – 2680 (2001).

[48] J.B. Restorff, M. Wun-Fogle, A.E. Clark, Th.A. Lograsso, A.R. Ross, D.L. Schlagel, “Magnetostriction of ternary Fe-Ga-X alloys (X = Ni, Mo, Sn, Al)” *Journal of Applied Physics* **91** (10) 8225 – 8227 (2002).

[49] R.A. Kellogg, A. Flatau, A.E. Clark, M. Wun-Fogle, Th.A. Lograsso, "Temperature and stress dependencies of the magnetic and magnetostrictive properties of $Fe_{81}Ga_{19}$" *Journal of Applied Physics* **91** (10) 7821 – 7823 (2002).

[50] A.E. Clark, M. Wun-Fogle, J.B. Restorff, Th.A. Lograsso, "Magnetostrictive properties of Galfenol alloys under compressive stress" *Materials Transactions, The Japan Institute of Metals, Special Issue on Smart Materials – Fundamentals and Applications* **43** (5) 881 – 886 (2002).

[51] Th.A. Lograsso, A.R. Ross, D.L. Schlagel, A.E. Clark, M. Wun-Fogle, "Structural transformations in quenched Fe-Ga alloys" *Journal of Alloys and Compounds* **350**, 95 – 101 (2003).

[52] R.A. Kellogg, A.B. Flatau, A.E. Clark, M. Wun-Fogle, Th.A. Lograsso, "Texture and grain morphology dependencies of saturation magnetostriction in rolled polycrystalline $Fe_{83}Ga_{17}$" *Journal of Applied Physics* **93** (10) 8495 – 8497 (2003).

[53] A.E. Clark, K.B. Hathaway, M. Wun-Fogle, J.B. Restorff, Th.A. Lograsso, V.M. Keppens, G. Petculescu, R.A. Taylor, "Extraordinary magnetoelasticity and lattice softening in b.c.c. Fe-Ga alloys" *Journal of Applied Physics* **93** (10) 8621 – 8623 (2003).

[54] R.A. Kellogg, A.M. Russell, T.A. Lograsso, A.B. Flatau, A.E. Clark, M. Wun-Fogle, "Tensile properties of magnetostrictive Iron-Gallium alloys" *Acta Materialia* **52**, 5043 – 5050 (2004); available online at www.sciencedirect.com.

[55] J.B. Restorff, M. Wun-Fogle, A.E. Clark, "High magnetomechanical coupling of transduction elements under tension" *The 11th CF/DRDC International Meeting on Naval Applications of Materials Technology* (Dartmouth, Nova Scotia) 5 pages (2005).

[56] N. Srisukhumbowornchai, S Guruswamy, "Influence of ordering on the magnetostriction of Fe-27.5 at. % Ga alloys" *Journal of Applied Physics* **92** (9) 5371 – 5379 (2002).

[57] L.-Ya. Dai, J. Cullen, M. Wuttig, Th.A. Lograsso, E. Quandt, "Magnetism, elasticity, and magnetostriction of FeCoGa alloys" *Journal of Applied Physics* **93** (10) 8627 – 8629 (2003).

[58] D. Viehland, J.F. Li, Th.A. Lograsso, A Ross, M. Wuttig, "Structural studies of $Fe_{0.81}Ga_{0.19}$ by reciprocal space mapping" *Applied Physics Letters* **81** (17) 3185 – 3187 (2002).

[59] M. Wun-Fogle, J.B. Restorff, A.E. Clark, E. Dreyer, E. Summers, "Stress annealing of Fe-Ga alloys" the Gelfanol Workshop ("Galfenol Day 2005") University of Maryland, College Park, Maryland, available online at http://www.aerosmart.umd.edu/Galfenol/index.html , 20 pages (2005).

[60] Sh.-X. Dong, J.-Y. Zhai, N.-G. Wang, F.-M. Bai, J.-F. Li, D. Viehland, Th.A. Lograsso, "Fe-Ga/$Pb(Mg_{1/3}Nb_{2/3})O_3$ – $PbTiO_3$ magnetoelectric laminate composites" *Applied Physics Letters* **87** (11) 222504-1 – 222504-3 (2005).

[61] R.A. Kellogg, A.M. Russell, Th.A. Lograsso, A.B. Flatau, A.E. Clark, M. Wun-Fogle, "Tensile strength and non-axial auxetic properties of Fe-Ga alloys" *U.S. Navy Workshop on Acoustic Transduction Materials and Devices*, State College, Pennsylvania, May 6-8, 1 page (2003).

[62] J.B. Restorff, M. Wun-Fogle, A.E. Clark, Th.A. Lograsso, A.R. Ross, D.L. Schlagel, "Magnetostriction and magnetization of ternary Fe-Ga-X alloys (X = Sn, Ni, Mo)" *46th Conference on Magnetism & Magnetic Materials* (Abstracts, Seattle, Washington) 274 – 275 (2001).

[63] M. Wun-Fogle, A.E. Clark, J.B. Restorff, Th.A. Lograsso, "Piezomagnetic properties of polycrystalline Galfenol transduction elements" *U.S. Navy Workshop on Acoustic Transduction Materials and Devices*, State College, Pennsylvania, May 6-8, 1 page (2003).

[64] H. Okamoto, L.E. Tanner (Editors), *Phase diagrams of binary Beryllium alloys*, ASM International, Metals Park, Ohio, 1987, pp. 81-96.

[65] H. Okamoto (Editor), *Phase diagrams of binary Iron alloys*, ASM International, Materials Park, OH, 1993, 147 – 151.

[66] A.E. Clark, M. Wun-Fogle, J.B. Restorff, T.A. Lograsso, G. Petculescu, "Magnetostriction and elasticity of body centered cubic $Fe_{100-x}Be_x$ alloys" *Journal of Applied Physics* **95** (11) 6942 – 6944 (2004).

[67] J. Slaughter, J. Raim, M. Wun-Fogle, J.B. Restorff, "Effect of cyclic stresses and magnetic fields on stress-annealed Galfenol" *The Galfenol Workshop* ("Galfenol Day 2005") University of Maryland, College Park, Maryland, available online at http://www.aerosmart.umd.edu/Galfenol/index.html , 15 pages (2005).

[68] A.E. Clark, J.B. Restorff, M. Wun-Fogle, T.A. Lograsso, "Magnetostrictive properties of Fe-Ga alloys under large compressive stresses" *The 2000 IEEE International Magnetics Conference*, Digest Intermag 2000, **BS-12**, 2 pages (2000).

[69] N. Srisukhumbowornchai, S. Guruswamy, "Large magnetostriction in directionally solidified FeGa and FeGaAl alloys" *Journal of Applied Physics* **90** (11) 5680 – 5688 (2001).

[70] U.S. Application No. 10/750,634, filed Dec. 24, 2003, entitled "Magnetostrictive materials, devices and methods using high magnetostriction, high strength Fe-Ga alloys" joint inventors A.E. Clark, J.B. Restorff, M. Wun-Fogle.

[71] U.S. Application No. 60/178,615, filed Jan. 28, 2000, entitled "Strong, ductile, and low field magnetostrictive alloys" joint inventors A.E. Clark, J.B. Restorff, M. Wun-Fogle.

[72] U.S. Application No. 10/182,095, filed Jul. 24, 2002, entitled "Magnetostrictive materials, devices and methods using high magnetostriction, high strength Fe-Ga alloys" joint inventors A.E. Clark, J.B. Restorff, M. Wun-Fogle.

[73] U.S. Application No. 11/007,953, filed Dec. 7, 2004, entitled "Magnetostrictive materials, devices and methods using high magnetostriction, high strength Fe-Ga alloys" joint inventors A.E. Clark, J.B. Restorff, M. Wun-Fogle.

[74] U.S. Application No. 60/543,650, filed Feb. 12, 2004, entitled "Preparation of positive magnetostrictive materials for operation under tension" joint inventors A.E. Clark, J.B. Restorff, M. Wun-Fogle.

[75] International Application filed under the Patent Cooperation Treaty (PCT), International Application No. PCT/US2007/015688, international filing date Jul. 10, 2007, title "Galfenol steel" joint inventors A.E. Clark, M. Wun-Fogle, Th.A. Lograsso (18 pages of text and 3 sheets of drawings).

[76] U.S. Application No. 11/822,778, filed Jul. 10, 2007, entitled "Galfenol steel" joint inventors A.E. Clark, M. Wun-Fogle, Th.A. Lograsso.
[77] U.S. Application No. 11/058,710, filed Feb. 11, 2005, entitled "Preparation of positive magnetostrictive materials for use under tension" joint inventors A.E. Clark, M. Wun-Fogle, J.B. Restorff.
[78] U.S. Application No. 11/296,726, filed Nov. 29, 2005, entitled "Magnetostrictive materials, devices and methods using high magnetostriction, high strength FeGa and FeBe alloys" joint inventors A.E. Clark, M. Wun-Fogle, J.B. Restorff, Th.A. Lograsso, R.A. Kellogg.
[79] U.S. Application No. 60/832,007, filed Jul. 11, 2006, entitled "Galfenol steel" joint inventors A.E. Clark, M. Wun-Fogle, Th.A. Lograsso.
[80] U.S. Application No. 60/882,259, filed Dec. 28, 2006, entitled "Fe-X (X = A1, Ga) bimetallic strips for energy harvesting, actuating and sensing" joint inventors A.E. Clark, M. Wun-Fogle, J.B. Restorff.
[81] U.S. Application No. 11/274,635, filed Nov. 15, 2005, entitled "Method of achieving high transduction under tension or compression" joint inventors A.E. Clark, M. Wun-Fogle, J.B. Restorff.
[82] R. Malmhäll, G. Bäckström, K.V. Rao, S.M. Bhagat, M. Meichle, M.B. Salamon, "Metglas 2826B – transport, magnetic and thermal properties" *Journal of Applied Physics* **49** (3) 1727 – 1729 (1978).
[83] J. Henaff, M. Feldmann, M.A. Kirov, "Piezoelectric crystals for surface acoustic waves (Quartz, $LiNbO_3$, $LiTaO_3$, Tl_3VS_4, Tl_3TaSe_4, $AlPO_4$, GaAs)" *Ferroelectrics* **42**, 161 – 185 (1982).
[84] A.A. Zakharenko, "Love type waves in layered systems consisting of two piezoelectric cubic crystals" *Journal of Sound and Vibration* **285** (4–5) 877 – 886 (2005).
[85] V.P. Kamenov, Y. Hu, E. Shamonina, K.H. Ringhofer, V.Ya. Gayvoronsky, "Two-wave mixing in (111)-cut $Bi_{12}SiO_{20}$ and $Bi_{12}TiO_{20}$ crystals: characterization and comparison with the general orientation" *Physical Review E* **62** (2) 2863 – 2870 (2000).

[86] Sh.-X. Dong, J.-Y. Zhai, F.-M. Bai, J.-F. Li, D. Viehland, Th.A. Lograsso, "Magnetostrictive and magnetoelectric behavior of Fe-20 at. % Ga/Pb(Zr,Ti)O_3 laminates" *Journal of Applied Physics* **97** (10) 103902 (2005).

[87] J.Y. Zhai, S.X. Dong, Z.P. Xing, J.-F. Li, D. Viehland, "Giant magnetoelectric effect in Metglas/Polyvinylidene-Fluoride laminates" *Applied Physics Letters* **89**, 083507 (2006).

[88] A. Melkumyan, "Twelve shear surface waves guided by clamped/free boundaries in magneto-electro-elastic materials" *International Journal of Solids and Structures* **44**, 3594 – 3599 (2007).

[89] A.A. Zakharenko, *Propagation of seven new SH-SAWs in piezoelectromagnetics of class 6 mm*, Saarbruecken – Krasnoyarsk, LAP LAMBERT Academic Publishing GmbH & Co. KG, 76 pages, 2010, ISBN: 978-3-8433-6403-4.

[90] J.L. Bleustein, "A new surface wave in piezoelectric materials" *Applied Physics Letters* **13** (12) 412 – 413 (1968).

[91] Yu.V. Gulyaev, "Electroacoustic surface waves in solids" *Soviet Physics Journal of Experimental and Theoretical Physics Letters* **9** (1) 37 – 38 (1969).

[92] R. Ribichini, F. Cegla, P.B. Nagy, P. Cawley, "Quantitative modeling of the transduction of electromagnetic acoustic transducers operating on ferromagnetic media" *IEEE Transactions on Ultrasonics, Ferroelectrics, and Frequency Control* **57** (12) 2808 – 2817 (2010).

[93] R.B. Thompson, "Physical principles of measurements with EMAT transducers" in *Physical Acoustics*, W.P. Mason and R.N. Thurston, Eds., New York, NY: Academic Press, 1990, **vol. 19**, pp. 157 – 200.

[94] M. Hirao, H. Ogi, *EMATs for Science and Industry: Non-contacting Ultrasonic Measurements*, Boston, MA: Kluwer Academic, 2003.

[95] E.A. Kolosovskii, A.V. Tsarev, I.B. Yakovkin, "Improved procedure for measuring SAW velocity in anisotropic structures" *Acoustical Physics Reports* (Moscow) **44**, 793 – 800 (1998).

[96] M.I. Kaganov, I.L. Sklovskaya, "On surface waves in piezoelectrics" *Soviet Physics of Solid State* (Moscow) **8** (12) 3480 – 3483 (1966), in Russian.

[97] S. Kaliski, “On the existence of transversal surface waves in an elastic half-space with surface impedance” *Bulletin of L'Academie Polonaise Science* **15**, 353 – 358 (1967).

[98] C.C. Tseng, “Piezoelectric surface waves in cubic crystals” *Journal of Applied Physics* **41**, 2270 – 2276 (1970).

[99] C.C. Tseng, “Piezoelectric surface waves in cubic and orthorhombic crystals” *Applied Physics Letters* **16** (6) 253 – 255 (1970).

[100] G. Koerber, R.F. Vogel, “Generalized Bleustein modes” *IEEE Transactions on Sonics and Ultrasonics* **SU-19**, 3 – 8 (1972).

[101] V.M. Bright, W.D. Hunt, “Bleustein-Gulyaev waves in gallium arsenide and other piezoelectric cubic crystals” *Journal of Applied Physics* **66**, 1556 – 1564 (1989).

[102] Yu.V. Gulyaev, F.S. Hickernell, “Acoustoelectronics: history, present state and new ideas for a new Era” *Acoustical Physics* **51** (1) 81 – 88 (2005) [*Akusticheskii Zhurnal* (Moscow) **51** (1) 101 – 110 (2005)].

[103] A.A. Zakharenko, “New solutions of shear waves in piezoelectric cubic crystals” *Journal of Zhejiang University SCIENCE A* **8** (4) 669 – 674 (2007).

[104] S.S. Rao, M. Sunar, “Piezoelectricity and its use in disturbance sensing and control of flexible structures: a survey” *Applied Mechanics Review* **47**, 113 – 123 (1994).

[105] F.S. Hickernell, “Shear horizontal BG surface acoustic waves on piezoelectrics: a historical note” *The IEEE Transactions on Ultrasonics, Ferroelectrics, and Frequency Control* **52**, 809 – 811 (2005).

[106] V.I. Al’shits, A.N. Darinskii, J. Lothe, “On the existence of surface waves in half-infinite anisotropic elastic media with piezoelectric and piezomagnetic properties” *Wave Motion* **16** (3) 265 – 283 (1992).

[107] V.I. Al’shits, V.N. Lyubimov, “On existence of piezoelectric and piezomagnetic properties of anisotropic media” *Soviet Kristallografia* (Moscow) **35** (2) 483 – 484 (1990).

[108] Yu.V. Gulyaev, I.E. Dikshtein, V.G. Shavrov, "Magnetoacoustic surface waves in magnetic crystals at reorientation phase transitions" *Uspekhi Phizicheskikh Nauk* (Moscow) **167** (7) 735 – 750 (1997).

[109] P. Curie, "Sur la symétrie des phénomènes physiques: symétrie d'un champ électrique et d'un champ magnétique" *Journal de Physique,* 3e Série, 393 – 415 (1894).

[110] L.D. Landau, E.M. Lifshitz, *Electrodynamics of Continuous Media*, Second Edition, Pergamon Press, Oxford (1984).

[111] I.E. Dzyaloshinskii, "On the magneto-electrical effects in antiferromagnetics" *Soviet Physics – Journal of Experimental and Theoretical Physics* (*JETP*) **10**, 628 – 629 (1960) [Zhurnal Experientalnoi i Teoreticheskoi Fiziki (USSR) **37**, 881 – 882 (1959)].

[112] D.N. Astrov, "The magnetoelectric effect in antiferromagnets" *Soviet Physics – Journal of Experimental and Theoretical Physics* (*JETP*) **11**, 708 – 709 (1960) [Zhurnal Experientalnoi i Teoreticheskoi Fiziki (USSR) **38**, 984 – 985 (1960)].

[113] G.T. Rado, V.J. Folen, "Observation of the magnetically induced magnetoelectric effect and evidence for antiferromagnetic domains" *Physical Review Letters* **7** (8) 310 – 311 (1961).

[114] G.A. Smolenskii, V.A. Ioffe, *Communications de Colloque International de Magnetisme de Grenoble* (France), 2 – 6 Jullet, Communication No. 1 (1958).

[115] D.N. Astrov, B.I. Al'shin, R.V. Zorin, L.A. Drobyshev, "Spontaneous magnetoelectric effect" *Soviet Physics – Journal of Experimental and Theoretical Physics* (*JETP*) **28**, 1123 – 1128 (1969) [Zhurnal Experientalnoi i Teoreticheskoi Fiziki (USSR) **55**, 2122 – 2127 (1968)].

[116] D.N. Astrov, "Magnetoelectric effect in antiferromagnetic Cr_2O_3" *Soviet Physics – Journal of Experimental and Theoretical Physics* (*JETP*) **13** (4) 729 – 733 (1961).

[117] V.J. Folen, G.T. Rado, E.W. Stalder, "Anisotropy of the magnetoelectric effect in Cr_2O_3" *Physical Review Letters* **6** (11) 607 – 608 (1961).

[118] S. Foner, M. Hanabusa, "Magnetoelectric effect in Cr_2O_3 and $(Cr_2O_3)_{0.8}(Al_2O_3)_{0.2}$" *Journal of Applied Physics* **34** (4) 1246 – 1247 (1963).

[119] T.J. Martin, J.C. Anderson, "Magneto-electric annealing effects of Cr_2O_3" *Physics Letters* **11** (2) 109 – 110 (1964).

[120] T.H. O'Dell, "Magnetoelectrics - a new class of materials" *Electronics and Power* **11**, 266 – 267 (1965).

[121] T.J. Martin, J.C. Anderson, "Antiferromagnetic domain switching in Cr_2O_3" *The IEEE Transactions on Magnetics*, **MAG-2**, 446 (1966).

[122] S. Alexander, S. Shtrikman, "On the origin of the axial magnetoelectric effect of Cr_2O_3" *Solid State Communications* **4**, 115– 117 (1966).

[123] R.M. Hornreich, S. Shtrikman, "Statistical mechanics and origin of the magnetoelectric effect in Cr_2O_3" *Physical Review* **161** (2) 506 – 512 (1967).

[124] R.M. Hornreich, "The magnetoelectric effect: Some likely candidates" *Solid State Communications* **7** (15) 1081 – 1085 (1969).

[125] R.M. Hornreich, "Theory of the magnetoelectric effect in polycrystalline powders" *Journal of Applied Physics* **41** (3) 950-951 (1970).

[126] L.M. Holmes, L.G. van Uitert, G.W. Hull, "Magnetoelectric effect and critical behavior in the Ising-like antiferromagnet, $DyAlO_3$" *Solid State Communications* **9** (16) 1373 – 1376 (1971).

[127] E. Fischer, G. Gorodetsky, R.M. Hornreich, "A new family of magnetoelectric materials: $A_2M_4O_9$(A = Ta, Nb; M = Mn, Co)" *Solid State Communications* **10** (12) 1127 – 1132 (1972).

[128] R.M. Hornreich, "The magnetoelectric effect: Materials, physical aspects, and applications" *The IEEE Transactions on Magnetics*, **MAG-8**, 584 – 589 (1972).

[129] G.A. Smolenskii, I.E. Chupis, *Problems in Solid State Physics*, Mir Publishers, Moscow (1984).

[130] I.H. Ismailzade, R.M. Ismailov, A.I. Alekberov, F.M. Salaev, "Magnetoelectric investigation of the system BiFeO-$Pb(Fe_{0.5}Nb_{0.5})O_3$" *Physica Status Solidi* (a) **57** (1) 99 – 103 (1980).

[131] R.S. Singh, T. Bhimasankaram, G.S. Kumar, S.V. Suryanarayana, "Dielectric and magnetoelectric properties of $Bi_5FeTi_3O_{15}$" *Solid State Communications* **91** (7) 567 – 569 (1994).

[132] H. Schmid, "Magnetic ferroelectric materials" *Bulletin of Materials Science* **17** (7) 1411 – 1414 (1994).

[133] J. van Suchtelen, "Product properties: a new application of composite materials" *Philips Research Reports* **27** (1) 28 – 37 (1972).

[134] J. van den Boomgaard, D.R. Terrell, R.A.J. Born, H.F.J.I. Giller, "*In-situ* grown eutectic magnetoelectric composite-material. 1. Composition and unidirectional solidification" *Journal of Materials Science* **9** (10) 1705 – 1709 (1974).

[135] A.M.J.G. van Run, D.R. Terrell, J.H. Scholing, "*In-situ* grown eutectic magnetoelectric composite-material. 2. Physical properties" *Journal of Materials Science* **9** (10) 1710 – 1714 (1974).

[136] J. van den Boomgaard, A.M.J.G. van Run, J. van Suchtelen, "Piezoelectric-piezomagnetic composites with magnetoelectric effect" *Ferroelectrics* **14** 727 – 728 (1976).

[137] V.E. Wood, A.E. Austin, in *Magnetoelectric Interaction Phenomena in Crystals*, A.J. Freeman, H. Schmid, Eds., Gordon and Breach Science Publishers, Newark, New York, 1975, pp. 181 – 194.

[138] B.A. Bednarcyk, "A fully coupled micro/macro theory for thermo-electro-magneto-elasto-plastic composite laminates" NASA/CR—2002-211468 (2002) 46 pages; available electronically at http://gltrs.grc.nasa.gov/GLTRS.

[139] M. Sunar, A.Z. Al-Gami, M.H. Ali, R. Kahraman, "Finite element modeling of thermopiezomagnetic smart structures" *AIAA Journal* **40** (9) 1846 – 1851 (2002).

[140] T.J.-Ch. Liu, Ch.-H. Chue, "On the singularities in a bimaterial magneto-electro-elastic composite wedge under antiplane deformation" *Composite Structures* **72**, 254 – 265 (2006).

[141] P. Chen, Ya.-P. Shen, "Propagation of axial shear magneto–electro-elastic waves in piezoelectric–piezomagnetic composites with randomly distributed

cylindrical inhomogeneities" *International Journal of Solids and Structures* **44**, 1511 – 1532 (2007).

[142] Y.-Z. Wang, F.-M. Li, W.-H. Huang, X. Jiang, Yu.-Sh. Wang, K. Kishimoto, "Wave band gaps in two-dimensional piezoelectric/piezomagnetic phononic crystals" *International Journal of Solids and Structures* **45**, 4203 – 4210 (2008).

[143] J.F. Nye, *Physical properties of crystals. Their representation by tensors and matrices*, Oxford, Clarendon Press, 1989, 385 pages.

[144] H. Schmid, "Some symmetry aspects of ferroics and single phase multiferroics" *Journal of Physics: Condensed Matter* **20**, 434201 (2008) 24 pages.

[145] C.W. Nan, "Magnetoelectric effect in composites of piezoelectric and piezomagnetic phases" *Physical Review B* **50** (9) 6082 – 6088 (1994).

[146] Sh.-F. Li, "The electromagneto-acoustic surface wave in a piezoelectric medium: The Bleustein–Gulyaev mode" *Journal of Applied Physics* **80** (9) 5264 – 5269 (1996).

[147] M.I. Bichurin, I.A. Kornev, V.M. Petrov, A.S. Tatarenko, Yu.V. Kiliba, G. Srinivasan, "Theory of magnetoelectric effects at microwave frequencies in a piezoelectric/magnetostrictive multilayer composite" *Physical Review B* **64**, 094409 (2001).

[148] K. Mori, M. Wuttig, "Magnetoelectric coupling in Terfenol-D/polyvinylidenedifluoride composites" *Applied Physics Letters* **81** (1) 100 – 101 (2002).

[149] M.I. Bichurin, D.A. Filippov, V.M. Petrov, V.M. Laletsin, N. Paddubnaya, G. Srinivasan, "Resonance magnetoelectric effects in layered magnetostrictive-piezoelectric composites" *Physical Review B* **68** (13) 132408 (2003) 4 pages.

[150] X.-F. Li, "Dynamic analysis of a cracked magnetoelectroelastic medium under anti-plane mechanical and in-plane electric and magnetic impacts" *International Journal of Solids and Structures* **42** (11-12) 3185 – 3205 (2005).

[151] S. Srinivas, J.Y. Li, Y.C. Zhou, A.K. Soh, "The effective magnetoelectroelastic moduli of matrix-based multiferroic composites" *Journal of Applied Physics* **99**, 043905 (2006) 7 pages.

[152] A.-K. Soh, J.-X. Liu, "Interfacial shear horizontal waves in a piezoelectric-piezomagnetic bi-material" *Philosophical Magazine Letters* **86** (1) 31 – 35 (2006).
[153] P. Yang, K. Zhao, Y. Yin, J.G. Wan, J.S. Zhu, "Magnetoelectric effect in magnetostrictive/ piezoelectric laminate composite Terfenol-D/$LiNbO_3$ [(*zxtw*)−129°/30°]" *Applied Physics Letters* **88**, 172903 (2006) 3 pages.
[154] J. Chen, E. Pan, H. Chen, "Wave propagation in magneto-electro-elastic multilayered plates" *International Journal of Solids and Structures* **44** (3-4) 1073 – 1085 (2007).
[155] A. Melkumyan, Y.-W. Mai, "Influence of imperfect bonding on interface waves guided by piezoelectric/piezomagnetic composites" *Philosophical Magazine* **88** (23) 2965 – 2977 (2008).
[156] V.M. Petrov, G. Srinivasan, "Enhancement of magnetoelectric coupling in functionally graded ferroelectric and ferromagnetic bilayers" *Physical Review B* **78**, 184421 (2008).
[157] Y. Huang, X.-F. Li, K.Y. Lee, "Interfacial shear horizontal (SH) waves propagating in a two-phase piezoelectric/piezomagnetic structure with an imperfect interface" *Philosophical Magazine Letters* **89** (2) 95 – 103 (2009).
[158] Y.N. Venevtsev, V.V. Gagulin, I.D. Zhitomirsky, "Material science aspects of seignette-magnetism problem" *Ferroelectrics* **73**, 221 – 248 (1987).
[159] A.A. Zakharenko, *Dispersive SAWs in Layered Systems Consisting of Cubic Piezoelectrics*, Saarbruecken – Krasnoyarsk, LAP LAMBERT Academic Publishing GmbH & Co. KG, 62 pages, 2010, ISBN: 978-3-8433-7523-8.
[160] D.A. Berlincourt, D.R. Curran, H. Jaffe, "Piezoelectric and piezomagnetic materials and their function in transducers", in *Physical Acoustics: Principles and Methods*, edited by W.P. Mason, **Vol. 1**, Part A, Academic Press, New York, 1964, pages 169 – 270.
[161] V.E. Lyamov, *Polarization effects and interaction anisotropy of acoustic waves in crystals*, Moscow, MSU Publishing, 1983, 224 pages; in Russian.

[162] J.X. Liu, X.L. Liu, Y.B. Zhao, "Green functions for anisotropic magnetoelectroelastic solids with an elliptical cavity or a crack" *International Journal of Engineering Science* **39**, 1405 – 1418 (2001).

[163] W.Y. Tian, U. Gabbert, "Macrocrack–microcrack interaction problem in magnetoelectroelastic solids" *Mechanics of Materials* **37**, 565 – 592 (2005).

[164] R. Rojas-Diaz, A. Saez, F. Garcia-Sanchez, Ch. Zhang, "Time-harmonic Green's functions for anisotropic magnetoelectroelasticity" *International Journal of Solids and Structures* **45**, 144 – 158 (2008).

[165] E. Pan, "Exact solution for simply supported and multilayered magneto-electro-elastic plates" *Journal of Applied Mechanics* **68**, 608 – 618 (2001).

[166] A.R. Annigeri, N. Ganesan, S. Swarnamani, "Free vibrations of simply supported layered and multiphase magneto-electro-elastic cylindrical shells" *Smart Materials and Structures* **15**, 459 – 467 (2006).

[167] R.E. Newnham, *Properties of materials: anisotropy, symmetry, structure*, Oxford University Press, 2004, 620.112 N55P.

[168] S.G. Lekhnitskii, *Theory of Elasticity of an Anisotropic Elastic Body*, Holden-Day, San Francisco, 1963.

[169] B.A. Auld, *Acoustic Fields and Waves in Solids*, **volume 1**, John Wiley and Sons, New York, 1973.

[170] F.I. Fedorov, *Theory of Elastic Waves in Crystals*, Plenum Press, New York, 1968.

[171] W.A. Wooster. *Tensors and Group Theory for the Physical Properties of Crystals*, Clarendon Press, Oxford, 1973.

[172] M.A. Jaswon, M.A. Rose, *Crystal Symmetry: Theory of Colour Crystallography*, Ellis Horwood Limited, Chichester, 1983.

[173] A.H. Nayfeh, *Wave Propagation in Layered Anisotropic Media with Applications to Composites*, Elsevier, Amsterdam, 1995.

[174] C. Hammond, *The Basics of Crystallography and Diffraction*, Oxford University Press, Oxford, 1997.

[175] G.W. Farnell, E.L. Adler, "Elastic wave propagation in thin layers" in *Physical Acoustics: Principles and Methods*, W.P. Mason and R.N. Thurston (Eds.), **Vol. 9,** Academic Press, New York, 1972, pp. 35 – 127.

[176] E. Dieulesaint, D. Royer, *Elastic waves in solids: applications to signal processing* / translated by A. Bastin and M. Motz, Chichester [English]; New York, J. Wiley, 1980, 511 pages.

[177] D. Royer, E. Dieulesaint, *Elastic waves in solids I*, Springer Verlag, New York, 2000, 158 pages.

[178] C. Lardat, C. Maerfeld, P. Tournois, "Theory and performance of acoustical dispersive surface wave delay lines" *Proceedings of the IEEE* **59** (3) 355 – 364 (1971).

[179] G.W. Farnell, Types and properties of surface acoustical waves, in: A.A. Oliner (Ed.), *Acoustic Surface Waves*, **Vol. 24**, Springer Verlag, Berlin–Heidelberg–New York, 1978, pp. 26 – 109.

[180] Lord Rayleigh (J.W. Strutt), "On waves propagated along the plane surfaces of an elastic solid" *Proceedings of the London Mathematical Society* **17**, 4–11 (1885).

[181] A.A. Zakharenko, "On cubic crystal anisotropy for waves with Rayleigh-wave polarization" *Non-destructive Testing and Evaluation* **21** (2) 61 – 77 (2006).

[182] A.A. Zakharenko, "Acoustic waves with the in-plane polarization in piezoelectric cubic structures" *Canadian Journal of Pure & Applied Sciences* (*SENRA Academic Publishers, Burnaby, British Columbia, Canada*) **3** (1) 675 – 690 (2009); ISSN: 1715-9997 (on-line at http://www.cjpas.org).

[183] W. Kleber, *An introduction to Crystallography*, Veb–Verlag Technik, Berlin, 1971, 336 pages.

[184] Yu.I. Sirotin, M.P. Shaskol'skaya, *Basics of Crystallophysics*, Moscow, Nauka Publishers, 640 pages (1979).

[185] I.N. Bronstein, K.A. Semendyaev, *The reference-book on mathematics for engineers and higher school students*, Science, Moscow, 608 pages (2000).

[186] A.A. Zakharenko, "New interfacial shear-horizontal waves in piezoelectric cubic crystals" *Journal of Electromagnetic Analysis and Applications* (*Scientific Research Publishing*, *California*, *USA*) **2** (11) 633 – 639 (2010).

[187] C. Maerfeld, P. Tournois, "Pure shear elastic surface wave guide by the interface of two semi-infinite media" *Applied Physics Letters* **19** (4) 117 – 118 (1971).

[188] M. Bichurin, V. Petrov, A. Zakharov, D. Kovalenko, S.Ch. Yang, D. Maurya, V. Bedekar, Sh. Priya, "Magnetoelectric interactions in lead-based and lead-free composites" *Materials* **2011** (4) 651 – 702 (2011).

[189] Y.P. Guo, K. Kakimoto, H. Ohsato, "Phase transitional behavior and piezoelectric properties of $(Na_{0.5}K_{0.5})NbO_3$-$LiNbO_3$ ceramics" *Applied Physics Letters* **85**, 4121 – 4123 (2004).

[190] Y.P. Guo, K. Kakimoto, H. Ohsato, "$(Na_{0.5}K_{0.5})NbO_3$-$LiTaO_3$ lead-free piezoelectric ceramics" *Materials Letters* **59**, 241 – 244 (2005).

[191] G.Z. Zang, J.F. Wang, H.C. Chen, W.B. Su, C.M. Wang, P. Qi, B.Q. Ming, J. Du, L.M. Zheng, "Perovskite $(Na_{0.5}K_{0.5})_{1-x}(LiSb)_xNb_{1-x}O_3$ lead-free piezoceramics" *Applied Physics Letters* **88**, 212908:1 – 212908:3 (2006).

[192] B.Q. Ming, J.F. Wang, P. Qi, G.Z. Zang, "Piezoelectric properties of (Li,Sb,Ta) modified $(Na,K)NbO_3$ lead-free ceramics" *Journal of Applied Physics* **101**, 054103:1 – 054103:4 (2007).

[193] C.W. Ahn, H.Y. Park, S. Nahm, K. Uchino, H.G. Lee, H.J. Lee, "Structural variation and piezoelectric properties of $0.95(Na_{0.5}K_{0.5})NbO_3$-$0.05BaTiO_3$ ceramics" *Sensors and Actuators A Physics* **136**, 255 – 260 (2007).

[194] R.P. Wang, R.J. Xie, K. Hanada, K. Matsusaki, H. Bando, M. Itoh, "Phase diagram and enhanced piezoelectricity in the strontium titanate doped potassium-sodium niobate solid solution" *Physica Status Solidi A Applications and Materials* **202**, R57 – R59 (2005).

[195] R.P. Wang, R.J. Xie, K. Hanada, K. Matsusaki, H. Bando, T. Sekiya, M. Itoh, "Phase diagram of the $(Na_{0.5}K_{0.5})NbO_3$-$ATiO_3$ solid solution" *Ferroelectrics* **336**, 39 – 46 (2006).

[196] H.Y. Park, K.H. Cho, D.S. Paik, S. Nahm, H.G. Lee, D.H. Kim, "Microstructure and piezoelectric properties of lead-free (1-x)($Na_{0.5}K_{0.5}$)NbO_3-x$CaTiO_3$ ceramics" *Journal of Applied Physics* **102**, 124101:1 – 124101:5 (2007).

[197] J.H. Huang, "Analytical predictions for the magnetoelectric coupling in piezomagnetic materials reinforced by piezoelectric ellipsoidal inclusions" *Physical Review B* **58** (1) 12 – 15 (1998).

[198] J.Y. Li, "Magnetoelectroelastic multi-inclusion and inhomogeneity problems and their applications in composite materials" *International Journal of Engineering Science* **38** (18) 1993 – 2011 (2000).

[199] J. Kiang, L. Tong, "Nonlinear magneto-mechanical finite element analysis of Ni–Mn–Ga single crystals" *Smart Materials and Structures* **19**, 015017 (2010) 17 pages.

[200] A.A. Zakharenko, "Analytical investigation of surface wave characteristics of piezoelectromagnetics of class 6 mm" *International Scholarly Research Network ISRN Applied Mathematics* **2011**, Article ID 408529, 8 pages (2011); Doi:10.5402/2011/408529.

[201] R.G. Kulkarni, "On the solution to octic equations" *The Montana Mathematics Enthusiast* (The Montana Council of Teachers of Mathematics) **4** (2) 193 – 209 (2007); ISSN 1551-3440.

[202] E.N. Mikhalkin, "Solution of fifth-degree equations" *Russian Mathematics* **53** (6) 15 – 23 (2009).

[203] A. Ishikawa, T. Tanaka, S. Kawata, "Negative magnetic permeability in the visible light region" *Physical Review Letters* **95**, 237401, 4 pages (2005).

[204] T.F. Gundogdu, I. Tsiapa, A. Kostopoulos, G. Konstantinidis, N. Katsarakis, R.S. Penciu, M. Kafesaki, E.N. Economou, Th. Koschny, C.M. Soukoulis, "Experimental demonstration of negative magnetic permeability in the far-infrared frequency regime" *Applied Physics Letters* **89**, 084103, 3 pages (2006).

[205] S.T. Chui, W.H. Wang, L. Zhou, Z.F. Lin, "Longitudinal elliptically polarized electromagnetic waves in off-diagonal magnetoelectric split-ring composites" *Journal of Physics*: *Condensed Matter* **21**, 292202, 4 pages (2009).

[206] H. Liu, S.N. Zhu, Y.Y. Zhu, Y.F. Chen, N.B. Ming, X. Zhang, "Piezoelectric-piezomagnetic multilayer with simultaneously negative permeability and permittivity" *Applied Physics Letters* **86**, 102904, 3 pages (2005).

[207] Zh.X. Liu, W.Y. Wang, "Study of the phonon–polaritons in piezomagnetic superlattices using a generalized transfer matrix method" *Journal of Physics: Condensed Matter* **18**, 9083 – 9092 (2006).

[208] C. Potel, S. Devolder, A. Ur-Rehman, J.-F. Belleval, J.-M. Gherbezza, O. Leroy, M. Wevers, "Experimental verification of the theory of multi-layered Rayleigh waves" *Journal of Applied Physics* **86** (2) 1128 – 1135 (1999).

[209] A.M. Shuvaev, S. Engelbrecht, M. Wunderlich, A. Schneider, A. Pimenov, "Strong dynamic magnetoelectric coupling in metamaterial" *The European Physical Journal B* **79** (2) 163 – 167 (2011).

[210] W.T. Chen, Ch.J. Chen, P.Ch. Wu, Sh. Sun, L. Zhou, G.-Y. Guo, Ch.T. Hsiao, K.-Y. Yang, N.I. Zheludev, D.P. Tsai, "Optical magnetic response in three-dimensional metamaterial of upright plasmonic metamolecules" *Optics Express* **19** (13) 12837 – 12842 (2011).

[211] K. Fan, A.C. Strikwerda, H. Tao, X. Zhang, R.D. Averitt, "Stand-up magnetic metamaterials at terahertz frequencies" *Optics Express* **19** (13) 12619 – 12627 (2011).

[212] G.V. Naik, A. Boltasseva, "A comparative study of semiconductor-based plasmonic metamaterials" *Metamaterials* **5** (1) 1 – 7 (2011).

[213] M. Huang, J. Yang, S. Jun, Sh. Mu, Ya. Lan, "Simulation and analysis of a metamaterial sensor based on a microring resonator" *Sensors* **2011** (11) 5886 – 5899 (2011).

[214] J. Yang, M. Huang, Ch. Yang, J. Peng, R. Zong, "Metamaterial electromagnetic superabsorber with arbitrary geometries" *Energies* **2010** (3) 1335 – 1343 (2010).

[215] L.-M. Si, T. Jiang, K. Chang, T.-Ch. Chen, X. Lv, L. Ran, H. Xin, "Active microwave metamaterials incorporating ideal gain devices" *Materials* **2011** (4) 73 – 83 (2011).

[216] S. Arslanagić, O. Breinbjerg, “Sub-wavelength resonances in metamaterial-based multi-cylinder configurations” *Materials* **2011** (4) 117 – 130 (2011).

[217] N. Dutta, I.O. Mirza, Sh. Shi, D.W. Prather, “Fabrication of large area fishnet optical metamaterial structures operational at near-IR wavelengths” *Materials* **2010** (3) 5283 – 5292 (2010).

[218] A. Sihvola, “Metamaterials in electromagnetics” *Metamaterials* **1** (1) 2 – 11 (2007).

[219] N.A. Hill (N.A. Spaldin), “Why are there so few magnetoelectric materials?” *Journal of Physical Chemistry B* **104**, 6697 – 6709 (2000).

[220] W. Prellier, M.P. Singh, P. Murugavel, “The single-phase multiferroic oxides – from bulk to thin film” *Journal of Physics: Condensed Matter* **17** (30) R803 (2005).

[221] N.A. Spaldin, M. Fiebig, “The renaissance of magnetoelectric multiferroics” *Science* **309** (5733) 391 – 392 (2005).

[222] D.I. Khomskii, “Multiferroics: Different ways to combine magnetism and ferroelectricity” *Journal of Magnetism and Magnetic Materials* **306** (1) 1 – 8 (2006).

[223] G.A. Smolenskii, I.E. Chupis, “Ferroelectromagnets” *Soviet Physics Uspekhi* (*Uspekhi Phizicheskikh Nauk*, Moscow) **25** (7) 475 (1982).

[224] S.-W. Cheong, M. Mostovoy, “Multiferroics: A magnetic twist for ferroelectricity” *Nature Materials* **6**, 13 – 20 (2007).

[225] R. Ramesh, N.A. Spaldin, “Multiferroics: Progress and prospects in thin films” *Nature Materials* **6**, 21 – 29 (2007).

[226] T. Kimura, “Spiral magnets as magnetoelectrics” *Annual Review of Materials Research* **37**, 387 – 413 (2007).

[227] T. Kimura, T. Goto, H. Shintani, K. Ishizaka, T. Arima, Y. Tokura, “Magnetic control of ferroelectric polarization” *Nature* **426**, 55 – 58 (2003).

[228] K.F. Wang , J.-M. Liu, Z.F. Ren, “Multiferroicity: The coupling between magnetic and polarization orders” *Advances in Physics* **58** (4) 321 – 448 (2009).

[229] M. Pregelj, O. Zaharko, A. Zorko, Z. Kutnjak, P. Jeglic, P.J. Brown, M. Jagodic, Z. Jaglicic, H. Berger, D. Arcon, “Spin amplitude modulation driven

magnetoelectric coupling in the new multiferroic $FeTe_2O_5Br$" *Physical Review Letters* **103**, 147202 (2009).

[230] R. Ramesh, "Materials science: Emerging routes to multiferroics" *Nature* **461**, 1218 – 1219 (2009).

[231] K.T. Delaney, M. Mostovoy, N.A. Spaldin, "Superexchange-driven magnetoelectricity in magnetic vertices" *Physical Review Letters* **102** (15) 157203, 4 pages (2009).

[232] A. Fert, "Origin, development, and future of spintronics (Nobel lectures)" *Reviews of Modern Physics* **80** (4) 1517 – 1530 (2008).

[233] A. Fert, "Origin, development, and future of spintronics (Nobel lectures)" *Physics – Uspekhi* **51** (12) 1336 – 1348 (2008) [*Uspekhi Phizicheskikh Nauk*, Moscow, **178** (12) 1336 – 1348 (2008)].

[234] C. Chappert, J.-V. Kim, "Metal spintronics: Electronics free of charge" *Nature Physics* **4**, 837 – 838 (2008).

[235] M. Bibes, A. Barthélémy, "Multiferroics: Towards a magnetoelectric memory" *Nature Materials* **7**, 425 – 426 (2008).

[236] S.S.P. Parkin, *Shiftable magnetic shift register and method of using the same*, US Patent 6,834,005 (2004).

[237] S.S.P. Parkin, *Magnetic shift register with shiftable magnetic domains between two regions, and method of using the same*, US Patent 7,031,178 (2006).

[238] M. Hayashi, L. Thomas, C. Rettner, R. Moriya, S.S.P. Parkin, "Direct observation of the coherent precession of magnetic domain walls propagating along permalloy nanowires" *Nature Physics* **3** (1) 21 – 25 (2007).

[239] M. Hayashi, L. Thomas, C. Rettner, R. Moriya, Y.B. Bazaliy, S.S.P. Parkin, "Current driven domain wall velocities exceeding the spin angular momentum transfer rate in Permalloy nanowires" *Physical Review Letters* **98** (3) 037204 (2007).

[240] L. Thomas, M. Hayashi, X. Jiang, C. Rettner, S.S.P. Parkin, "Oscillatory dependence of current-driven magnetic domain wall motion on current pulse length" *Nature* **443**, 197 – 200 (2006).

[241] L. Thomas, M. Hayashi, X. Jiang, R. Moriya, C. Rettner, S.S.P. Parkin, "Resonant amplification of magnetic domain-wall motion by a train of current pulses" *Science* **315**, (5818) 1553 – 1556 (2007).

[242] C. Israel, N.D. Mathur, J.F. Scott, "A one-cent room-temperature magnetoelectric sensor" *Nature Materials* **7**, 93 – 94 (2008).

[243] M.I. Bichurin, V.M. Petrov, D.A. Filippov, G. Srinivasan, S.V. Nan, *Magnetoelectric materials*, Academia Estestvoznaniya Publishers, Moscow (2006).

[244] Y.K. Fetisov, A.A. Bush, K.E. Kamentsev, A.Y. Ostashchenko, G. Srinivasan, "Ferrite-piezoelectric multilayers for magnetic field sensors" *The IEEE Sensor Journal* **6** (4) 935 – 938 (2006).

[245] G. Srinivasan, Y.K. Fetisov, "Microwave magnetoelectric effects and signal processing devices" *Integrated Ferroelectrics* **83** (1) 89 – 98 (2006).

[246] T.-J. Lin, C.C. Chen, W. Lee, S. Cheng, Y.F. Chen, "Electrical manipulation of magnetic anisotropy in the composite of liquid crystals and ferromagnetic nanorods" *Applied Physics Letters* **93** (1) 013108 (2008).

[247] T.K. Chung, G.P. Carman, K.P. Mohanchandra, "Reversible magnetic domain-wall motion under an electric field in a magnetoelectric thin film" *Applied Physics Letters* **92** (11) 112509, 3 pages (2008).

[248] V.R. Palkar, K. Prashanthi, "Observation of magnetoelectric coupling in $Bi_{0.7}Dy_{0.3}FeO_3$ thin films at room temperature" *Applied Physics Letters* **93** (13) 132906, 3 pages (2008).

[249] Y.H. Chu, L.W. Martin, M.B. Holcomb, M. Gajek, Sh.-J. Han, Q. He, N. Balke, Ch.-H. Yang, D. Lee, W. Hu, Q. Zhan, P.-L. Yang, A. Fraile-Rodríguez, A. Scholl, Sh.X. Wang, R. Ramesh, "Electric-field control of local ferromagnetism using a magnetoelectric multiferroic" *Nature Materials* **7**, 478 – 482 (2008).

[250] T. Yang, T. Kimura, Yo. Otani, "Giant spin-accumulation signal and pure spin-current-induced reversible magnetization switching" *Nature Physics* **4**, 851 – 854 (2008).

[251] D. Chiba, M. Sawicki, Y. Nishitani, Y. Nakatani, F. Matsukura, H. Ohno, "Magnetization vector manipulation by electric fields" *Nature* **455**, 515 – 518 (2008).

[252] H. Zheng, F. Straub, Q. Zhan, P.-L. Yang, W.-K. Hsieh, F. Zavaliche, Y.-H. Chu, U. Dahmen, R. Ramesh, "Self-assembled growth of $BiFeO_3$-$CoFe_2O_4$ nanostructures" *Advanced Materials* **18** (20) 2747 – 2752 (2006).

[253] H. Zheng, Q. Zhan, F. Zavaliche, M. Sherburne, F. Straub, M.P. Cruz, L.-Q. Chen, U. Dahmen, R. Ramesh, "Controlling self-assembled Perovskite-Spinel nanostructures" *Nano Letters* **6** (7) 1401 – 1407 (2006).

[254] H. Zheng, J. Wang, S.E. Lofland, Z. Ma, L. Mohaddes-Ardabili, T. Zhao, L. Salamanca-Riba, S.R. Shinde, S.B. Ogale, F. Bai, D. Viehland, Y. Jia, D.G. Schlom, M. Wuttig, A. Roytburd, R. Ramesh, "Multiferroic $BaTiO_3$-$CoFe_2O_4$ nanostructures" *Science* **303** (5658) 661 – 663 (2004).

[255] G. Srinivasan, E.T. Rasmussen, J. Gallegos, R. Srinivasan, Yu.I. Bokhan, V.M. Laletin, "Magnetoelectric bilayer and multilayer structures of magnetostrictive and piezoelectric oxides" *Physical Review B* **64** (21) 214408, 6 pages (2001).